博士論文

Caging Technology for Delivery of Oligonucleotides into Cells

（細胞へのオリゴヌクレオチド送達のためのケージング技術）

カルンソムワン　ウィランパット

Overview

Oligonucleotide delivery has an essential role in oligonucleotide therapeutics according to their poor bioavailability and cellular penetration. However, the application of oligonucleotides as therapeutic agents has been limited due to poor bioavailability and cellular penetration. The physicochemical properties of cell membranes are the barriers of the oligonucleotide delivery into the cells. In addition, the polyanionic and hydrophilic properties of oligonucleotides are the major factors that prevent the passive diffusion to the cells. The development of the efficient delivery of oligonucleotides to a specific target site is highly required for the therapeutic application.

In chapter 1, oligonucleotide based therapeutics and oligonucleotides delivery techniques are overviewed. In the first section, the mechanisms oligonucleotides therapeutics and the limitation of oligonucleotides therapeutics were described. In the second section, oligonucleotides delivery techniques have been reviewed. Chemical modifications of oligonucleotides and chemically caged nucleic acids are also outlined.

In chapter 2, polyunsaturated fatty acids conjugated oligonucleotides has been developed as the pro-oligonucleotides to assist the oligonucleotides delivery. The cleavage of polyunsaturated fatty acids to release the naked oligonucleotides has been performed. The application of polyunsaturated fatty acids conjugated oligonucleotides has been evaluated in HeLa Cells.

In chapter 3, 4-nitrobenzyl caged oligonucleotides has been synthesized. Linolenate-linked 4-nitrobenzyl caged oligonucleotides has been developed via the CuAAC reaction of the alkyne-linked 4-nitrobenzyl caged oligonucleotides. Alkyne-linked 4-nitrobenzyl caged oligonucleotides has been introduced as a conjugatable functional group to develop the molecules for oligonucleotides delivery.

In chapter 4, the whole research has been summarized and possibility of further development in future has been proposed.

Table of Contents

Pages

Chapter 1

General Introduction

1.1 Oligonucleotides Based Therapeutics.

Oligonucleotides play important roles in biology. The potential use of oligonucleotides for therapeutics has been influenced to treat many human diseases. Small molecule therapeutics are primarily target protein-binding sites to provide biological effect. In contrast, oligonucleotide-based therapeutics exert the gene expressions creating new treatment patterns in which called "undruggable" targets[1]. The significant advantage of oligonucleotide-based therapeutics over currently small molecule drugs is the selectivity of molecular targets and specificity of biological actions. Oligonucleotides-based therapeutics can be used to relieve disease states at the early stage, consequently preventing disease progression and its complications[2]. Presently, there are currently five FDA-approved nucleic acid therapeutics.

Table 1-1 FDA-Approved Nucleic Acid Therapeutics[1]

Name	Mechanism of Action	Administration	Indication
Fomivirsen	Antisense (RNAse H)	Local (intravitreal)	Cytomegalovirus retinitis
Mipomersen	Antisense (RNAse H)	Systemic (iv)	Familial hypercholesterolemia
Pegaptinib	Aptamer	Local (intravitreal)	Neovascular age-related macular degeneration (wet AMD)
Eteplirsen	Splice blocking	Systemic (iv)	Duchenne's muscular dystrophy
Nusinersen	Splice blocking	Local (intrathecal)	Spinal muscular atrophy

Oligonucleotide therapeutics can be grouped into four categories on mechanism of action.[1]

1. Decreasing translation and transcription of mRNA or Increasing degradation of mRNA
2. Increasing translation and transcription of mRNA
3. Creating new translation to produce new gene product
4. Translation agonist or antagonist or Receptor binding

The four mechanism of action along with the size of the oligonucleotides and the examples of oligonucleotides are summarized in **Figure 1-1** and **Table 1-2**.

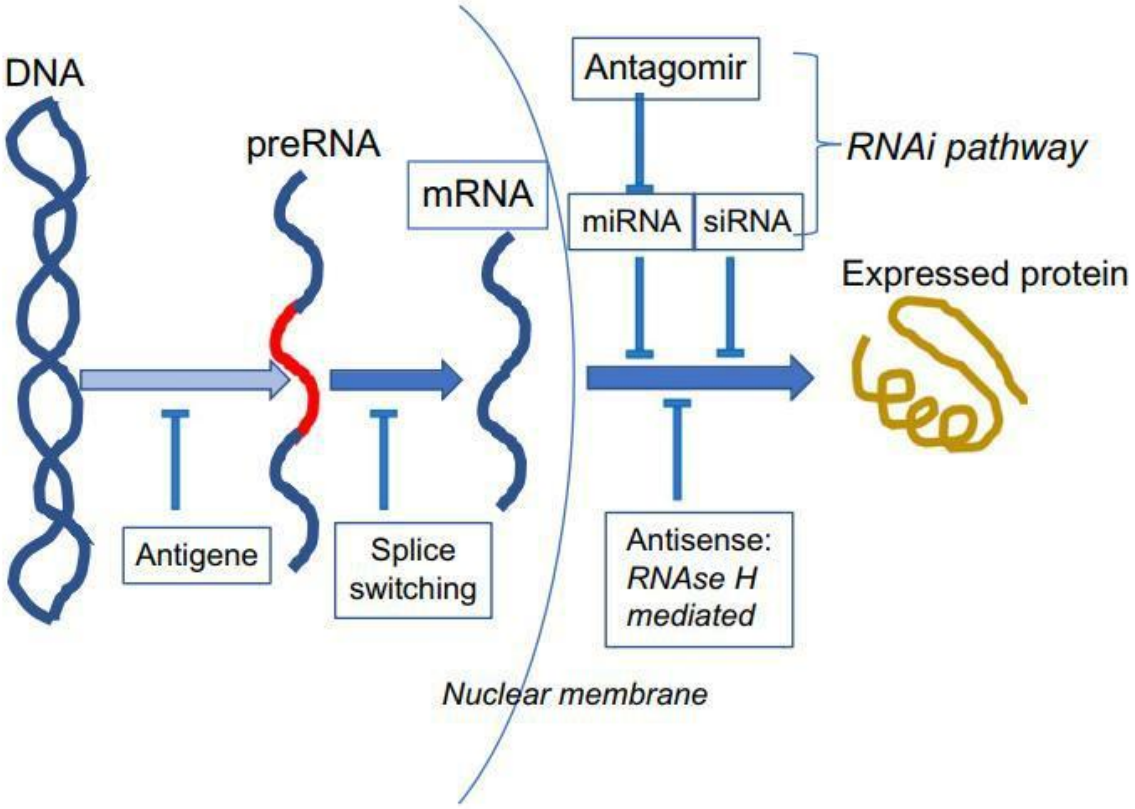

Rozema D.B., Annual Reports in Medicinal Chemistry. 2017, 50: 18-29

Figure 1-1 Mechanisms of oligonucleotides-based therapeutics. Different oligonucleotide therapeutic modalities are in box.

Table 1-2 Mechanism of Action and Size of Oligonucleotides[1]

Mechanism of Action	Examples	Size
Decreased Gene Expression	Antisense	15-25 nucleotides
	RNA interference	18-24 base pairs
	Antigene	~16 nucleotides
Increased transcription	Antagomirs, IncRNA binding	17-22 nucleotides
New gene expression	Splice blocking	15-30 nucleotides
	mRNA	>1500 nucleotides
Receptor binding	Aptamers	~15-60 nucleotides
	Toll receptor agonists	~20 nucleotides
	Telomere agonists	~15 nucleotides

.

There are various sizes and mechanism of actions of oligonucleotides therapeutics. However, there are several drawbacks to the application of unmodified oligonucleotides owing to their intrinsic chemical structures and properties. The major limitations are the development of oligonucleotides delivery into the target cells and the low stability of oligonucleotides under physiological conditions, especially RNA, towards their low nuclease resistance that are abundant in the human body. In addition, oligonucleotides are too large, even the small siRNA and microRNA (**Table 1-2**). Moreover, the polyanionic and hydrophilic properties of oligonucleotides are the major factors that prevent the passive diffusion into the cells[3-5]. Consequently, there are a variety of methodologies to overcome the drawbacks of unmodified nucleic acids by controlling their properties and rendering them with new functions.

1.2 Oligonucleotides delivery techniques

To date, various delivery systems have been developed for the efficiency delivery of oligonucleotides therapeutics. The optimal delivery system depends on the target cells and its characteristics. Delivery systems strategies of oligonucleotides are provided as follows: Viral vector delivery systems, Non-viral vector delivery systems and Chemical modification of the oligonucleotides.

1.2.1 Viral Vector of Oligonucleotides Delivery Systems

During evolution, nonpathogenic attenuated viruses have been developed in various mechanisms to carry genetic material into the target cells and suppress or modify of mechanism protection in the host organism[6 -7]. For therapeutic purposes, the viral genome integrated with interest transgene, infected to the cells, then release the expression cassette. The gene that delivers into the nucleus, is assembled into the host gene pool, thus is latterly expressed[8]. The ability of transfer oligonucleotides therapeutics into target cells are reported in retroviruses, parvoviruses, adenoviruses, lentiviruses, adeno-associated viruses, and the herpes simplex virus[9-11]. Transfection efficiencies in tissues such as kidney, heart, muscle, eye, and ovary were succeeded with gene expression using viral vectors[12-14]. Viruses are preferably applied more than 70% of human clinical gene therapy trials [15]. The summary of viral delivery systems are shown in **Table 1-3**.

The advantage of viral DNA vectors is the greatest high transfection efficiency in a variety of human tissues. Retroviral vectors are widely used in cells that are extremely difficult to transfect including primary human endothelial, smooth muscle cells[16]. A recent report showed that adenoviral vectors can transfer gene higher than liposomal delivery systems in COS-7 cells[17].

Even the impressive of virus gene transfer, there are several issues of viral vector delivery of DNA therapeutics in humans. The major problems are the toxicity and the strong immune response of viruses due to virus proteinaceous capsid. The toxicities have been remarked in numerous animal models. In addition, animal studies are generally studied under abnormal conditions such as specific strains and regimented nutrition, it is difficult to use animal model results to predict human immune response in various patient population[18-20]. The death of a patient participation in a Food and Drug Administration-approved gene therapy clinical trial from respiratory and multiple organ failure in 1999, led to temporary discontinue gene therapy trials in the United States. Though clinical experimentation has resumed, this serious issues tremendous concern over the safety of viruses for future gene therapy applications. Moreover, the assembly of therapeutic genes into the host genome by the virus takes place in a random manner. There is no control over the exact location of gene insertion. Random gene transfer can generate insertional mutagenesis in which may inhibit expression of normal cellular genes or activate oncogenes, with deleterious consequences[21].

The limitations of using viral vectors for therapeutic applications according to the viral envelope has a finite capacity that limit on the size of the expression plasmid in which can incorporate. First generation adeno-associated viral vector had been developed with very small capacity of ~4.7 kilobase (kb) for encapsulation of the plasmid DNA cargo. Recent studies showed the efficient production in the development of second-generation adeno-associated viruses with higher encapsulating capabilities[22].

It has been proved that the formulations of adnoviruses may lose their potency after keeping in commonly used pharmaceutical vials. Adenoviral vectors are known to originate inflammatory responses in tissues with short-lived gene expression[23]. There is concern using viruses for transfection in which the loss of transgene expression over tissue maturation may occurred [24]. Retroviral vector delivery for gene therapy are still expensive and difficult to produce on a large scale. The use of viruses for oligonucleotides delivery remains difficult till all of these problems are being solved[9].

Table 1-3 Viral Vector of Oligonucleotides Delivery Systems[5]

Transgene Delivery Method	Size of inserted transgene (kb)	Time of transgene expression	Preferential way of administration	Immuno genictiy	Safety
Adenoviral vectors	Up to 30	Short (days)	Subcutaneous Intratumoral, Local	high	Low; systemic administration can lead to a systemic inflammatory, lethal case described
Lentiviruses	Up to 10	Life –long	*Ex vivo* transduction of stem cells.	low	Correction of inherited genetic defects, mainly of hematopietic system
Retroviruses	Up to 10	Life –long	*Ex vivo* transduction of stem cells.	low	Unacceptably low; high risk of insertional oncogenesis
Adeno-asso-ciated viruses	Up to 4	Long (months, may be life-long)	Intramuscular	low	High
Poxviruses	Up to 20	Short (days)	Subcutaneous, Local	high	relatively high,
RNA viruses	Up to 2	Short (days)	Subcutaneous, Intratumoral, Local	medium	For the estimation, depends on each vector

1.2.2 Non-viral Vector of Oligonucleotides Delivery System

The non-viral vector are described as physical based, particle based and chemical based. The present non-viral vectors used for oligonucleotide delivery are classified using physical methods and chemical carriers.

1.2.2.1 Physical nonviral delivery systems

Oligonucleotides delivery techniques can be simply transfer genetic materials. These methods apply physical force to interact with membrane barrier of the cells eventually promoting intracellular delivery of the genetic material.

1. Needle: Needle can carry genetic material into tissue through a needle carrying syringe or systemic injection from a vessel. Needle injection are commonly used in muscle, skin, liver, cardiac muscle and solid tumors. Nevertheless, the efficiency of needle injection is relatively low owing to rapid degradation by nucleases in the body and mononuclear phagocyte system clearing [25].

2. Gene gun: Gene gun was first used as gene transfer technique to the plants. This method is based on the delivery of DNA coated heavy metal particles by crossing target tissue at a certain speed. The proper speed is accomplished by high voltage electronic discharge, spark discharge or helium pressure discharge. Gas pressure, particle size, dose frequency are the critical parameters to determine the efficiency of gene transfer. Gold, tungsten and silver are commonly used as metal particles with 1 μm diameter. The major advantage of gene gun is accurate delivery of DNA doses. It is most widely applied in ovarian cancers research[26].

3. Electroporation: Electroporation is the method in which the application of electric field that is greater than the membrane capacitance causing opposite charges polarity to line up on either side of cell membrane thus forming a potential difference at a specific point on the cell surface. Membrane eventually breakdown to form a pore and allows the gene to pass. Pore formation occurs in approximately 10 nanoseconds. The pore of the membrane can be reversible based on the field strength and pulse duration. The resulting of electroporation can maintain the reversible and viable of the cells. Irreversible electroporation is commonly used in cancer treatment to destroy cancer cells. The amplitude and duration of pulse will control the permeability of the cell membrane for gene transfer. High field strength [>700V/cm] or low field strength [< 700 V/cm] with short pulses (microseconds) or long pulses (milliseconds) are currently applied to control field strength. Target tissue determines this combination of variables. Electroporation is considering as a reliable physical method for plasmid DNA delivery. Electroporation can transfer gene by intradermal, intramuscular and intratumoural[25-26].

4. Sonoporation: Sonoporation is the noninvasive technique using ultrasound wave to temporarily permeablize the cell membrane providing internalization of DNA into the target cells. Sonoporation allowed genetic material assembly with micro bubble and administered into systemic circulation. The ultrasound wave's rotated the micro bubble within the microcirculation of target tissue producing the deposition of targeted transfection of genetic material. Micro bubbles are consisted of gas filled core with high molecular weight such as per fluorocarbon or sulfur hexafluoride. The outer shell composed of lipids, proteins or synthetic biopolymers. Micro bubbles is similar to red blood cells in circulation. Sonoporation method is generally performed in brain, cornea, kidney, peritoneal cavity, muscles and heart tissues.

5. Photoporation: Photoporation is a technique using single laser pulse to form transient pores on a cell membrane providing DNA delivery into the target cells. The efficiency of this method depends on focal point and pulse frequency of the laser. Transgene expression results are resemble to electroporation. Though, this method remains lack documented evidence[28].

6. Hydroporation: Hydroporation is a technique using hydrodynamic pressure to attack the cell membrane. Hydrodynamic pressure is made from injection of large volume DNA in a period of time. The methods can create the capillary endothelium permeability and form pore in encircling parenchyma cells. The therapeutic gene can transfer to the target cell through membrane pores. The membrane pores can be closed later to store the therapeutic gene in the target cells. This method is mostly used in hepatic cells for gene therapy studies[29].

7. Magnetofection: Magentofection is the method based on gathering therapeutics gene with magnetic nanoparticle. Magenetic particle was produced from earth electromagnets to increase the complex sedimentation and transfection. In vivo studies, the gene-magetic particle complex is taken via intravenous administration using strong gradient of external magnets, then the complex is captured and transfer to the target cell. The enzyme cleavage hydrolyze the genetic material of crosslink molecules rendering the degradation of the matrix. Magenetofection is commonly used in vitro studies for the transfecting primary cells and cells that are difficult to transfect[30].

1.2.2.2 Chemical nonviral delivery systems

Chemical nonviral delivery systems are more common application than physical nonviral delivery systems. Additionally, there are several advantages of chemical nonviral delivery systems over viral delivery systems such as low toxicity and antigenicity. Chemical nonviral delivery are commonly produced from biological lipids that showed less risk of oncogene insertion, but this method are still having low efficiency[31]. Chemical nonviral delivery systems are included in 2 categories: **Inorganic particles** and **synthetic/natural biodegradable**.

A. Inorganic particles[32]

Nanoparticles come from various size, shape and porosity in order to protect the molecule from degradation and reticuloendothelial system.

1. Calcium phosphate: Calcium phosphate particles were the first inorganic particles, which is biocompatible and biodegradable. Calcium plays an important roles in endocytosis that poses the high binding affinity. However, calcium phosphate nano crystals can be produced resulting the storage capacity. This problem can be solved by adding magnesium.

2. Silica: Silica are commonly used as gene delivery vehicle to functionalized nanoparticles with amono silicanes that poses low toxicity. A major limiting factor is the low delivery efficiency of silica in serum containing medium from the interaction between serum proteins

3. Gold: Gold particles are determined as the method that is easy preparation, unlimited surface characterization and inert nature. Gold nanoparticles poses strong absorption with light near infra-red region, which can penetrate deeply into the target tissues. Modification of the gold surface with DNA can be applied by thermal denaturation to induce photo thermal effect that control the delivery of DNA into the cells. Studies had demonstrated that the gold nanoparticles transfection ability showed lower toxicity in *in vitro* compared to lipoplexes. The major issue of gold particles is high chemical stability that is difficulty to dissolve in the cells occurring the production of gold particles in target cells in which harmful to the cell growth.

B. Synthetic/natural biodegradable

1. Cationic liposomes[33]: Cationic liposomes are widely used in gene therapy research. They are produced from positive charged lipids. The positive charged lipids will bind with negative charged of phosphate group on the internucleotide linkages of oligonucleotides resulting the forming of structure called **lipoplexs**. Cationic liposomes can incorporate hydrophilic and hydrophobic molecules, possess low toxicity, activated non immune system and specifically targeted the delivery of lipoplexs to the target sites. 1,2-dioleoyl-3-trimethylammonium-propane (**DOTAP**) was the first cationic liposomes and synthesized by by Felgner et al. in 1987. There are several studies of new cationic liposomes or micelles systems for gene therapy both *in vitro* and *in vivo*. However, the cationic liposomes can be rapidly degraded by reticuloendothelial system resulting the unstability of sustained gene delivery in a fraction of time. This issues have been solved by the modification of the surface of liposome with hydrophilic polymers. **polyethylene glycol (PEG)** was the cationic liposomes are considered as good stability and efficiency in gene delivery systems.

2. Polyethyleninemine, PEI [34]: PEI is a second generation of cationic polymers that can form nanosized complex, which is called **polyplexes**, when mixing with DNA. PEI is considered as a gold standard for gene transfer. However, PEI have high density amine groups, which exert protein sponge effect that ultimately stops the acidification of endosomal pH. This leads to influx of chloride within the compartment and increases the osmotic pressure, leading to the swelling rupture of endosomal membrane.

3. Dendrimers[35]: Dendrimers are organic high branched molecules that bind with oligonucleotides and transfer genetic materials into the target cells. Dendrimers come with symmetrical size and shape with terminal group functionality. The positive charge of dendrimers encounters with genetic material in physiological pH. Dendrimers effectively interact with cell membranes and proteins owing to their nanometric size. The terminal amino group of dendrimers that possess the positive charge are considering as toxicity concerns.

1.2.3 Chemical Modification of the Oligonucleotides

There are three parts of oligonucleotides chemical modification: nucleobase, ribose and phosphate group for targeting cells specific.

1. Oligonucleotides analogues replace the oligonucleotides skeleton

Phosphorothioate is a common chemical modification of oligonucleotides by the replacement of non-bridge oxygen atoms on diester bond with sulfer. Phosphorothioate can facilitate the cellular uptake in the human body and enhance the bioavailability of the modified oligonucletoides[36]. The chemical modified phosphorothioate siRNA is indicated to be stable in the human body. However, phosphorothioate can increase the cytotoxicity and reduce gene silence[37]. Several reports showed that the modification of siRNA using thiophosphate is not recommended according to the phosphorylated phosphate ester in the phosphorylation can damage RISC activity[38].

There are several functional groups have been considered to the replacement of phosphorodiester group on the internucletide linkages. There are numbers of negative charge functional groups of oligonucleotides skeleton such as phosphorodithioate[39] and thiophosphoramidates. Additionally, there are various of analogues identifying to be uncharged molecules such as phophorodiamidate morpholino oligomer (PMO) [40], peptide nucleic acid (PNA)[41], phosphotriesters[42], and phosphonates[43]. One advantage of uncharged functional groups is nuclease resistance. Furthermore the membrane permeability is also more stable. However, the uncharged oligonucleotides still have limitation in passive diffusion across membrane owing to the size and hydrophilic properties.

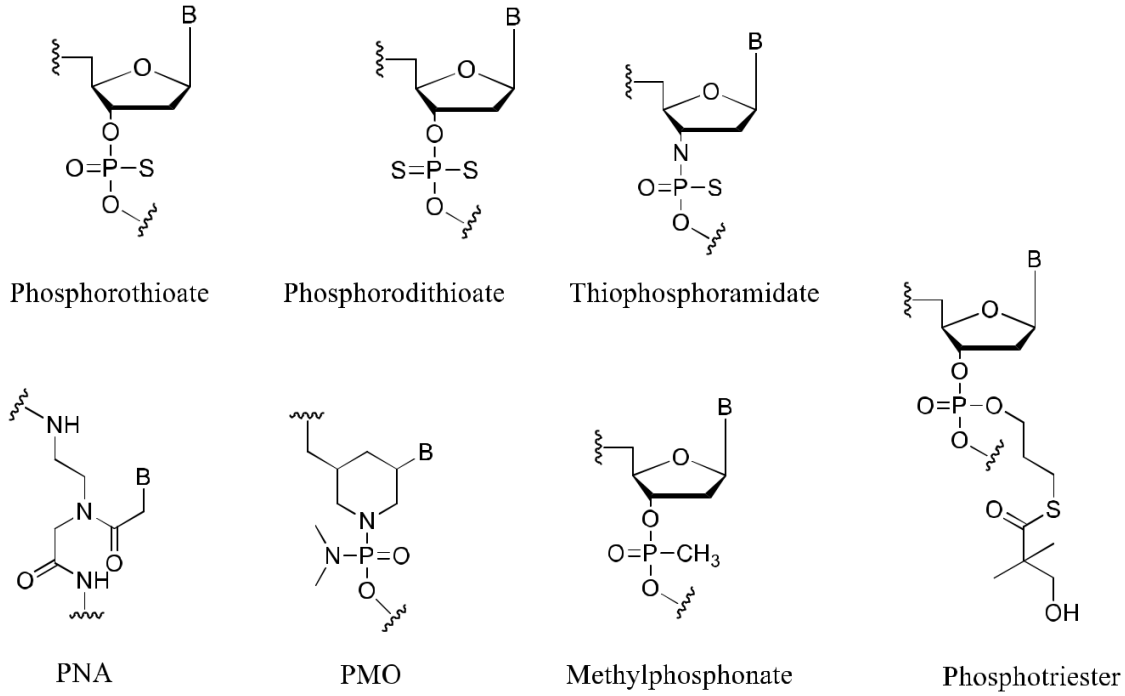

Figure 1-2 Oligonucleotides analogues replace the oligonucleotides skeleton

2. Modification of the Ribose

The gene expression of RNA does not depend of the 2'-OH of the ribose sugar on the oligonucleotides. Though, the chemical modification of 2'-OH have been studied in many research[44]. 2'-O-methyl ribonucleic acids are natural nucleoside that considered to enhance binding affinity and resistant to ribonucleases[45]. The design of 2'-O-methoxyethyl (MOE) was observed to protect ribonuclease resistance from O-methyl group alleviating protein– oligonucleotide interactions and increasing binding affinity of RNA[46]. The MOE is widely applied in antisense oligonucleotides technology and combined with the approved drugs Nusinersen and Mipomersen.

Fluorine is an analogues of nucleoside that possess highly electronegativity. C3'-endo conformations and adapt helical conformations to characterize the ribose RNA. 2'-fluoro derivatives were first used with ribozymes[47] and antisense oligonucleotides[48]. Macugen (pegatanib), the FDA-approved oligonucleotides therapeutics, composed of 2'-F pyrimidines. In sense and antisense of RNAi can be substantial 20 -fluoro modification [49] (**Figure 1-3**).

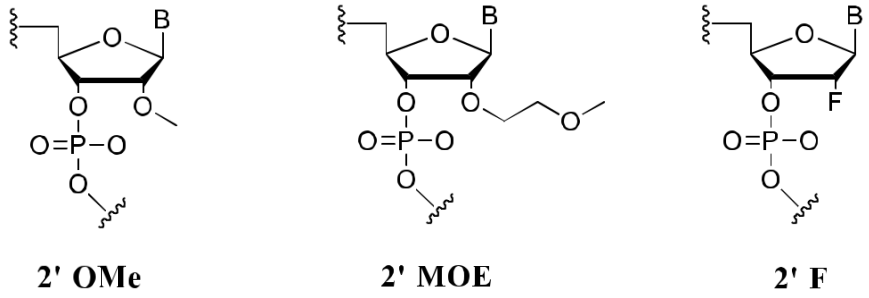

Figure 1-3 Ribose modification at 2' position

3. Base Modification

Base modification plays vital roles in the oligonucleotides formality. This method can increase base paring resulting to enhance the function and the stability of siRNA that interact with target mRNA. G-clamp[50] is the most famous base modification that is cytidine conjugates. G-clamp can increase the affinity of guanosine bases according to hydrogen bond forming with aminoehtyl group. C5 propynyl pyrimidines are considered to create more duplex stable, but the possible toxicity are emerged.

The base modifications of mRNA are shown to be benefit as gene therapy. Uridine and cytidine residues replacement with pseudouridine,[52] N-methyladenosine,[53] 2-thiouridine,[53] and 5-methylcytidine[54] can decreases the innate immune response, besides these modification can mRNA tolerance to the nuclease. One issues to concern is the large molecules of mRNA (>500,000 MW) and hydrophilic properties resulting to reach the cytoplasm of target cells (**Figure 1-4**).

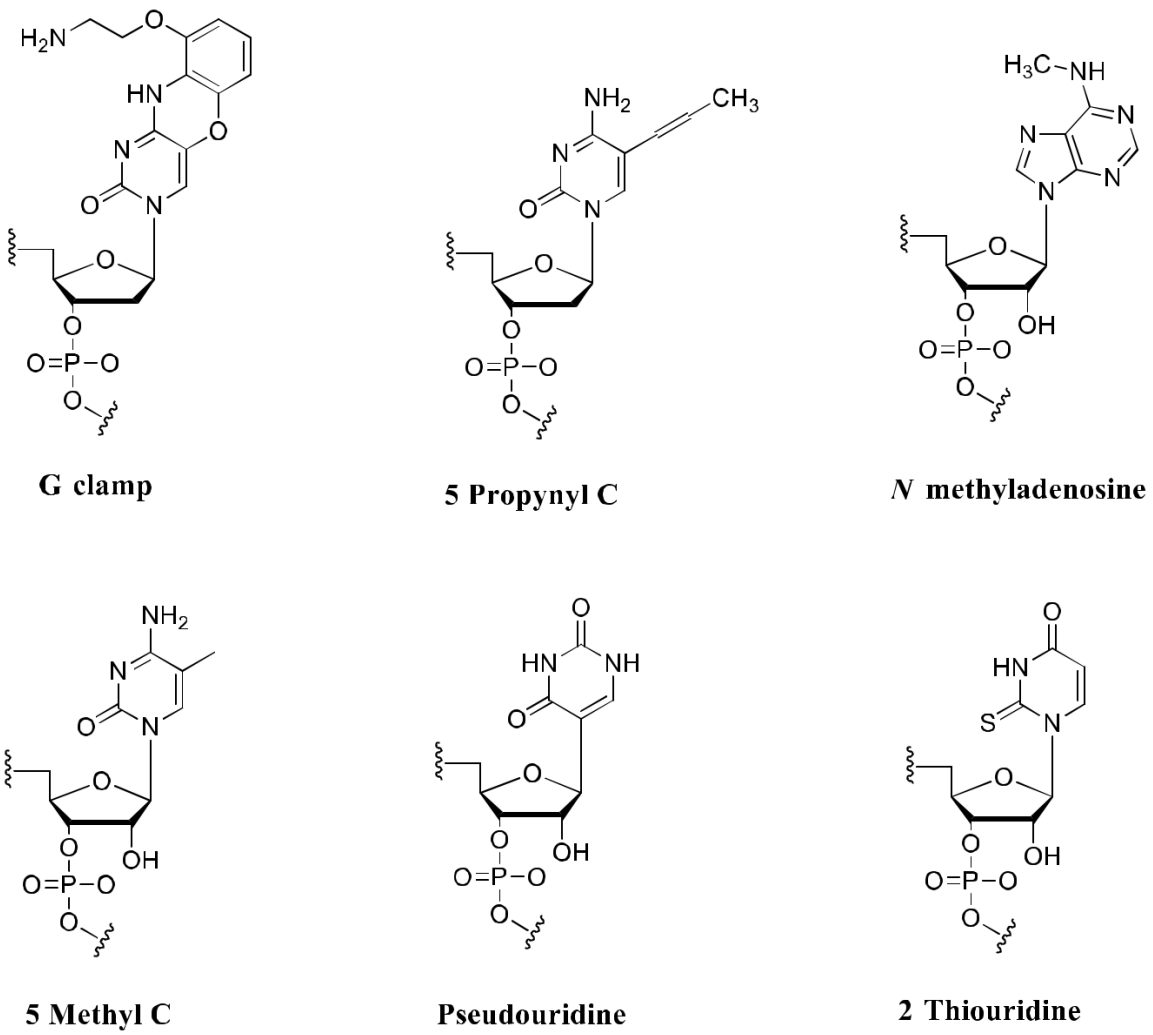

Figure 1-4 Base Modifications

1.2.4 Chemically Caged Nucleic Acids

The caged oligonucleotides composed of two main parts: nucleic acid moiety and a responsive unit (a synthetic moeity). Caged nucleic acid are chemically design for the conjugation into three different parts: nucleobase, ribose and phosphate group[55].

1. Introduction of a responsive unit at the nucleobase

Many research have developed the photocaged nucleobase[56]. Moreover, photocaged nucleobase oligonucleotides have been commonly used for the commercially available. Nucleobase caging can disrupt base paring or enzyme recognition by changing hydrogen donor acceptor platforms. Most of nucleobases modification are pre-synthetic modification. Common photocaged nucleobases group are shown in **Figure 1-5.**

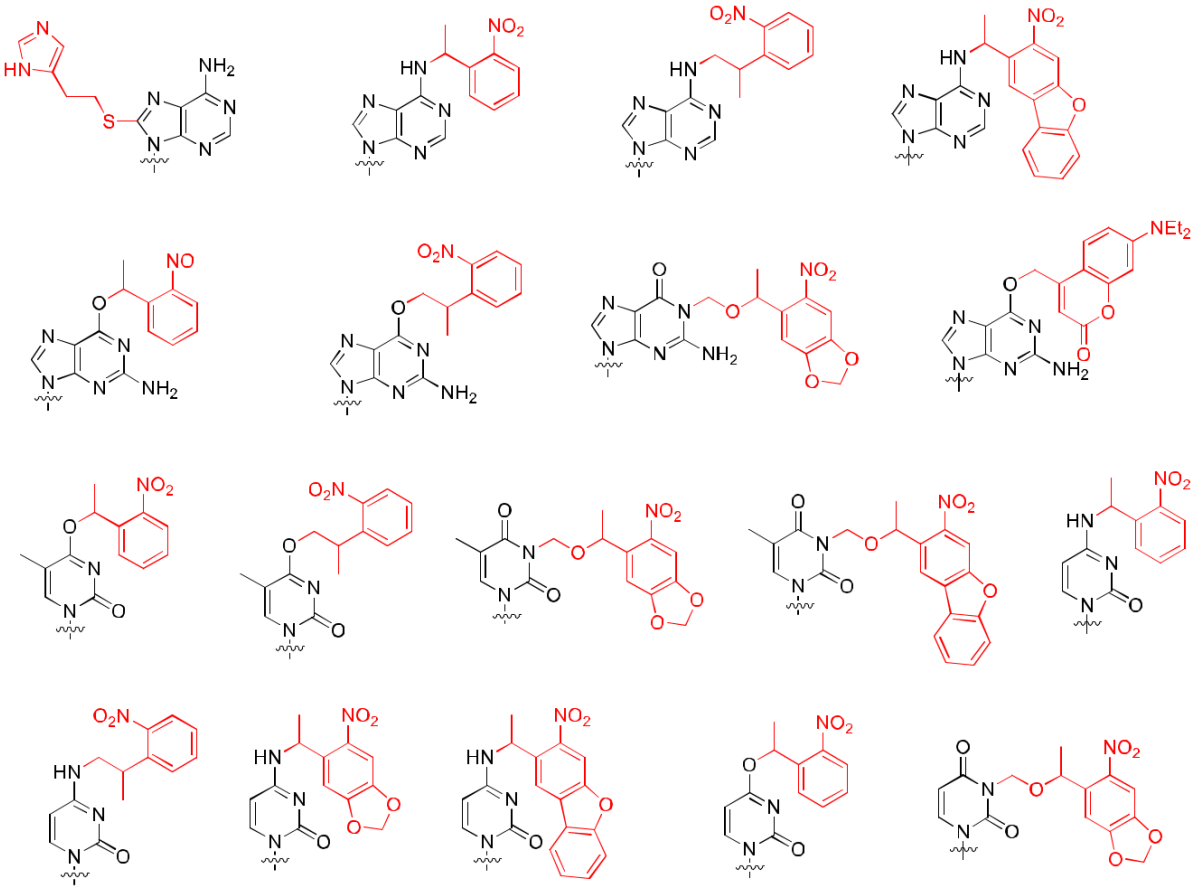

Figure 1-5 Chemical structures of photocaged nucleobases incorporated with oligonucleotides. The light-removable caging groups are shown in red.

However, the limitation of chemically caged nucleobases have been reported. In recent research, O^6-(2,2,2,-trichloroethyl)-modified guanosine (**Figure 1-6 (a)**) was synthesized and introduced to RNA. It was considered that zinc dust can eliminate the trichloroethyl group from the guanosie base [57]. 4-azidobenzyl group bearing guanine have been developed at O^6-position (G^{AB}) (**Figure 1-6 (b)**). It was applied as a protective group of DNA analogues and removed into a phosphine derivatives [58]. O^6-(4-nitrobenzyl)-modified guanosine (G^{NB}) incorporated with G-quadruplex-forming DNA have been developed (**Figure 1-6 (c)**). Chemical and enzymatic removal were demonstrated to trigger G-quadurplex formation[59]. O4-(4-nitrobenzyl)-modified thymine (T^{NB}) have been developed introduced into DNA (**Figure 1-6 (d)**). The investigation of the DNA duplex stability were confirmed before and after reduction treatment[60].

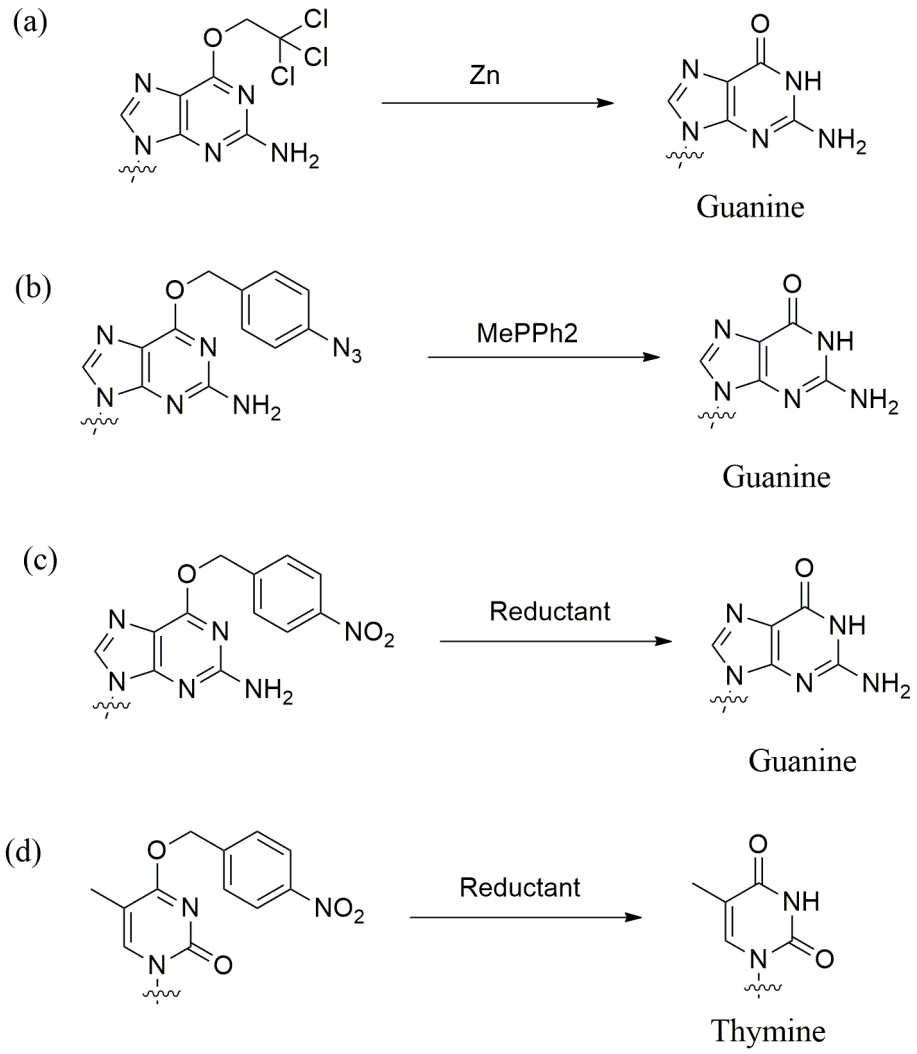

Figure 1-6 Introduction of a responsive unit at the nucleobase

2. Introduction of a responsive unit at the ribose

The biological activities of RNA are controlled by 2'-position of ribose ring. The caged units of 2'-postion are available only for RNA. General method were described as the preparation of RNA can be modified in a reversible manners using caging strategy owing to hydrogen-bonding properties[61]. Nitro-benzyl ether bearing the 2'-positon (**Figure 1-7 (a)**) were incorporated with RNAs by chemical synthesis. The modified can RNAs can be removed by photolysis using a laser or xenon lamp. The disulfide bridge at the 2'-position of prodrug mRNAs were developed (**Figure 1-7 (b)**) [62]. The disulfide bridge can be eliminated under reducing environment or glutathione (GSH). Azide-substituted was acylated 2'-OH of RNA strands in an aqueous buffer. The cloaked RNAs can blocked the hybridization of the complementary oligonucleotides. The treatment of water-soluble phosphine triggers under a Staudinger reduction can spontaneous loss of acyl groups (**Figure 1-7 (c)**) [63]. Methyldithomethyl group were synthesized and removed under the intracellular reducing environments (**Figure 1-7 (d)**) [64]. Additionally, 2,2-dimethyl-2-(2-nitrophenyl)acetyl group was introduced to ribose sugar (**Figure 1-7 (e)**) [65] can be removed when adding the iron powders reducing ammonium chloride.

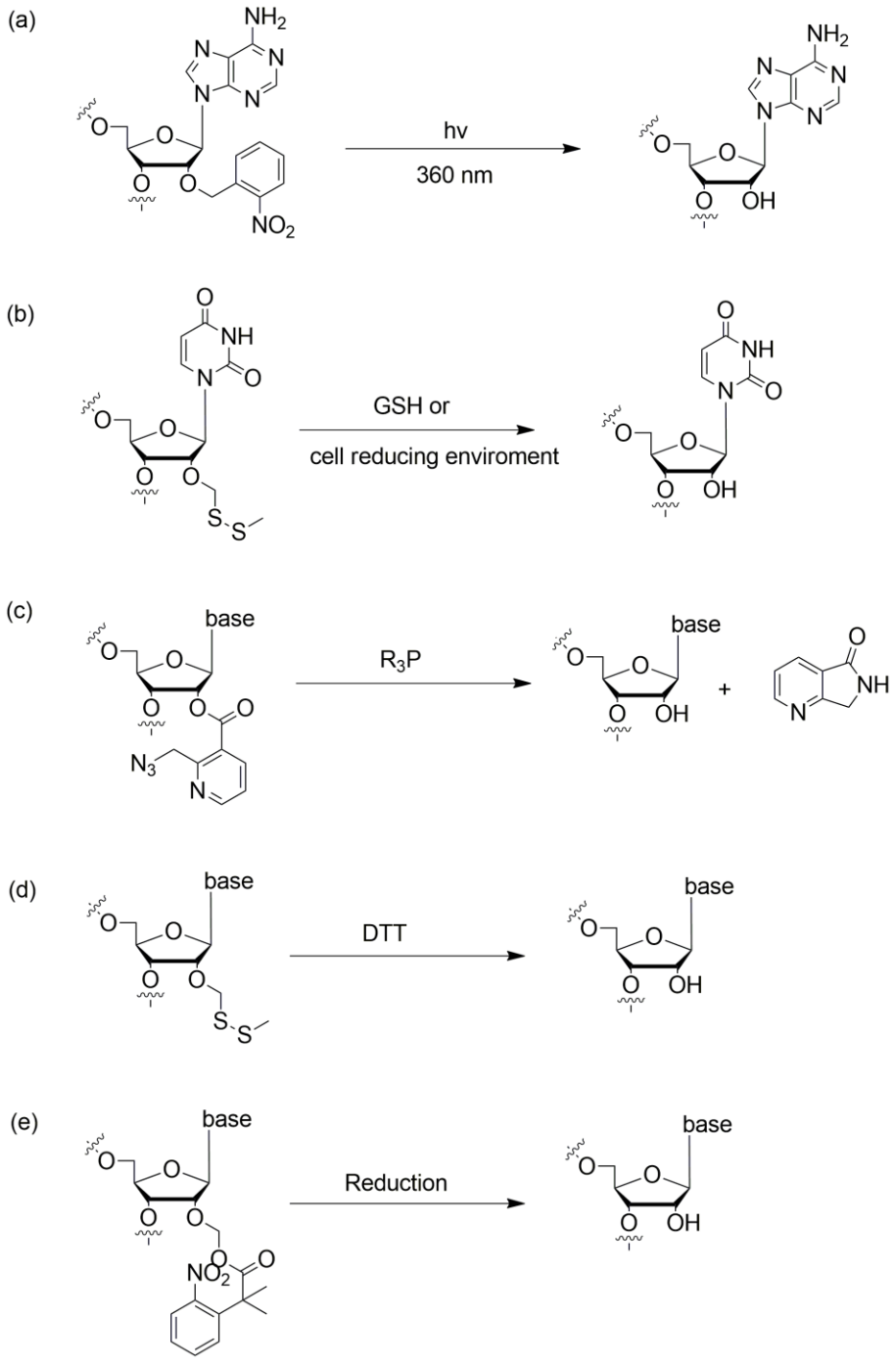

Figure 1-7 Introduction of a responsive unit at the ribose

3. Introduction of a responsive unit at the phosphate diester group

The polyanionic properties of phosphate group of oligonucleotides are major factor that interrupt the gene transfer into the hydrophobic biomembranes of target cells. Phophate caged oligonucleotides can enhance cellular uptake by the reduction anionic charge of oligonucleotides. Pioneering research has been developed neutral phosphate moeity bearing oligonucleotides to remove the polyanionic on phosphate group[66]. 6-bromo-4-dizomethyl-7-hydroxycoumarins (Bhc-diazo) were developed by forming a covalent bond with phosphate moiety on the backbond of mRNA (**Figure 1-8 (a)** [67]. The binding of 6-bromo-7-hydroxycoumarin-4-ylmethyl (Bhc) group and phosphate moieties were approximately 30 moieties on internucleotide linkages of RNA sequence. Moreover, Bhc-caged mRNA can be uncage using photolysis under long-wave ultraviolet light (350-365 nm). The enzyme cleavage units were introduced to the phosphate diester linkages resulting delivery of RNA into living cells (**Figure 1-8(b)**) without any transfection reagents[68]. It was demonstrated that ligand groups can improve the penetration of the cells and incorporated into the target sites. Additionally, the phosphate trimester groups of RNA duplex were transformed into the phosphate diester groups by cytosolic enzymes, then release RNA of target through RNAi pathway. The reduction-responsive groups can be treated and release the desired nucleic acids under hypoxia conditions (**Figure 1-8 (c)**) [69]. Additionally, cell permeable oligonucleotides bearing reduction-activated groups were developed as pro-oligonucleotides. The oligonucleotides were prepare by solid-phase DNA synthesis. The cleavage of the reductive group could be hydrolyzed by nitroreductase and NADH (**Figure 1-8 (d)**) [70].

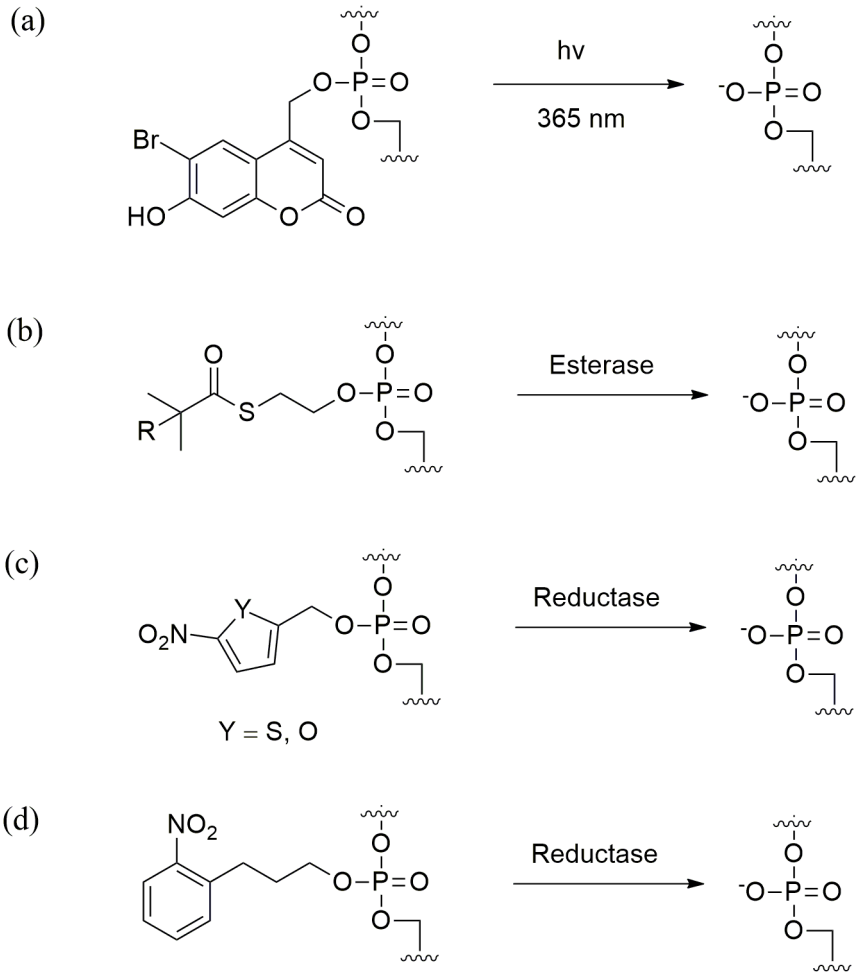

Figure 1-8 Introduction of a responsive unit at the phosphate diester group

1.2 Objectives of this thesis

The aim of this thesis is to develop a versatile strategy for the construction of prodrugs of oligonucleotides, which involves the conversion of a hydrophilic oligonucleotides into a lipophilic and less ionic oligonucleotide conjugates. It would be cell-membrane-permeable and bioreversible. The key point of this research is to develop a highly specific and efficient caging reaction for oligonucleotides strands. Based on the introduction above, the application of oligonucleotides as therapeutic agents has been limited due to poor bioavailability and cellular penetration. The physicochemical properties of cell membranes are the barriers of the oligonucleotides delivery into the cells. The polyanionic and hydrophilic properties of oligonucleotides are the major factors that prevent the passive diffusion to the cells. Thus, the development of the efficient delivery of oligonucleotides to a specific target site is highly required for the therapeutic application. In this doctor thesis, I've tried to provide the best functional group design for DNA strands and perform cellular uptake in the HeLa cells. Moreover, enzyme deprotection of the functional group were proceeded. Briefly, the objectives of this study include: i) develop safe functional group conjugated oligonucleotides strands to facilitate the cellular uptake of oligonucleotides; ii) monitor cellular uptake experiment of functional group conjugated oligonucleotides in HeLa cells and iii) perform enzyme deprotection of the functional group conjugated oligonucleotides to release the naked oligonucleotides.

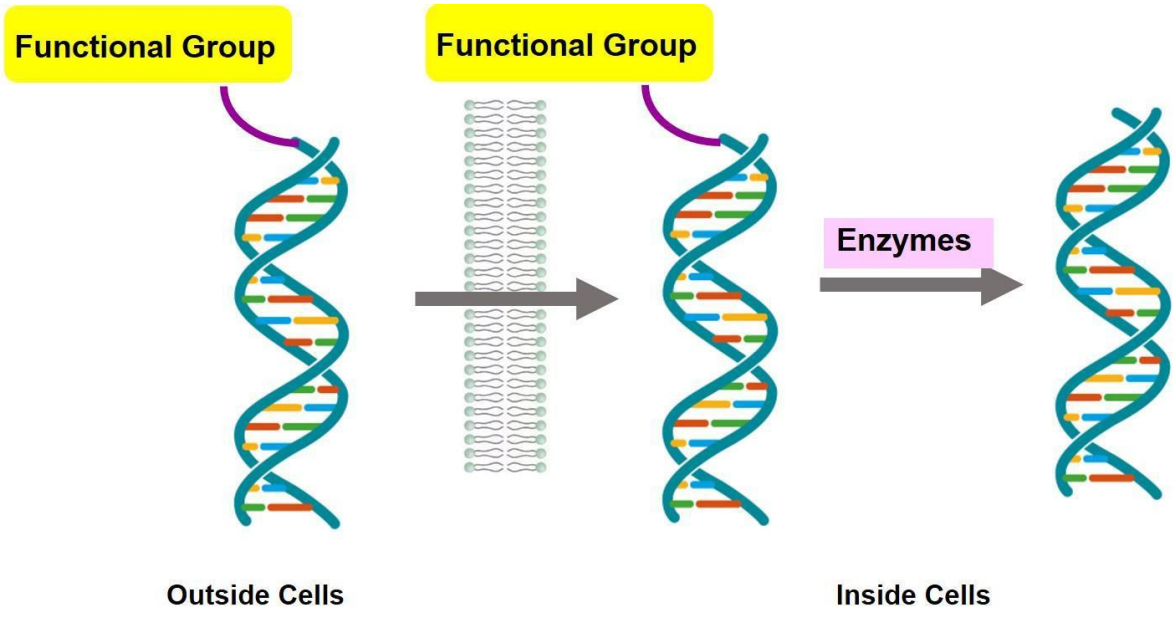

Figure 1-9 Cell permeation and bioreversible reaction of pro-oligonucleotides

1.3 Reference

1. Rozema D.B., The Chemistry of Oligonucleotides, Annual Reports in Medicinal Chemistry. 2017, 50, 17-59.
2. Patil S.D., Rhodes D.G., and Burgess D.J., DNA-based Therapeutics and DNA Delivery Systems: A Comprehensive Review. The AAPS Journal. 2005, 7 (1), E61-E77.

3. LV, H., Zhang, S., Wang, B., Cui, S., and Yan, J., Toxicity of Cationic Lipids and Cationic Polymers in Gene Delivery, Journal of Controlled Release, 2006, 14: 100-109.

4. Debart, F., Abes, S., Deglane, G., Moulton H.M., Clair, P., Gait., M.J., Vasseur, J., and Lebleu, B., Chemical Modifications to Improve the Cellular Uptake of Oligonucleotides, Current Topics in Medicinal Chemistry, 2007, 7: 727-737.

5 Lukashev, A.N., and Zamyatnin, A.A., Viral Vectors for Gene Therapy: Current State and Clinical Perspectives, Biochemistry, 2016, 81: 700-708.

6. Mah, C., Byrne, B.J., and Flotte, T.R., Virus-based Gene Delivery Systems, Clinical Pharmacokinetics, 2004, 41: 901-911.

7. Lotze, M.T., and Kost, T.A., Viruses as Gene Delivery Vectors: Application to Gene Function, Target Validation, and Assay Development, Cancer Gene Therapy, 2002:692-699.

8. Kamiya, H., Tsuchiya, H., Yamazaki, J., and Harashima, H., Intracellular Trafficking and Transgene Expression of Viral and Non-viral Gene Vectors, Advanced Drug Delivery Reviews, 2001, 52: 153-164.

9. McTaggart, S., and Al-Rubeai, M., Retroviral Vectors for Human Gene Delivery, Biotechnology Advances, 2002, 20: 1-31.

10. Galimi, F., and Verma, I.M., Opportunities for the Use of Lentiviral Vectors in Human Gene Therapy, Current Topics in Microbiology and Immunology, 2002, 261: 245-254.

11. Martin, K.R., Klein, R.L., and Quigley, H.A., Gene Delivery to the Eye Using Adeno-Associated Viral Vectors, Methods, 2002, 28: 267-275.

12. Lien, Y-H.H., and Lai, L-W., Gene Therapy for Renal Disorders: What Are the Benefits for the Elderly? Drugs and Aging, 2002, 19: 553–560.

13. Chamberlain, J.S., Gene Therapy of Muscular Dystrophy, Human Molecular Genetics, 2002, 11: 2355–2362.

14. Wolf, J.K., and Jenkins, A.D., Gene Therapy for Ovarian Cancer (Review), International Journal of Oncology, 2002, 21: 461–468.

15. Walther, W., and Stein, U., Viral Vectors for Gene Transfer: A Review of Their Use in the Treatment of Human Diseases. Drugs, 2000, 60: 249–271.

16. Garton, K.J., Ferri, N., and Raines, E.W., Efficient Expression of Exogenous Genes in Primary Vascular Cells using IRES-based Retroviral Vectors, BioTechaniques, 2002, 32: 830–843.

17. Heider, H., Verca, S.B., Rusconi, S., and Asmis, R., Comparison of Lipid-Mediated and Adenoviral Gene Transfer in Human Monocyte-Derived Macrophages and COS-7 Cells, BioTechaniques, 2000, 28: 260–270.

18. Kay, M.A., Glorioso, J.C., and Naldini, L., Viral Vectors for Gene therapy: the Art of Turning Infectious Agents into Vehicles of Therapeutics, Natural Medicine, 2001, 7: 33-40.

19. Favre, D., Provost, N., Blouin, V., Blancho, G., Cherel, Y., Salvetti, A., and Moullier, P., Immediate and Long-term Safety of Recombinant Adeno-associated Virus Injection into the Nonhuman Primate Muscle. Molecular Therapy, 2001, 4: 559–566.

20. Timme, T.L., Hall, S.J., Barrios, R., Woo, S,L., Aguilar-Cordova, E., and Thompson, T.C., Local Inflammatory Response and Vector Spread After Direct Intraprostatic Injection of a Recombinant Adenovirus Containing the Herpes Simplex Virus Thymidine Kinase Gene and Ganciclovir Therapy in Mice. Cancer Gene Therapy, 1998, 5:74–82.

21. Raper, S.E., Chirmule, N., Lee, F.S., Wivel, N.A., Bagg, A., Gao, G-P., Wilson, J.M., Batshaw, M.L., Fatal Systemic Inflammatory Response Syndrome in a Ornithine Transcarbamylase Deficient Patient Following Adenoviral Gene Transfer. Molecular Genetics and Metabolism, 2003, 80:148–158.

22. Owens, R.A., Second Generation Adeno-Associated Virus type 2-Based Gene Therapy Systems with the Potential for Preferential Integration into AAVSI. Current Gene Therapy, 2002, 2: 145–159.

23. Nyberg-Hoffman, C., and Aguilar-Cordova, E., Instability of Adenoviral Vectors during Transport and its Implication for Clinical Studies, Natural Medicine, 1999, 5: 955–957.

24. Cao, B., Mytinger, J.R., and Huard, J., Adenovirus Mediated Gene Transfer to Skeletal Muscle. Microscopy Research and Techniques, 2002, 58: 45–51.

25. Al-Dosari, M.S., and Gao, X., Non-viral Gene Delivery: Principle, Limitations and Recent Progress. The AAPS Journal, 2009, 11: 671–681.

26. Li, S.D., and Huang, S.L., Gene Therapy Progress and Prospects; Decade Strategy, Gene Therapy, 2006, 13: 1313–1319.

27. Newman, C.M., and Bettinger, T., Gene Therapy Progress and Prospects: Ultrasound for Gene Transfer, Gene therapy, 2007, 14: 465–475.

28. Li, S.D., and Huang, L., Non-viral is Superior to Viral Gene Delivery, Journal of Control Release, 2007, 123: 181–183.

29. Herweiger, H., and Wolff, J.A., Progress and Prospects: Hydrodynamic Gene Delivery, Gene Therapy, 2006, 14: 99–107.

30. Dabson, J., Gene Therapy Progress and Prospects; Magnetic Nanoparticle based Gene Delivery, Gene Therapy, 2006, 13: 283–287.

31. Nayerossadat, N., Maedeh, T., and Ali, P.A., Viral and Nonviral Delivery Systems for Gene Delivery, Advanced Biomedical Research, 2012, 1: 1-19.

32. Al-Dosari, M.S., and Gao, X., Non-viral Gene Delivery: Principle, Limitations and Recent Progress. The American Association of Pharmaceutical Scientists, 2009, 11: 671–681.

33. Simoes, S., Filipe, A., Faneca, H., Mano, M., Penacho, N., Duzgunes, N., and de Lima, M.P., Cationic Liposomes for Gene Delivery. Expert Opinion on Drug Delivery, 2005, 2: 237-254.

34. Yang, G., Multifional Non-viral Delivery Systems Based on Conjugated Polymers, Macromolecular Bioscience, 2012, 12: 1600-1614.

35. Dufes, C., Uchegbu, L.F., and Schatzlein, A.G., Dendrimers in Gene Delivery. Advanced Drug Delivery Reviews, 2005, 57: 2177-2202.

36. Chen, X., Dudgeon, N., Shen, L., and Wang, J.H., Chemical modification of gene silencing oligonucleotides for drug discovery and development. Drug Discovery Today, 2005, 10: 587–593.

37. Braasch, D.A., Paroo, Z., Constantinescu, A., Ren, G., Oz, O.K., Mason, R.P., Corey, D.R., Biodistribution of phosphodiester and phosphorothioate siRNA. Bioorganic Medicinal Chemistry Letters, 2004, 14: 1139–1143.

38. Soutschek, J., Akinc, A., Bramlage, B., Charisse, K., Constien, R., Donoghue, M., Elbashir, S., and Vornlocher, H.P., Therapeutic silencing of an endogenous gene by systemic administration of modified siRNAs. Nature, 2004, 432: 173–178.

39. Marshall, W. S., and Caruthers, M. H., Phosphorodithioate DNA as a potential therapeutic drug. Science. 1993, 259: 1564–1570.

40. Summerton, J., and Weller, D., Morpholino antisense oligomers: design, preparation, and properties. Antisense and Nucleic Acid Drug Development, 1997, 7: 187–195.

41. Nielsen, P. E., Egholm, M., Berg, R. H., and Buchardt, O., Sequence-selective recognition of DNA by strand displacement with a thymine-substituted polyamide. Science, 1991, 254: 1497–1500.

42. Meade, B. R., Gogoi, K., Hamil, A. S., Palm-Apergi, C., van den Berg, A., Hagopian, J. C., Springer, A. D., Eguchi, A., Kacsinta, A. D., Dowdy, C. F., Presente, A., Lonn, P., Kaulich, M., Yoshioka, N., Gros, E., Cui, X. S., and Dowdy, S. F., Efficient delivery of RNAi prodrugs containing reversible charge neutralizing phosphotriester backbone modifications. Nature Biotechnology, 2014, 32: 1256–1261.

43. Miller, P. S., McParland, K. B., Jayaraman, K., and Ts'o, P. O., Biochemical and biological effects of nonionic nucleic Acid methylphosphonates, Biochemistry, 1981, 20: 1874–1880.

44. Lam, J.K., Chow, M.Y., Zhang, Y., and Leung, S.W, siRNA versus miRNA as therapeutics for gene silencing. Molecular Therapy Nucleic Acids, 2015, 4: e252.

45. Inoue, H., Hayase, Y., Imura, A., Iwai, S., Miura, K., Ohtsuka, E., Synthesis and hybridization studies on two complementary nona(2'-O-methyl)ribonucleotides. Nucleic Acids Research, 1987, 15: 6131–6148.

46. Baker, B. F., Lot, S. S., Condon, T. P., Cheng-Flournoy, S., Lesnik, E. A., Sasmor, H. M., and Bennett, C. F., 2'-O-(2-Methoxy)ethyl-modified anti-intercellular adhesion molecule 1 (ICAM-1) oligonucleotides selectively increase the ICAM-1 mRNA level and inhibit formation of the ICAM-1 translation initiation complex in human umbilical vein endothelial cells, Journal of Biological Chemistry, 1997, 272: 11994–12000.

47. Pieken, W. A., Olsen, D. B., Benseler, F., Aurup, H., and Eckstein, F., Kinetic characterization of rbonuclease-resistant 2'-modified hammerhead ribozymes, Science, 1991, 253: 314–317.

48. Kawasaki, A. M., Casper, M. D., Freier, S. M., Lesnik, E. A., Zounes, M. C., Cummins, L. L., Gonzalez, C., and Cook, P. D., Uniformly modified 2'-deoxy-2'-fluoro phosphorothioate oligonucleotides as nuclease-resistant antisense compounds with high affinity and specificity for RNA targets, Journal of Medicinal Chemistry, 1993, 36: 831–841.

49. Braasch, D. A., Jensen, S., Liu, Y., Kaur, K., Arar, K., White, M. A., and Corey, D. R., RNA interference in mammalian cells by chemically-modified RNA. Biochemistry, 2003, 42: 7967–7975.

50. Flanagan, W. M., Wolf, J. J., Olson, P., Grant, D., Lin, K. Y., Wagner, R. W., and Matteucci, M. D., A cytosine analog that confers enhanced potency to antisense oligonucleotides, Proceeding of the National Academy of Sciences of the United States of America, 1999, 96: 3513–3518.

51. Shen, L., Siwkowski, A., Wancewicz, E. V., Lesnik, E., Butler, M., Witchell, D., Vasquez, G., Ross, B., Acevedo, O., Inamati, G., Sasmor, H., Manoharan, M., and Monia, B. P., Evaluation of C-5 propynyl pyrimidine-containing oligonucleotides in vitro and in vivo, Antisense and Nucleic Acid Drug Development, 2003, 13: 129–142.

52. Kariko´, K., Muramatsu, H., Welsh, F. A., Ludwig, J., Kato, H., Akira, S., and Weissman, D., Incorporation of pseudouridine into mRNA yields superior nonimmunogenic vector with increased translational capacity and biological stability, Molecular Therapy, 2008, 16: 1833–1840.

53. Anderson, B. R., Muramatsu, H., Jha, B. K., Silverman, R. H., Weissman, D., and Kariko´, K., Nucleoside modifications in RNA limit activation of 2'-5'-oligoadenylate synthetase and increase resistance to cleavage by RNase L. Nucleic Acids Research, 2011, 39: 9329–9338.

54. Kormann, M. S., Hasenpusch, G., Aneja, M. K., Nica, G., Flemmer, A. W., HerberJonat, S., Huppmann, M., Mays, L. E., Illenyi, M., Schams, A., Griese, M., Bittmann, I., Handgretinger, R., Hartl, D., Rosenecker, J., and Rudolph, C., Expression of therapeutic proteins after delivery of chemically modified mRNA in mice, Nature Biotechnology, 2011, 29: 154–157.

55. Ikeda, M., and Kabumoto, M., Chemically caged nucleic acids, Chemistry Letters, 2017, 46: 634-640.

56. Liu, Q., and Deiters, A., Optochemical control of deoxyoligonucleotide function via a nucleobase-caging approach, Account of Chemical Research, 2014, 47: 45-55.

57. Hobartner, C., Mittendorfer, H., Breuker, K., and Micura, R., Triggering of RNA secondary structures by a functionalized nucleobase, Angewandte Chemie International Edition, 2003, 43: 3922-3925.

58. Kawanka, T., Shimizu, M., Shintani, N., and Wada, T., Solid-phase synthesis of backbone-modified DNA analogs by the boranophosphotriester method using new protecting groups for nucleobases, Bioorganic and Medicinal Chemistry Letters, 2008, 18: 3783-3786.

59. Ikeda, M., Kamimura, M., Hayakawa, Y., Shibata, A., and Kitade, Y., Reduction-responsive guanine incorporated into G-quadruplex-forming DNA, Chembiochem Communcations, 2016, 17:1304-1307.

60. Saneyoshi, H., Hiyoshi, Y., Iketani, K., Kondo, K., and Ono, A., Bioreductive deprotection of 4-nitrobenzyl group on thymine base in oligonucleotides for the activation of duplex, Bioorganic and Medicianl Chemistry Letter, 2015, 25: 5632-5635.

61. Chaulk, S.G., and MacMillan, A.M., Synthesis of oligo-RNAs with photocaged adenosine 2'-hydroxyls, Nature Protocols, 2007, 2, 1052-1058.

62. Debart, F., Dupouy, C., and Vasseur, J., Stimuli-responsive oligonucleotides in prodrug-based approaches for gene silencing, Beilstein Journal of Organic Chemistry, 2018, 14, 436-469.

63. Kadina, A., Kietrys, A.M., and Kool, E.T., RNA clocking by reversible acylation, Angewandie Chemie Communications, 2018, 57: 3059-3063.

64. Ochi, Y., Nakagawa, O., Sakaguchi, K., Wada, S., and Urata, H., Post-synthetic approach for the synthesis of 2'-O-methyldithiomethyl-modified oligonucleotides responsive to a reducing environment, Chemical Communications, 2013, 49: 7620-7622.

65. Chen, K., Wang, W., Qu, D., Zhao, H., Xiong, W., Luo, C., Yin, M., and Zhang, B., 2'-O-{[2,2-dimethyl-2-(2-nitrophenyl) acetyl] oxy} methyl protecting group for RNA synthesis, Tetrahedron Letters, 2013, 54: 4281-4284.

66. Miller, P.S., Barrett, J.C., and Ts'O, P.O., Synthesis of oligodeoxyribonucleotide ethyl phosphotriesters and their specific complex formation with transfer ribonucleic acid, Biochemistry, 1974, 13: 4887-4896.

67. Ando, H., Furuta, T., Tsien, R.Y., and Okamoto, H., Photo-mediated gene activation using caged RNA/DNA in zebrafish embryos, Nature Genetics, 2001, 28: 317-325.

68. Meade, B.R., Gogoi, K., Hamil, A., Apergi, C.P., Berg, A., Hagopian, J., Springer, A.D., Eguchi, A., Kacsinta, A.D., Dowdy, C.F, Presente, A., Lonn, P., Kaulich, M., Yoshioka, N., Gros, E., Cui, X., and Dowdy, S.F., Efficient delivery of rNAi prodrugs containing reversible charge-neutralizing phosphotriester backbone modifications, Nature Biotechnology, 2014, 32, 1256-1263.

69. Zhange, N., Tan, C., Cai, P., Zhang, P., Zhao, Y., and Jiang, Y., The design, synthesis and evaluation of hypoxia-activated pro-oligonucleotides, Chemical Communications, 2009: 3216-3218.

70. Saneyoshi, H., Iketani, K., Kondo, K., Saneyoshi, T., Okamoto, I., and Ono, A., Synthesis and characterization of cell-permeable oligonucleotides bearing reduction-activated protecting groups on the internucleotide linkages, Bioconjugate Chemistry, 2016, 27: 2149-2156.

Chapter 2

Polyunsaturated fatty acids conjugated oligonucleotides

2.1 Abstract

Oligonucleotide delivery has an essential role in oligonucleotide therapeutics according to their poor bioavailability and cellular penetration. Herein, we have developed the postsynthetic DNA modification via direct conjugation of polyunsaturated fatty acids with oligonucleotides. Linolenate-protecting oligonucleotides showed the best cellular uptake into HeLa cells among the oligonucleotides protected by several polyunsaturated fatty acids. FRET assay of polyunsaturated fatty acids showed the unstable of polyunsaturated fatty acids micelles that indicated the partition of polyunsaturated fatty acids conjugated oligonucleotides into the cell membranes. Linolenate was removed from oligonucleotides by ester cleavage with esterase to give the unprotected oligonucleotides. Moreover, there were no cytotoxicity of linolenate conjugated oligonucleotides on HeLa Cells. Direct protection of nucleic acids by linolenate drastically facilitates the cellular penetration of nucleic acids and subsequent esterase digestion reproduces the original nucleic acids to work in cells.

2.2 Introduction

The therapeutic use of oligonucleotides has gained a lot of attention. The high specificity of oligonucleotides covering a wide range of biomedical applications allows the inhibition of target proteins that are not easily accessed and modulated by conventional small molecule or protein drugs[1-3]. A key challenge in realizing the full potential of oligonucleotides do not cross the intact cell membranes to any significant degree via simple diffusion. This is primarily due to the highly hydrophilic and anionic character of these molecules, which have poor affinity for the negatively charged cell membranes. Thus, development of efficient delivery systems is one of the most challenging hurdles to turn oligonucleotides into clinically acceptable therapeutic drugs. Therefore, various delivery systems have been developed for the oligonucleotides delivery including viral vectors and nonviral vectors delivery systems. However, genotoxicity of viral vectors delivery systems have been investigated due to immunogenicity and possible recombination of oncogenes[4]. On the other hand, most of nonviral vectors composed from polycationic lipids or liposomes have been well- documented of cytotoxicity.[5] Thus, the use of neutral lipid-oligonucleotide conjugates have become an outstanding interest to improve the safe delivery of oligonucleotides and enhance their pharmacokinetic behavior of transmembrane delivery[6].

The synthetic approaches of lipid-oligonucleotide conjugates are separated into 2 major categories: the postsynthetic conjugation approach (or solution-phase approach) and the presynthetic conjugation approach (or stepwise solid-phase synthesis approach)[6]. According to the postsynthetic conjugation approach, the oligonucleotides is equipped with an appropriate functionality, to which the lipid moiety is coupled in solution after release and purification of the oligonucleotides. When using stepwise solid-phase approach, the lipid-oligonucleotide conjugates is prepared on a single support by assembling the conjugate group (i.e., lipophilic group) by a stepwise process prior to or after oligonucleotides synthesis and using suitable protecting groups or/and functional moieties which minimize side reactions. Conjugation strategies of lipid conjugated oligonucleotides are summarized in **Table 2-1**.

According to the **Table 2-1**, recent work in the area of neutral lipid-oligonucleotides conjugates has been used different types of cholesterol-conjugated oligonucleotides to elucidate the requirements for oligonucleotides delivery. However, cholesterol may be linked with cardiovascular events via intravenous administration[7]. In this concept, polyunsaturated fatty acids are safe and naturally essential neutral lipids that play crucial roles in cell growth[8]. Previous studies were proven that polyunsaturated fatty acids conjugates of clinical anticancer drugs have provided significant advances in improving drug's pharmacokinetics and efficacy[9-11]. We propose that polyunsaturated fatty acids conjugate such as linolenic acid, linoleic acid and oleic acid will be able to deliver oligonucleotides into the cells.

Table 2-1 Summary of Strategies Used for the Synthesis of Lipid-Oligonucleotide Conjugates[6]

Oligonucleotides Conjugates	Site of conjugation on the oligonucleotides	Linker or Functional Group	Conjugate Chemistry	Target siRNA
Cholesterol-siRNA[12]	3'-end of sense strand	Cholesterol-aminocaproic acid-4-hydroxyproline linker	Solid-phase synthesis (phosphoramidite)	Apo-B-1 siRNA
Cholesterol-siRNA[13]	5'-end of sense strand	Cholesterol phosphoramidite coupled to (CH_2-S-S-$(CH_2)_6$ linker	Solid-phase synthesis (phosphoramidite)	p38 MAP kinase siRNA
Squalene-siRNA[7]	3'-end of sense strand	Maleimide modified squalene acid	Postsynthesis conjugation (Michael addition)	RET/PTC 1siRNA
α-tocopherol-siRNA[14]	5'-end of antisense strand	R-tocopherol phosphoramidite	Solid-phase synthesis (phosphoramidite)	Apo-B-1 siRNA
Lipid-and steroid-siRNA[15]	3'-end	Not specified	Solid-phase synthesis (phosphoramidite)	Apo-B-1 siRNA
Lipid- and cholesteryl siRNA[16]	3'-end of sense strand	Not specified	Solid-phase synthesis (phosphoramidite)	Apo-B-1 siRNA

2.3 Results and Discussion

Rationale

Acyloxyalkyl ester is one of the most commonly prodrugs types for phosphonates. Enzymatic cleavage of the carbonate ester generates a transient hydroxymethyl intermediate, which rapidly loses formaldehyde to afford the acyloxyalkyl monoester[17] (**Figure 2-1**).

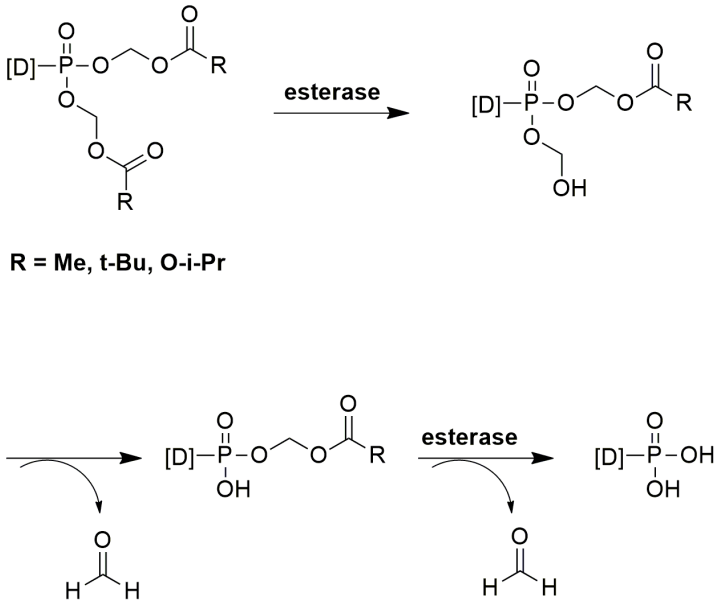

Figure 2-1 Activation of acyloxyalkyl ester prodrugs

Acyloxyl ester can be cleaved by the esterase enzymes, which is the enzyme that responsible for the delivery pharmacologically compounds in the most common prodrug approach. The esterase involved in drug metabolism that mainly localized in the liver. Esterase-activated prodrugs effectively mask polar moieties with a non-polar ester bond, often increasing lipophilicity, thus membrane permeability[18]. The production of formaldehyde as a byproduct generated following cleavage of acyloxyalkyl esters has long been a potential safety concern. However, our cells have defense mechanisms to against the danger from formaldehyde. Firstly, an enzyme coverts the formaldehyde into a less dangerous chemical, called formate, which is a component of one-carbon cycle uses to make the building blocks of life. And secondly, DNA damage caused by formaldehyde can be fixed by DNA repair enzymes[19].

In this study, we focused on development of the conjugation of polyunsaturated fatty acids to the oligonucleotides by postsynthetic modification. According to the previous studies were proven that polyunsaturated fatty acids conjugated anticancer drugs such as DHA-paclitaxel, linoleic acid-paclitaxel and oleic acid-paclitaxel can improve the

therapeutic efficacy of chemotherapy[20]. Moreover, polyunsaturated fatty acids are safe and naturally essential neutral lipids that play crucial roles in cell growth. We proposed that polyunsatured fatty acids conjugates oligonucleotides such as linolenic acid, linoleic acid and oleic acid will be able to deliver oligonucleotides in the cells. The caging reaction has applied from the pivaloyl oxytrimethyl conjugated oligonucleotides that derived from the previous studies showing that the phosphate group of ethyl(hydroxylmethyl)phosphonate can be selectively reacted with acetoxymethyl bromine resulting in acetoxymethyl esters of alkyl or aryl phoaphates that rapidly cleaved intracellularly, they facilitate the delivery of organophosphates into the cytoplasm without puncturing or disruption of the plasma membrane[21].

According to the previous research of Dr.Zhu Hao (former postdoc researcher in okamoto laboratory). Enzyme-labile acetoxymethylgroup was incorporated into a fluoresceinlabelled short model oligonucleotide (TpT-fluo). The caging reaction of TpT-fluo with bromomethyl acetate was conducted in DMF containing DIPEA (**Figure 2-2**). Unfortunately, TpT-fluo barely reacted even in the 3 presence of overwhelmed bromomethyl acetate and DIPEA, probably due to the low reactivity of bromomethyl acetate. We hypothesized that our strategy in which iodomethyl alkyl ester group that more reactivity than bromine can be reacted with the phosphate group on the internucleotide linkages.

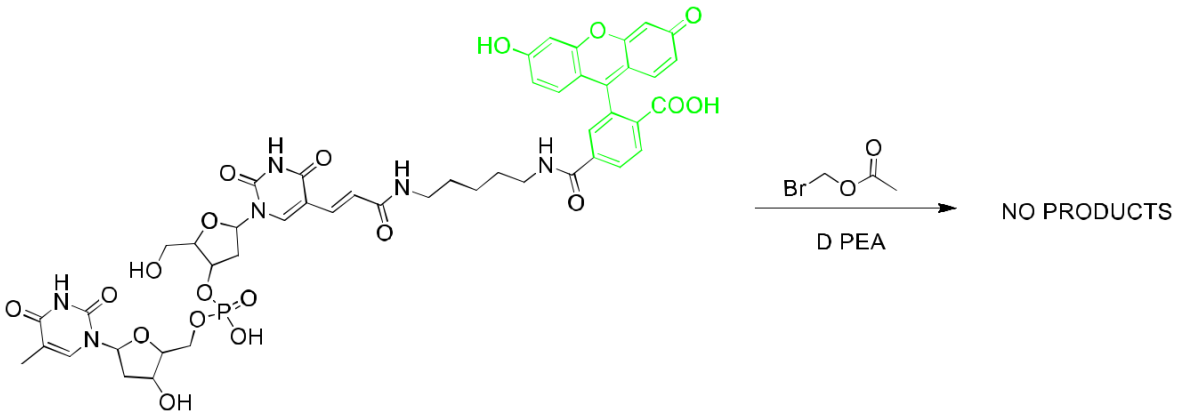

Figure 2-2 Conjugation of TpT-fluo using bromomethyl acetate

Conjugation of thymine dimer (T2) using iodomethyl pivalate

Thymine dimer (T2) was used for the conjugation of pivaloyl oxytrimethyl group. The optimized condition was validated by using silver nitrate (AgNO3) to for silver salt with short oligonucleotides, after that silver salt was achieved by using iodomethyl pivalate with N,N-diisopropylethylamine (DIEA) as a catalyze. The reaction was proceeded at 65ºC for 18 hours. Purification of reaction mixture of the linolenic acid conjugated T2 was subjected to HPLC analysis. The production of the conjugates were confirmed by ESI-MS. The ESI-MS data showed 1 conjugation of pivaloyl oxymethyl with thymine dimer.

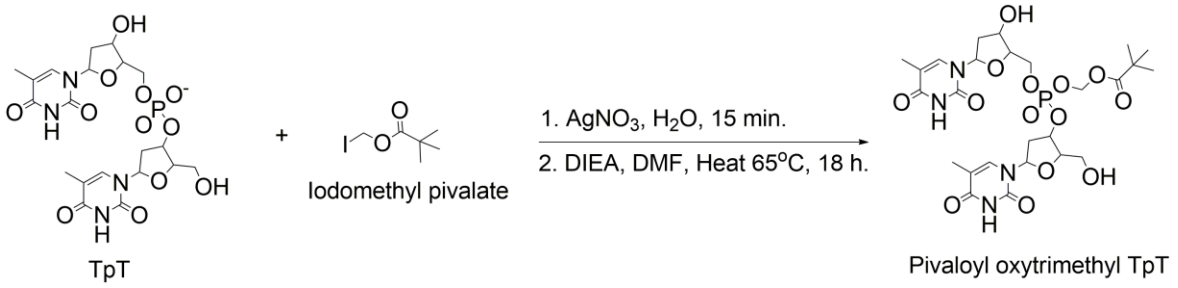

Figure 2-3 Conjugation of pivaloyl oxytrimethyl with thymine dimer (T2)

Conjugation of thymine 3-mer (T3) using iodomethyl pivalate

To confirm the addition of iodomethyl pivalate to the phosphate group and clearify the MS with MALDI-TOF, thymine 3-mer (T3) were applied for the synthesis of iodomethyl pivalate conjugation using the same method as the synthesis of pivaloyl oxymethyl thymine dimer. The MALDI-TOF performed 1 and 2 conjugation of pivaloyl oxymethyl with T3. However, there are many impurities in the obtained fractions that difficult to purify by HPLC.

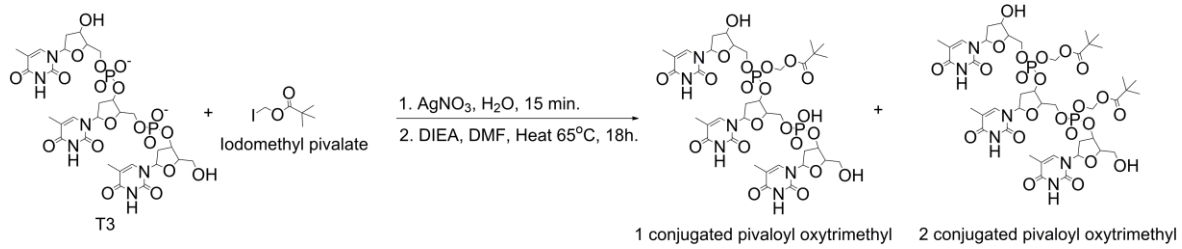

Figure 2-4 Conjugation of pivaloyl oxytrimethyl with thymine 3-mer (T3) by using $AgNO_3$ and iodomethyl pivalate

Thymine 3-mer was applied to synthesize pivaloyl oxytrimethyl thymine 3-mer by using only iodomethyl pivalate and N,N-diisopropylethylamine (DIEA) The reaction mixture was incubated at 40°C for 24 hours. Purification of reaction mixture of the linolenic acid conjugated thymine 3-mer was subjected to HPLC analysis. The production of the conjugates were confirmed by MALDI-TOF. The MALDI-TOF indicated 1 and 2 conjugation of pivaloyl oxymethyl with thymine 3-mer with a pure desired products (**Figure 2-5**).

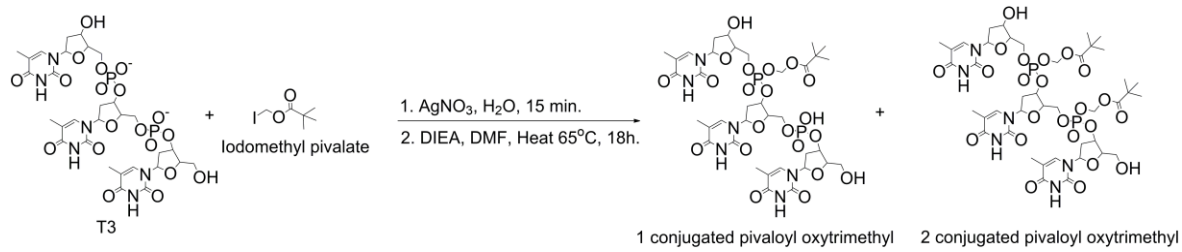

Figure 2-5 Conjugation of pivaloyl oxytrimethyl with thymine 3-mer (T3) by using iodomethyl pivalate

Optimization of the conjugation of thymine 3-mer (T3) using iodomethyl pivalate

The optimized reaction was validated in a variety of the time, solvent, and temperature. Summarize the yield of pivaolyl oxytrimethyl thymine 3-mer were shown in **Table 2-2**. The best condition for the conjugation of pivaloyl oxytrimethyl with nucleic acids is using water and acetronitrile (1:6) as a solvent. The reaction mixture was heated 60^{o}C for 6 hours. 1 and 2 conjugated pivaloyl oxytrimethyl with thymine 3-mer were obtained the highest %yield.

Table 2-2 Summary of the conjugation of thymine 3-mer using Iodomethyl pivalate

Trial No.	Iodomethyl pivalate	DIEA	Solvent	Temerature (°C)	Time (h.)	Yield	
						1 conjugated	2 conjugated
1	500 eq	500 eq	H_2O/MeCN : 1/6	40	24	20%	1%
2	500 eq	500 eq	H_2O/DMF : 1/6	40	24	None	None
3	500 eq	500 eq	MeCN	40	24	None	None
4	500 eq	500 eq	DMF	40	24	None	None
5	500 eq	500 eq	H_2O/MeCN : 1/6	40	12	12%	4%
6	500 eq	500 eq	H_2O/MeCN : 1/6	60	12	13%	9%
7	500 eq	500 eq	H_2O/MeCN : 1/6	80	12	None	None
8	500 eq	500 eq	H_2O/MeCN : 1/6	60	6	22%	10%

Conjugation of poly(dT)sequence (T20) using iodomethyl pivalate

The optimized condition of the conjugation of pivaloyl oxytrimethyl with thymine 3-mer was operated for the conjugation with poly(dT)sequence (T20) that is complementary to the poly(A) tails of mRNA. The MALDI-TOF showed the 7 conjugation of pivaloyl oxytrimethyl groups with T20.

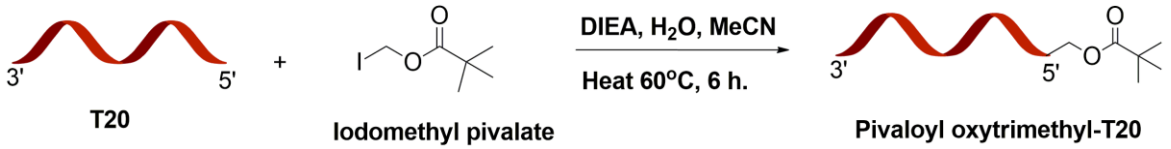

Figure 2-6 Conjugation of pivaloyl oxytrimethyl with poly(dT)sequences by using iodomethyl pivalate

Preparation of iodomethyl alkyl ester of unsaturated fatty acids and retinoic acid

The synthesis of iodomethyl alkyl ester of polyunsaturated fatty acids were synthesized through the two-step transformations according to previous report[22] (**Figure 2-7**). Firstly, the reaction of chlorination at carboxyl group of polyunsaturated fatty acids was employed to form chloromethyl alkyl ester group. Under this condition, chloromethyl chlorosulfate was used as the reagent to obtain the desired chloromethyl alkyl ester of polyunsaturated fatty acids (**2a-c**). Secondly, chloromethyl alkyl ester group were subjected into iodomethyl alkyl ester group. Sodium iodide was treated as the reagent to obtain iodomethyl alkyl ester of polyunsaturated fatty acids (**3a-c**).

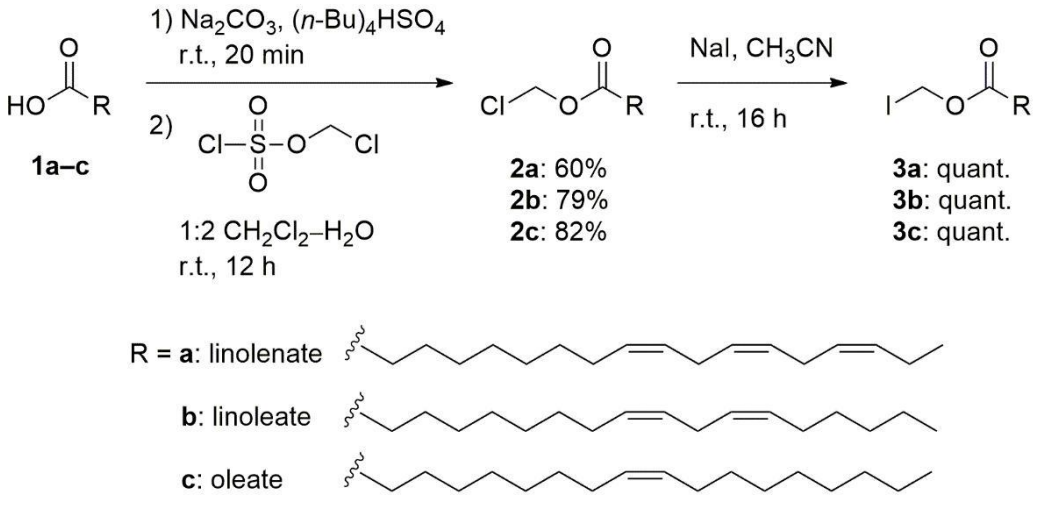

Figure 2-7 Synthesis of iodomethyl alkyl ester of polyunsatured fatty acids

Conjugation of oligonucleotides using iodomethyl alkyl ester of polyunsaturated fatty acids

Conjugated polyunsatured fatty acids with oligonucleotides was synthesized through postsynthetic modification of oligonucleotide by using iodomethyl alkyl ester of polyunsatured fatty acids. Poly(dT)sequence that is complementary to the poly(A) tails of mRNA was applied as the surrogate for oligonucleotides (**Figure 2-8**) DIPEA was added as a catalyst. The reaction mixture was incubated 60°C for 6 hours. Purification of reaction mixture of the linolenic acid conjugated a poly(dT)sequence was subjected to HPLC analysis. The production of the conjugates were confirmed by MALDI-TOF MS.

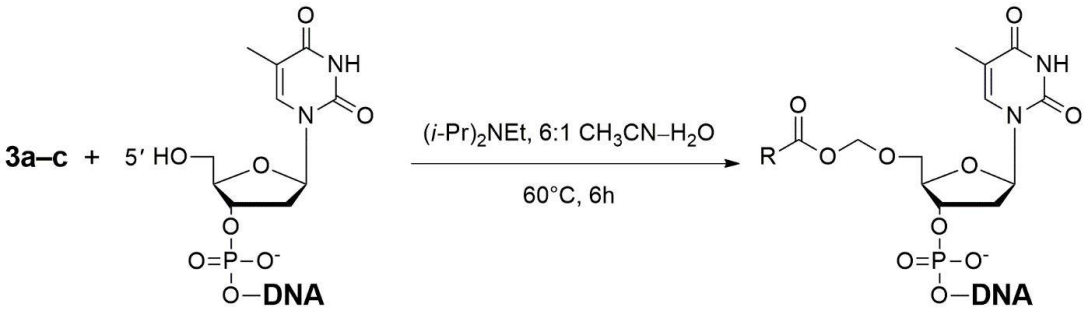

Figure 2-8 Conjugation of DNA with polyunsaturated fatty acids. R = linoleinate (a), linoleate (b), and oleate (c).

Table 2-3 Number of conjugated polyunsaturated fatty acids with oligonucleotides

	Conjugated polyunsaturated fatty acids	**Sequence**[a]	**MALDI-MS**	
			Cald.	Found.
ODN 1	Pivaloyl trimethyl	5’-TTT-3’	964.7	963.9
ODN 2	Pivaloyl trimethyl	5’-TTT TTT TTT TTT TTT TTT TT-3’	6139.5	6140.2
ODN 3	Linolenate	5’-TTT-3’	1093.1	1092.3
ODN 4	Linoleate	5’-TTT-3’	1143.1	1142.4
ODN 5	Oleate	5’-TTT-3’	1145.1	1143.6
ODN 6	Linolenate	5’-TTT TTT TTT TTT TTT TTT TT-3’	6313.4	6313.4
ODN 7	Linoleate	5’-TTT TTT TTT TTT TTT TTT TT-3’	6316.2	6316.2
ODN 8	Oleate	5’-TTT TTT TTT TTT TTT TTT TT-3’	6317.8	6317.9
ODN 9	Linolenate	5’-TTT TTT TTT TFT TTT TTT TT-3’	7136.8	7136.5
ODN 10	Linoleate	5’-TTT TTT TTT TFT TTT TTT TT-3’	7142.3	7141.3
ODN 11	Oleate	5’-TTT TTT TTT TFT TTT TTT TT-3’	7149.4	7150.1
ODN 12	-	5’-TTT TTT TTT TFT TTT TTT TT-3’	6838.6	6838.8
ODN 13	Linolenate	5’-AGA CAG CAG ACA TTG CCA TA -3’	6534.4	6534.1
ODN 14	Linolenate	5’-TAT GGC AAT GTC TGC TGT CT-3’	6404.4	6403.1

[a] F: fluorescein-labeled dT (**Figure 2-9**).

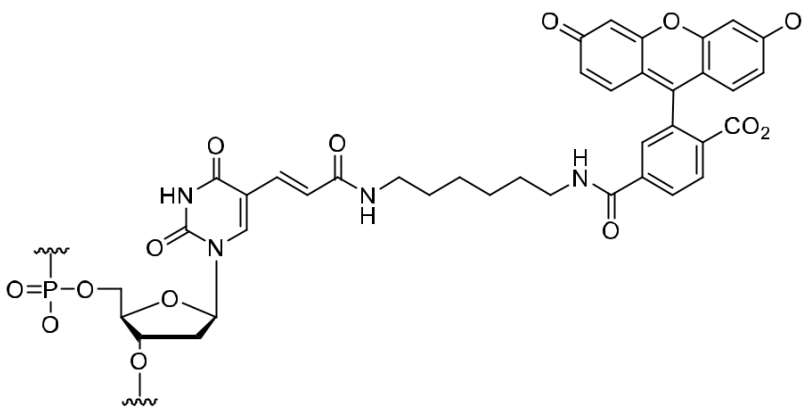

Figure 2-9 Structure of Fluorescein-labeled dT (F in **Table 2-3**).

MALDI-TOF MS suggested that a polyunsaturated fatty acid was attached to DNA strands (**ODN 1-11, ODN 13-14**). At first, we suspected that the conjugation site of oligonucleotides with polyunsaturated fatty acids can react at the phosphate group of the oligonucleotides. However, we observed only one conjugation of polyunsaturated fatty acids with poly(dT)sequences and mixed-sequence of DNA. To elucidate the reaction site of the conjugated unsaturated fatty acids with DNA, the 5'phosphorylation poly(dT)sequence (20-mer) were synthesized. The conjugation of linolenic acid with 5'phosphorylation poly(dT)sequence were proceeded same as the conditions for the conjugation of unsaturated fatty acids with 5'OH poly(dT)sequence. The conjugation of linolenic acid was failed to conjugate with 5'phosphorylation poly(dT)sequence. No desired products obtained from the reaction. Polyunsaturated fatty acids preferably attached to OH- group of deoxyribose on the oligonucleotides.

Cell culture, Oligonucleotides treatment, and Imaging Analysis

Investigation the cellular uptake properties of the polyunsaturated fatty acids conjugated oligonucleotides (**ODN 9-11**). **ODN 9**, **ODN 10** and **ODN 11** were individually incubated with HeLa cells without any transfecting reagent at 37ºC for 2 h. We propose that polyunsaturated fatty acids will facilitate the cellular uptake of oligonucleotides owing to their lipophilic nature that resulting in the interruption of the membrane structure and fluidity of active cells.[23] It is remarkable that, fluorescence signals could be detected when the synthesized probes reached the cytoplasm or nucleus where hybridization between the probes and the target mRNA poly A tails has been occurred.

The cellular uptake properties of the **ODN 9**, **ODN 10** and **ODN 11** were investigated without any transfecting reagent. The sample solutions containing 2 μM probes were incubated for 2 h with cultured HeLa cells and fluorescence positive cells were then detected for the non-modified probe and **ODN 9-11** under a confocal microscope. Surprisingly, the maximum intensity was observed for **ODN 9**, which exhibited 94.2% of cellular uptake intensity (**Figure 2-10)**. **ODN 10** showed slightly cellular uptake intensity. **ODN 11** did not show the cellular uptake intensity. The intensity of the fluorescence in the cells increased as the number of double bonds on the polyunsaturated fatty acids. The results suggest that **ODN 9** exhibited the outstanding of the cellular uptake intensity through 1 conjugation of linolenic acid was attached to fluorescence poly(dT)sequence.

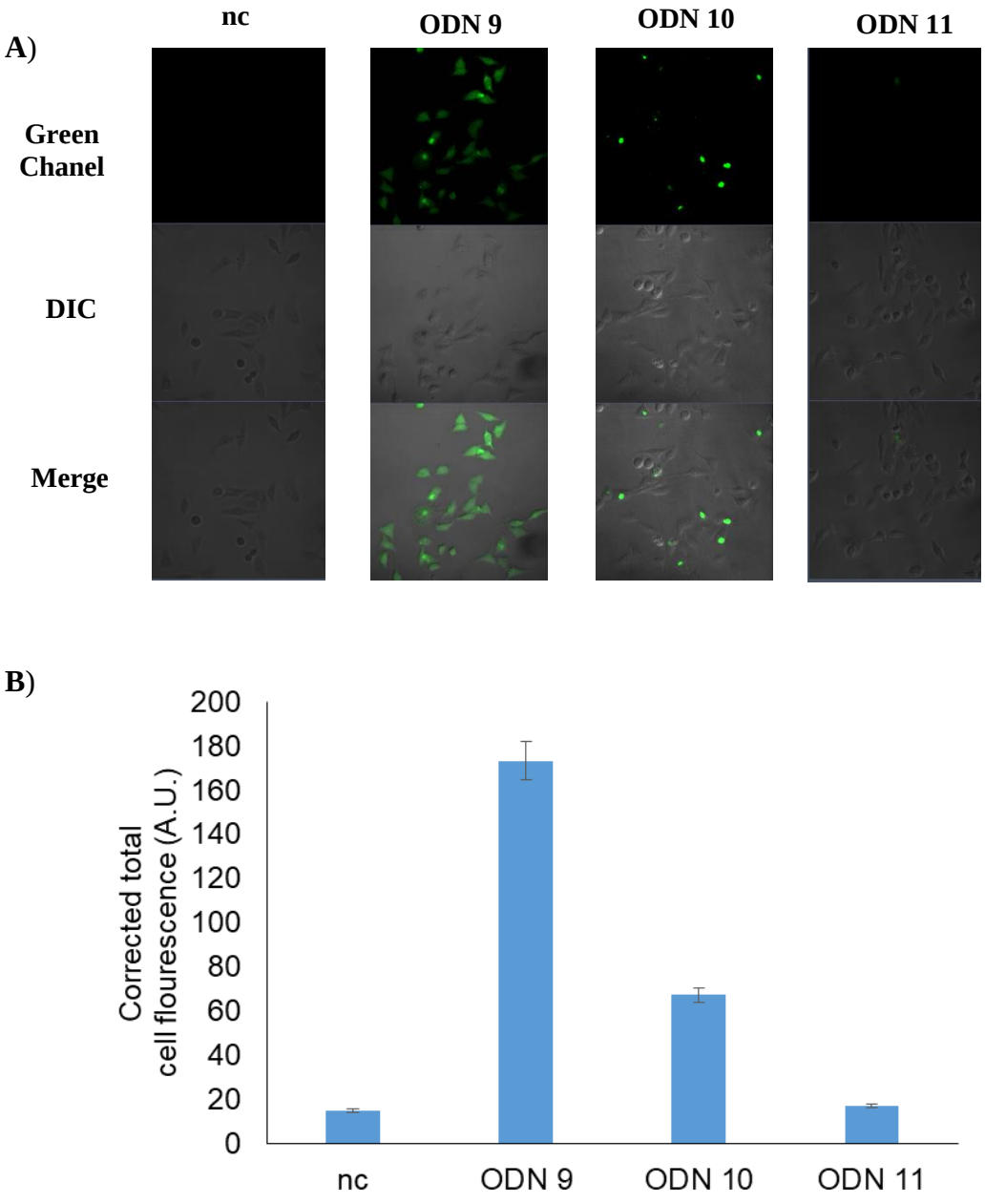

Figure 2-10 Cellular uptake experiments of polyunsaturated fatty acids conjugated fluorescent poly(dT)sequences. (A) Fluorescence imaging of living HeLa cells treated with polyunsaturated fatty acids conjugated poly(dT)sequences, linolenate, linoleate and oleate. Negative control (nc): unconjugated fluorescent poly(dT)sequence. Bar: 50 µm. (B) Quantification of corrected total cell fluorescence using ImageJ. Data shown mean ± standard deviation (n=10).

The fluorescence images from **ODN 9** indicate the oligonucleotides was mainly imported into the nucleus (**Figure 2-12**). Linolenic acid can deliver oligonucleotides into the nucleus domain. The behavior of linolenic acid conjugated oligonucleotides delivery system correspond to the short nucleic acid microinjection delivery, which was rapidly imported exogenous short-chain nucleic acids into the nucleus domain, although the pathway remains unknown. The efficiency of nuclear import is dependent on the size of the exogenous nucleic acids[24].

A)

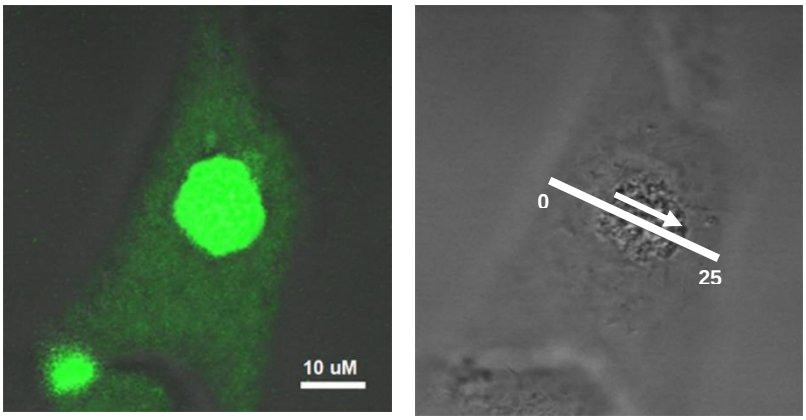

B)

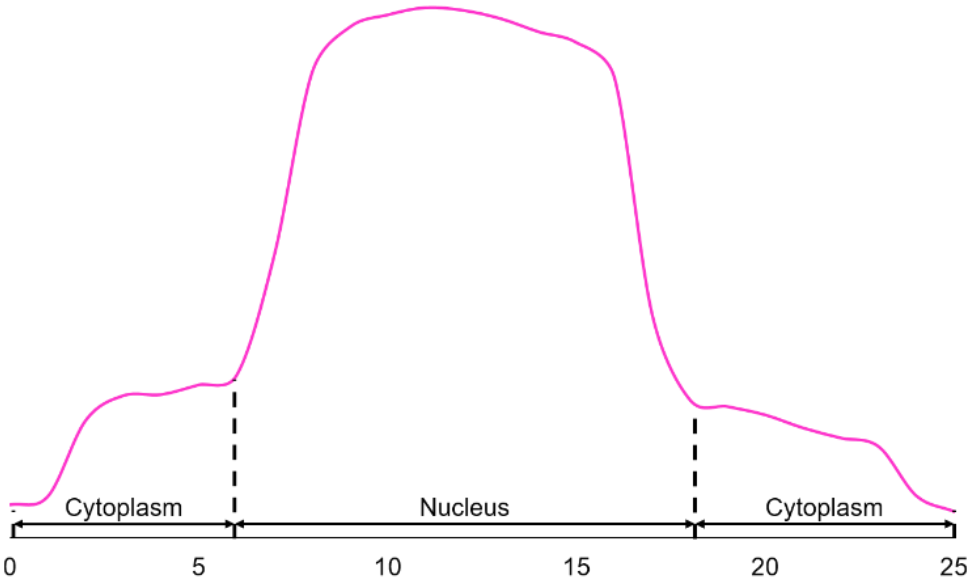

Figure 2-12 Images of an ODN 9 (linolenate)-transfected HeLa cell. (A) Fluorescent and differential interference contrast (DIC) images. Bar: 10 μm. (B) Fluorescent intensities along the white line drawn in the DIC image (right) were plotted. Bar: 10 μm.

Size characterization of polyunsaturated fatty acids conjugated poly(dT)sequences

Previous studies have been reported on the investigation of self-aggregation of lipid-conjugated oligonucleotides in aqueous environments[25]. On the other hand, only a few studies have investigate the deep detail of lipid-conjugated oligonucleotides structure in water. Lipid-conjugated oligonucleotides have a tendency to form supramolecular organization and self-aggregation due to their strong amphiphilic properties[26]. Moreover, previous report has been highlighted on the thermodynamically stable self-assemblies of lipid-conjugated oligonucleotides will not partition into the cell membrane[27] Previous work also confirmed that lipid-conjugated oligonucleotides can maintain the ability to specifically bind the targets and spontaneous insert into the cell membranes (**Figure 2-13**)[28-30] To examine the roles of unsaturated fatty acids- conjugated poly(dT)sequences on cellular pathways, we investigated the micellar size and monitored the micelles destabilization of unsaturated fatty acids-conjugated poly(dT)sequences. We proposed that the micelles stability value will define the competition between self-aggregation and insertion of the linolenate conjugated oligonucleotides into the cell membranes.

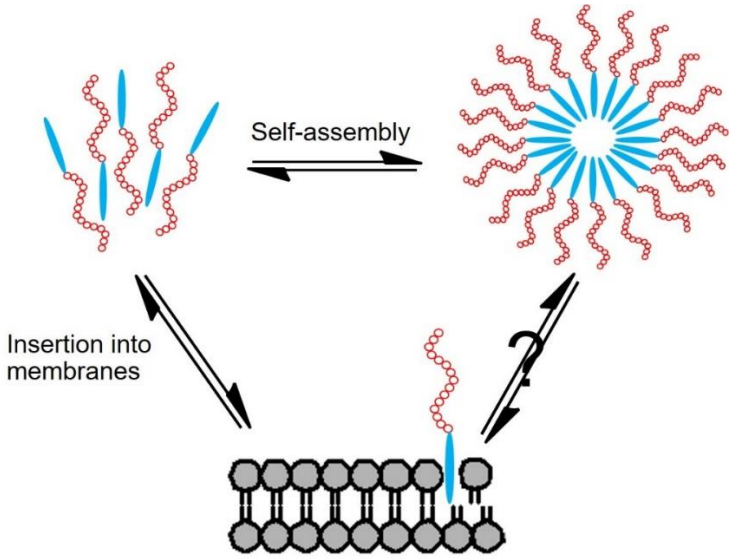

Figure 2-13 Competition between self-aggregation and insertion into membranes for LONs

Micellar size measurements were made of various polyunsaturated fatty acids conjugated poly(dT)sequence on a Zetasizer Nano-ZS90. **Table 2-4** summarizes the z-averages diameters in nanometers. The z-average is the mean hydrodynamic diameter.

Table 2-4 z-average diameters (in nanometers) obtained for polyunsaturated fatty acids conjugated poly(dT)sequences.

Conjugated polyunsaturated fatty acids	Sequence[a]	z-Average Diameter (nm)
-	5'-TTT TTT TTT TTT TTT TTT TT-3'	33.81
Linolenate	5'-TTT TTT TTT TTT TTT TTT TT-3'	111.95
Linoleate	5'-TTT TTT TTT TTT TTT TTT TT-3'	150.27
Oleate	5'-TTT TTT TTT TTT TTT TTT TT-3'	367.50
-	5'-TTT TTT TTT TFT TTT TTT TTT-3'	73.91
Linolenate	5'-TTT TTT TTT TFT TTT TTT TTT-3'	132.40
Linoleate	5'-TTT TTT TTT TFT TTT TTT TTT-3'	184.15
Oleate	5'-TTT TTT TTT TFT TTT TTT TTT-3'	411.62

Micellar size of polyunsaturated fatty acids conjugated poly(dT)sequences showed relatively large size, 110 nm to 400 nm, compared to the LONs that showed relatively small size of lipophilic part of lipid-conjugated oligonucleotides, 1.6 nm to 8 nm for an 18-mer of cholesteryl lipid-conjugated oligonucleotides[31]. Previous studiesconfirmed that the intracellular route was dependent on particle size, whereas the micelles of lipid-conjugated oligonucleotides cannot insert into the cell membrane as mentioned above[32]. Thus, micelle stability have been investigated to highlight the competition between micelles forming and the partition of the linolenate-conjugated poly(dT)sequence into the cell membranes.

Micelle stability via Forster Resonance Energy Transfer (FRET)

Micelle stability was assessed the release of hydrophobic probes from the core of the micelles overtime by monitoring Forester resonance energy transfer (FRET) efficiency. FRET pair was encapsulated using 3,3`-dioctadecyloxacarbocyanine perchlorate (DiO) acts as donor and 1,1`-dioctadecyl-3,3,3`,3`-tetramethylindocarbocyanine perchlorate (DiI) acts as acceptor[33,34]. Encapsulation of both dyes resulting in FRET, excitation at 450 nm (excitation of the donor) and the fluorescence emission is observed at 575 nm (emission of the acceptor). Dye release resulting results in separation of the FRET pair and an increase in fluorescence intensity at 505 nm. Linolenate conjugated poly(dT)sequence is diluted in 90% fetal bovine serum (FBS) in PBS (pH 7.4), the increase of fluorescence intensity at 505 nm as these lipids exchange with serum proteins was observed. Micelles have previously been shown to destabilize in FBS *in vivo* study due to the interactions with α/β globulins[35]. The destabilization of micelles was evaluated by a decrease in the FRET ratio ($I_{575}/[I_{575}+I_{505}]$), which experimentally indicated by the value of ~ 0.5 in 9 hours determining almost complete release of encapsulated cargo.

A FRET assay indicated the unstable of linolenate, linoleate and oleate conjugated poly(dT)sequence micelles due to the FRET molecules are released resulting the strong emission of FRET donor, DiO, is displayed at 505 nm over 9 h as shown in **Figure 2-14**. If the micelles are stable, the FRET pair will be observed at a strong emission of FRET acceptor, Dil, which displayed at 575 nm. Linolenate conjugated poly(dT)sequence micelles exhibited significant changes in the FRET pattern over time, indicating structural instability in FBS. It is important to consider that although the micellar size is one of the main factor to determine the micelle stability, however, this value is not enough to

determine the micelle stability. Consequently, the micellar size is not required for the stability in the serum proteins.

We also monitored the FRET assay of linolenate-conjugated oligonucleotide in acidic conditions using sodium acetate buffer (pH 5.2) according to cancer cells expressed more acidic environment than the surroundings area[36]. Linolenate conjugated oligonucleotides also showed the micelle unstable in acidic conditions.

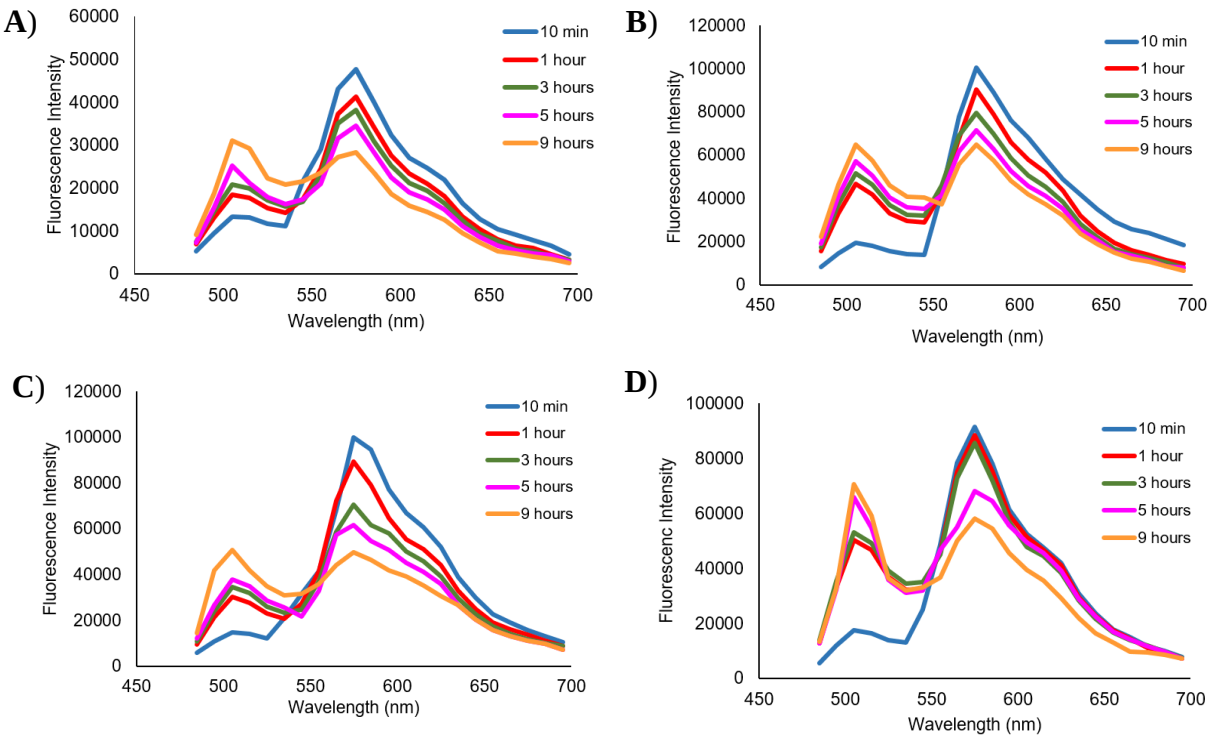

Figure 2-14 FRET assay to measure micelle stability. FRET spectra of polyunsaturated fatty acids-conjugated poly(dT)sequence micelles show and increase in fluorescence intensity at 505 nm indicating micelle destabilization. (A) Linolenate-conjugated oligonucleotide (B) Linolenate-conjugated oligonucleotide; acidic conditions pH 5.2 (C) Linoleate-conjugated oligonucleotide (D///) Oleate conjugated oligonucleotide

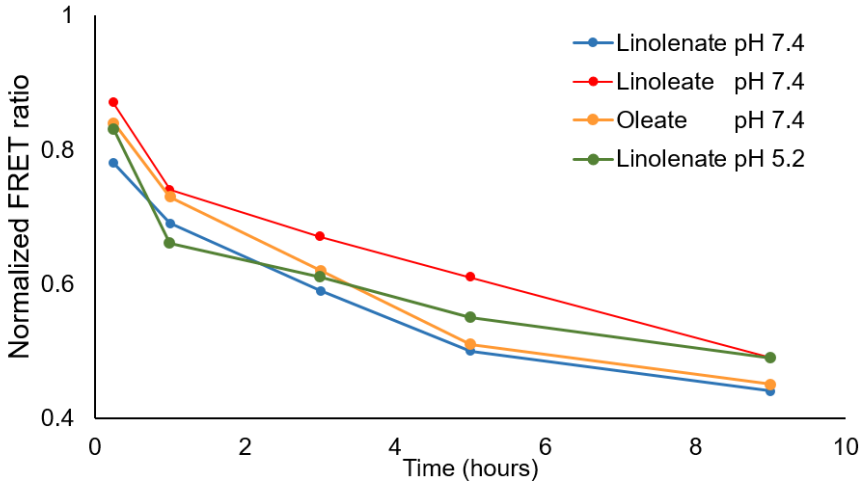

Figure 2-15 Graph of normalized FRET ratio ($I_{575}/[I_{575}+I_{505}]$) over 9 h.

Enzymatic deprotection of the linolenic acids conjugated oligonucleotides

Evaluation the deprotection of the linolenic acids on the oligonucleotides was conducted via esterase activities (**Figure 2-13**). **ODN 6** was treated with esterase from porcine liver, and the reaction was monitored by HPLC. Time course HPLC chromatogram are shown in **Figure 2-14**. A peak corresponding to **ODN 6** was observed in the HPLC chromatogram before the addition of the enzyme. After incubation with the enzyme for 2 hours, the intensity of the peak corresponding to **ODN 6** extremely decreased. The reaction proceeded until **ODN 6** had been finally converted to the deprotected product at 8 hours.

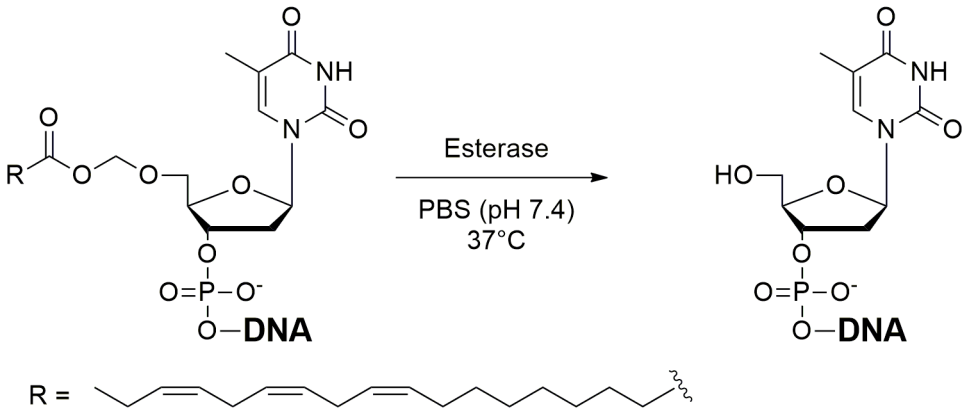

Figure 2-16 Esterase activities of the linolenic acid on oligonucleotides

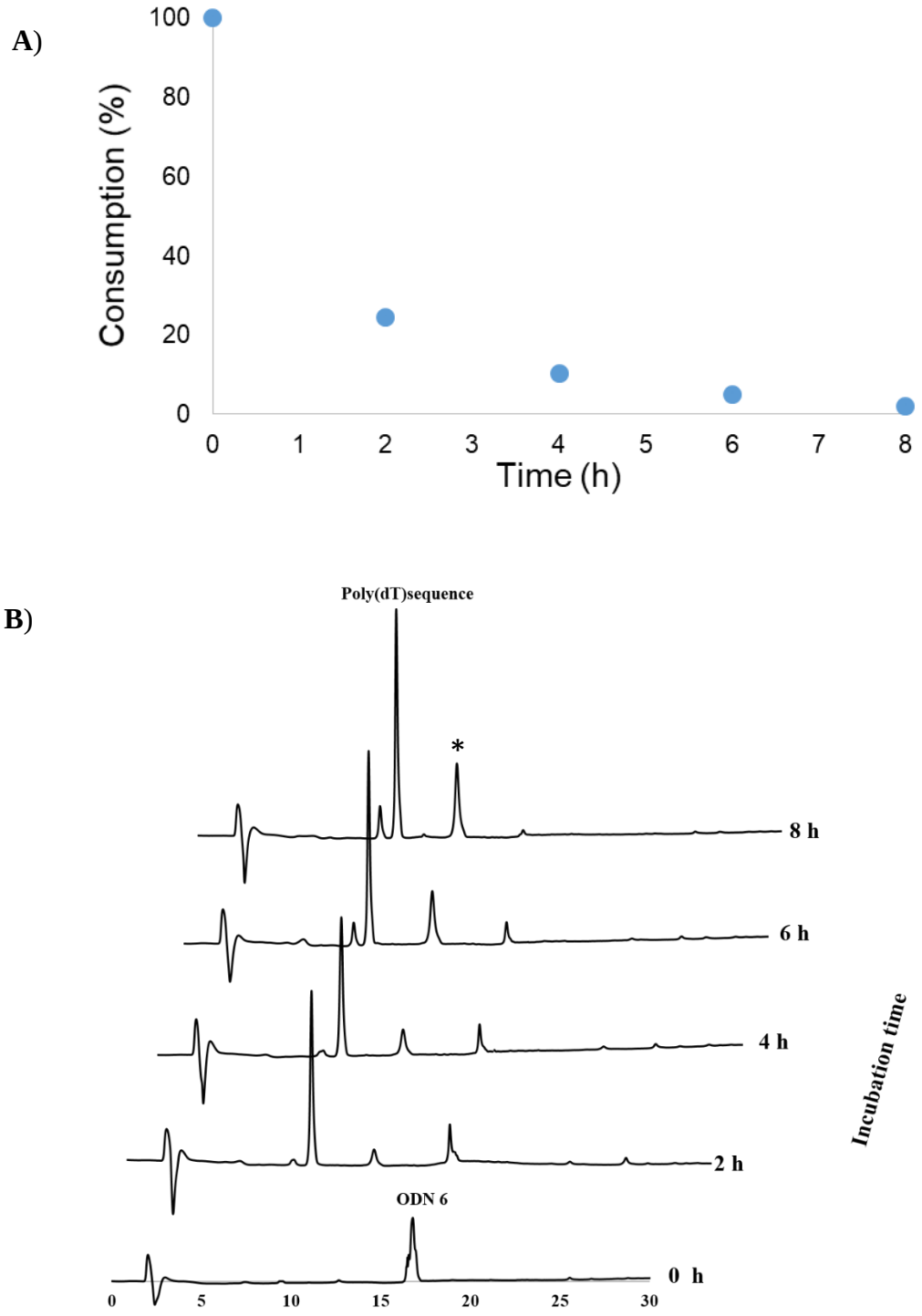

Figure 2-17 Deprotection of 5'-linolenate-protected poly(dT) with an esterase. (A) Consumption yield of starting material. (B) Reverse-phase HPLC profiles showing the time course for the deprotection reaction.

So far, the micelle stability of polyunsaturated fatty acids conjugated poly(dT)sequences has been demonstrated via FRET assay. The unstable of polyunsaturated fatty acids conjugated poly(dT)sequence micelles determined the insertion of linolenate conjugated poly(dT)sequence into the cell membranes. Moreover, the linolenate conjugated poly(dT)sequence showed micelle unstable in acidic condition. Therefore, after the partition of linolenate conjugated fluorescent poly(dT)sequence into the cell membranes, linolenate conjugated fluorescent poly(dT)sequence would be carried into cytoplasm, which is easily cleaved by esterase to release the free fluorescent poly(dT)sequence that can enter into the nucleus. According to the relatively large size of linolenate conjugated fluorescent conjugated poly(dT)sequence, it would not be able to penetrate to the nucleus without cleavage by the enzyme in the cells. Previous report demonstrated that the bulky ECHO probe was selectively penetrated only in the cytoplasm, whereas unbulky ECHO probe was nucleus-selective mRNA visualization[37].

Cell Viability Assay

Linolenate conjugated poly(dT)sequence were evaluated for *in vitro* cytotoxicity to determine the possibility of using as oligonucleotides delivery. Linolenate conjugated poly(dT)sequence was treated with HeLa cells to investigate the viability using Prestoblue® cell viability reagent. The cell viability after treating with the linolenate conjugated poly(dT)sequence for 72 hours with varying concentration was nearly 100% (**Figure 2-18**). Thus, linolenate conjugated poly(dT)sequence did not display any cytotoxicity in HeLa cells.

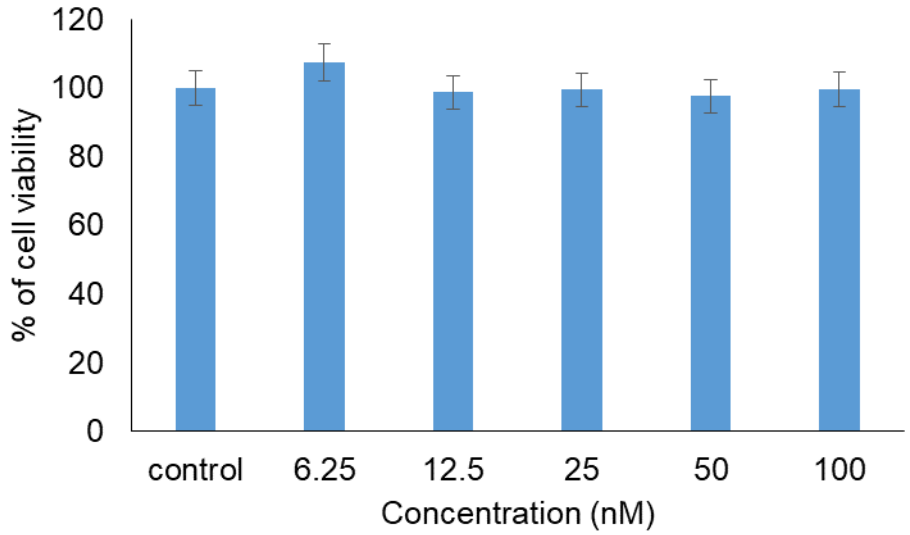

Figure 2-18 Cell viability at vary concentrations of linolenate conjugated poly(dT)sequence. Prestoblue® cell viability assay was performed on HeLa cells. No statistical difference was observed between untreated cells and linolenate conjugated poly(dT)sequence treated cells at 72 h.

2.4 Summary

We have designed and conjugated linolenic acid, linoleic acid, oleic acid to poly(dT)sequence via post-synthesis DNA modification. The reaction site of the polyunsaturated fatty acids attached to 5'-OH group of deoxyribose on oligonucleotides. Linolenate conjugated fluorescence poly(dT)sequence showed the outstanding cellular uptake in HeLa cells, as well as slightly cellular uptake was observed in linolenate conjugated fluorescence poly(dT) sequence. No fluorescence signals have been detected with unmodified probe and oleate conjugated fluorescence poly(dT) sequence. According to FRET assay, linolenate conjugated oligonucleotide would be partition into the cell membranes. Besides, linolenate conjugated poly(dT)sequence was readily cleaved by porcine liver esterase to release the naked oligonucleotides. The cell viability assay indicated the non-cytotoxicity and safety of linolenate conjugated oligonucleotides. These results showed that the linolenate conjugated poly(dT)sequence described in this study could be used as oligonucleotides delivery owing to its natural and safe essential substances.

2.5 Experimental procedures

General. All chemicals were purchased from Sigma-Aldrich, Wako Chemicals, and Tokyo Chemical Industry. 1H and 13C NMR spectra were measured with a Bruker Avance 600 (600 MHz). Electrospray ionization mass spectra (ESI-MS) were recorded by a Bruker microTOF II-NAC. MALDI-TOF mass spectra were recorded by a Bruker microflex-NAC. DNA was synthesized on a NTS H-8 DNA/RNA synthesizer (Nihon Techno Service). DNA oligonucleotides were purified by HPLC system composed by GILSON Inc. and JASCO Inc. modules. Absorption were recorded on Shimadzu UV-2550 spectrophotometer and RF-5300PC spectrofluorophotometer.

Compound 2a. To a suspension of linolenic acid (**1a**) (4.02 ml, 13 mmol) in water 40 ml was added Na_2CO_3 (5.51 g, 52 mmol). After 20 minutes, the reaction was cooled at 0ºC and nBu_4NHSO_4 (3.02 ml, 2.6 mmol), dichloromethane (80 ml) and chloromethyl chlorosulfate (1.71 ml, 16.9 mmol) were added. The reaction was allowed to warm 25ºC and stirred overnight. The reaction mixture was then quenched by the addition of water (50 ml) and dichloromethane (50 ml). The aqueous layer extracted with dichloromethane (2 × 100 ml). The combined organics was dried (Mg_2SO_4) and concentrated in vacuo. The product was purified by column chromatography eluting with dichloromethane–hexanes (1: 9, v/v) provided chloromethyl alkyl ester of linolenic acid (**2a**) as a colorless oil at a yield of 60%, 2.14 g. ^{1}H-NMR ($CDCl_3$, 600 MHz) δ 5.89 (s, 2-H), 5.41-5.29 (m, 6-H), 2.80 (m, 2-H), 2.32 (t, 2-H, *J* = 7.38 Hz), 2.07 (m, 4-H), 1.63 (m, 2-H), 1.59 (s, 2-H), 1.30 (m, 6-H), 0.97 (t, 3-H, *J* = 7.62 Hz); ^{13}C-NMR ($CDCl_3$, 600 MHz) δ 172.1, 132.3, 130.6, 128.7, 128.6, 128.2, 127.5, 69.0, 34.4, 29.9, 29.5, 29.4, 29.3, 27.6, 26.0, 25.9, 24.9, 21.0 ,14.6; ESI-MS $[M+H]^+$, $C_{19}H_{31}ClO_2$ 349.3085 (calcd.), 349.3080 (found).

Compound 3a. To a solution of chloromethyl alkyl ester of linolenic acid (**2a**) (1 g, 2.87 mmol) in acetronitrile (20 ml) was added sodium iodide (1.3 g, 8.61 mmol). The flask was covered in tin foil to exclude light and stirred at 25 ºC overnight. The reaction mixture was then quenched by the addition of water (50 ml) and dichloromethane (50 ml) and the aqueous layer extracted with dichloromethane (2 × 40 ml). The combined organics were washed with aq satd. $NaHCO_3$ (50 ml), 5% aq sodium sulfite solution (50 ml) and brine (2 × 25 ml) and concentrated to provided iodomethyl alkyl ester of linolenic acid (**3a**) as yellow oil at a yield of 100%, 1.82 g. ^{1}H-NMR ($CDCl_3$, 600 MHz) δ 5.70 (s, 2-H), 5.36 (m, 6-H), 2.80 (s, 4-H), 2.37 (t, 2-H, *J* = 7.32 Hz), 2.05 (m, 4-H), 1.65 (m, 2-H), 1.55 (s, 2-H), 1.31 (s, 6-H), 0.97 (t, 3-H, *J* = 7.32 Hz); ^{13}C-NMR ($CDCl_3$, 600 MHz) δ 172.2, 132.3, 130.6, 128.6, 128.6, 128.1, 127.5, 34.6, 31.1, 29.9, 29.5, 29.3, 27.6, 26.0, 25.9. 24.9, 21.0, 14.7; ESI-MS $[M+H]^+$, $C_{19}H_{31}IO_2$ 419.1445 (calcd.), 419.1447 (found).

Compound 2b. Compound **2b** was prepared by following the synthesis of chloromethyl alkyl ester of linolenic acid (**2b**). Linoleic acid (**1b**) was employed as the starting material to give chloromethyl alkyl ester of linoleic acid (**2b**) as a colorless oil at a yield of 79.1%, 2.47 g. ^{1}H-NMR ($CDCl_3$, 600 MHz) δ 5.69 (s, 2-H), 5.36-5.31 (m, 4-H), 2.76 (t, 2-H, *J* = 6.48 Hz), 2.37 (t, 2-H, *J* = 7.32 Hz), 2.06-2.02 (m, 4-H), 1.64 (m, 12-H), 1.30 (m, 2-H), 0.88 (t, 3-H, *J* = 0.62 Hz)); ^{13}C-NMR ($CDCl_3$, 600 MHz) δ 172.1, 130.6, 130.4, 128.5, 128.3, 69.0, 34.4, 31.9, 29.9, 29.7, 29.5, 29.4, 29.3, 27.6, 26.0, 24.9, 22.9, 14.5; ESI-MS [M+TFA-H], $C_{21}H_{33}ClF_3O_4$ 441.3095 (calcd.), 441.3094 (found).

Compound 3b. Compound **3b** was prepared by following the synthesis of iodomethyl alkyl ester of linolenic acid (**3a**). Chloromethyl alkyl ester of linoleic acid (**2b**) was employed as the starting material to give iodomethyl alkyl ester of linoleic acid (**3b**) as a yellow oil at a yield of 100%, 1.19 g. ^{1}H-NMR ($CDCl_3$, 600 MHz) δ 5.89 (s, 2-H), 5.37-5.31 (m, 4-H), 2.75 (t, 2-H, *J* = 6.78 Hz), 2.31 (t, 2-H, *J* = 7.32 Hz), 2.04-2.01 (m, 4-H), 1.62 (t, 2-H, *J* = 6.72 Hz), 1.29 (m, 16-H), 0.87 (t, 3-H, *J* = 7.08 Hz)); ^{13}C-NMR ($CDCl_3$, 600 MHz) δ 172.3, 130.6, 130.4, 128.5, 128.3, 34.7, 31.9, 31.0, 29.9, 29.6, 29.5, 29.4, 29.3, 27.6, 27.5, 26.0, 24.8, 23.0, 14.5; ESI-MS $[2M+H]^+$, $C_{38}H_{67}I_2O_4$ 841.3539 (calcd.), 841.3532 (found).

Compound 2c. Compound **2c** was prepared by following the synthesis of chloromethyl alkyl ester of linolenic acid (**2b**). Oleic acid (**1c**) was employed as the starting material to give chloromethyl alkyl ester of oleic acid (**2c**) as a colorless oil at a yield of 81.9%, 2.31 g. ^{1}H-NMR ($CDCl_3$, 600 MHz) δ 5.69 (s, 2-H), 5.33 (d, 2-H, *J* = 3.54 Hz), 2.37 (t, 2-H, *J* = 7.62 Hz), 2.03 (m, 4-H), 1.64 (t, 2-H, *J* = 6.48 Hz), 1.30 (m, 20-H), 0.87 (t, 3-H, *J* = 6.42 Hz); ^{13}C-NMR ($CDCl_3$, 600 MHz) δ 172.1, 130.4, 130.1, 68.9, 34.4, 32.3, 30.1, 30.0, 29.9, 29.7, 29.5, 29.4, 29.3, 27.6, 27.5, 26.0, 24.9, 23.1, 14.5; ESI-MS $[M+Na]^+$, $C_{19}H_{67}I_2O_4$ 353.1638 (calcd.), 353.1632 (found).

Compound 3c. Compound **3c** was prepared by following the synthesis of iodomethyl alkyl ester of linolenic acid (**3a**). Chloromethyl alkyl ester of oleic acid (**2c**) was employed as the starting material to give iodomethyl alkyl ester of linoleic acid (**3c**) as a yellow oil at a yield of 100%, 1.14 g. ^{1}H-NMR ($CDCl_3$, 600 MHz) δ 5.89 (s, 2-H), 5.32 (d, 2-H, *J* = 3.24 Hz), 2.31 (t, 1-H, *J* = 7.2 Hz), 2.02 (m, 2-H), 1.25 (m, 20-H); ^{13}C-NMR ($CDCl_3$, 600 MHz) δ 172.1, 130.4, 130.1, 34.7, 32.3, 30.9, 30.2, 30.0, 29.9, 29.7, 29.5, 29.4, 29.3, 27.6, 27.5, 26.0, 24.9, 23.1, 14.6; ESI-MS [M+2Na-H]+, $C_{19}H_{68}INa_2O_2$ 467.1468 (calcd.), 467.1466 (found).

Conjugation of Oligonucleotides A solution of oligonucleotides (30 nmol) in water 100 µl and MeCN 600µl was add iodomethyl alkyl ester of unsaturated fatty acids (500 eq) and DIEA (500 eq). The mixture was heated 60 ^{o}C for 6 hours, then cooled to room temperature. The crude reaction was purified by reverse phase HPLC.

Cellular Uptake of Conjugated Fatty Acid Fluorescein Labeled Pro-oligonucleotides Conjugated fatty acid fluorescein labeled pro-oligonucleotides (2 µM, 1.0 µL) was mixed with OPTI-MEM (9.0 µL). Each cultured cells in 3.5 cm glass bottom dish containingg 1× 10^5cells were washed with 1 mL of 1 × PBS (-) once and the sample solution was added to the center of glass base. These dishes were incubated at 37^{o}C for 2 hours. Subsequently, the sample solution was discarded and each dish was washed with 1 × PBS (-) and OPTI-MEM. The fluorescence images were recorded under confocal laser scanning microscope (Ex: 488 nm, wavelength longer than 505 nm was detected.

Dynamic Light Scattering The particle size of polyunsaturated fatty acids conjugated oligonucleotides were measured using a Malvern Zetasizer Nano-ZS90 and analyzed with Zetasizer software (Malvern Instruments). Each sample was prepared and diluted in nuclease-free water. All measurements were carried out at 25^{o}C, and three measurements with at least 10 sub-runs were performed for each sample.

Micelle stability via Forester Resonance Energy Transfer (FRET) The two dyes 3,3'-dioctadecyloxacarbocyanineperchlorate (DiO) and 1,1'-dioctadecyl-3,3,3',3'-tetramethylindocarbocyanineperchlorate (Dil) were suspended in ethanol at 2 mg/ml. The DNA-polyunsaturated fatty acids conjugates were also dissolved in ethanol and 5 wt% of each dyes was added to the samples. The ethanol was evaporated in a vaccum concentrator, resulting in a thin lipid film. The film was rehydrated with 25 mM NaHPO4, 50 mM KCl pH = 7.2 to reach a final concentration of 1 mg/ml. The mixture was heated to 65oC for 15 mins and the cooled slowly at room temperature. The sample was centrifuged in tube filters with a pore size 0.45 µm to remove aggregates. Micelles stability assays were added to 90%bovine serum albumin (BSA) in PBS in a half area 96-welll black plate. Using multi-well Cytation 5 plate reader (BioTek Instruments, JPN), samples were excited at 450 nm, and time dependent fluorescence intensity was recorded for 24 hours over the range of 475 nm to 650 nm. Samples were incubated 37^{o}C for the course of the FRET assay. The FRET ratio ($I_{575}/I_{575}+I_{505}$) was calculated at each time point to measure the change in micelle stability.

Enzymatic Deprotection of Linolenate PBS buffer (10x) solution in water 180 µl containing pig liver esterase (0.3mg/ml) was added to the tube containing ODN 1 10 µmol. The mixture was shaken at 37^{o}C in an incubator. Aliquots of sample solution were analyzed by reverse-phase HPLC at appropriate times. HPLC conditions: A buffer (0.1 M TEAA buffer), B buffer (CH_3CN); gradient (B) 5%→100% (30 min)

***In Vitro* Cell Viability Prestoblue® Assay** HeLa cells were grown in Dulbecco`s modified Eagle`s medium (DMEM) containing 10% (v/v) fetal bovine serum (FBS) and 1% (v/v) antibiotic-antimycotic solution at 37ºC in humidified atmosphere of 5% CO_2. The cells were grown until at 80% confluency, and then subcultured. Cells were seeded at an initial cell density of 5000 cells/well onto 96 well-plates and allowed to adhere overnight. After 72 h, the cells were individually treated with a series of linolenate conjugated poly(dT)sequence concentrations (6.25, 12.5, 25, 50, 100 nM). Cells were used as positive control. DMEM was used as a negative control. Cell viability was measured by Prestoblue® Assay. Prestoblue® solution was added to each well, and incubated at 37oC under 5%CO2 atmosphere for 1 h. The absorbance was measured at 540 nm using a multi-well Cytation 5 plate reader (BioTek Instruments, JPN) at a wavelength of 590 nm, excited by a wavelength of 560 nm.

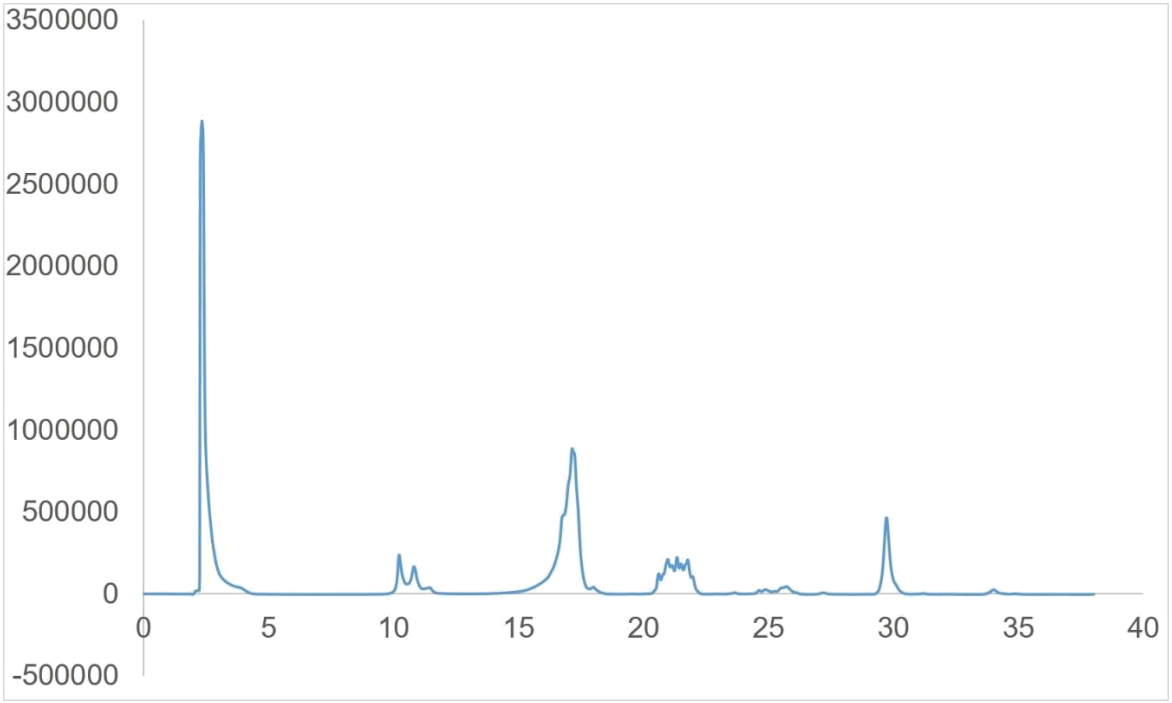

Figure 2-19 HPLC chromatogram of thymine 3-mer conjugation with pivaloyl oxytrimethyl (**ODN 1**). Similar chromatogram was obtained when the reaction was performed at 60°C for 6 hours. HPLC condition: 5C18-MS-II column, 4.6 mm I.D. × 250 mm, flow rate: 1 ml/min, gradient: 0 to 45 min 5% to 100% acetonitrile.

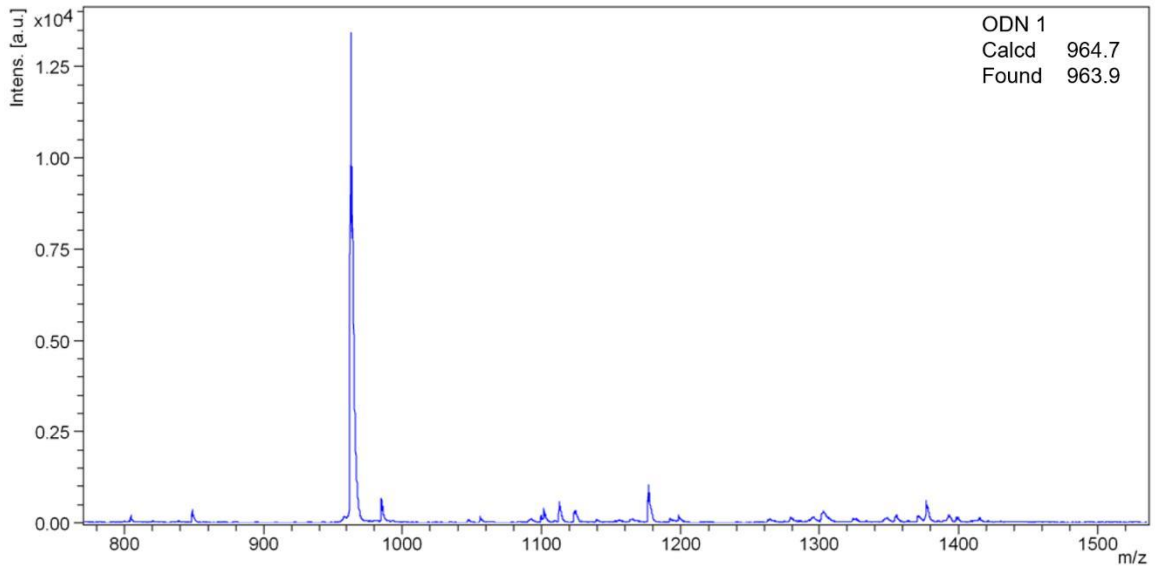

Figure 2-20 MALDI-TOF spectrum of the HPLC peak with R*t* = 16’ (see **Figure 2-19**) revealed the 1 conjugated pivaloyl oxytrimethyl with thymine 3-mer (**ODN 1**).

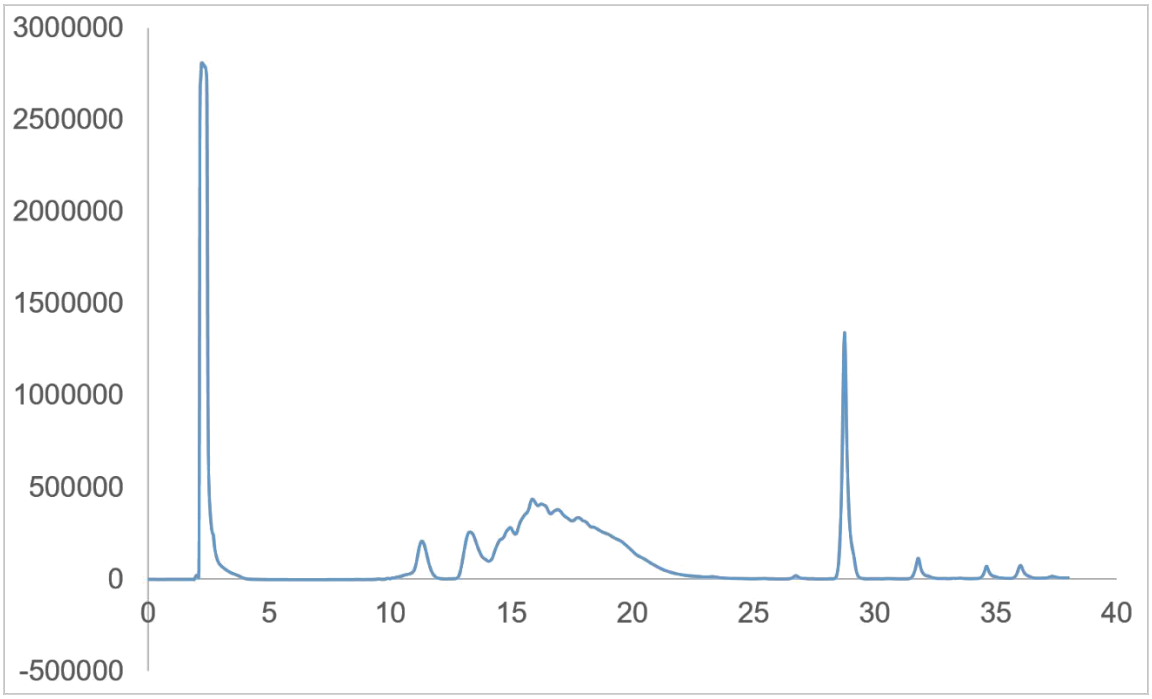

Figure 2-21 HPLC chromatogram of poly(dT)sequence conjugation with pivaloyl oxytrimethyl (**ODN 2**). Similar chromatogram was obtained when the reaction was performed at 60°C for 6 hours. HPLC condition: 5C18-MS-II column, 4.6 mm I.D. × 250 mm, flow rate: 1 ml/min, gradient: 0 to 45 min 5% to 100% acetonitrile.

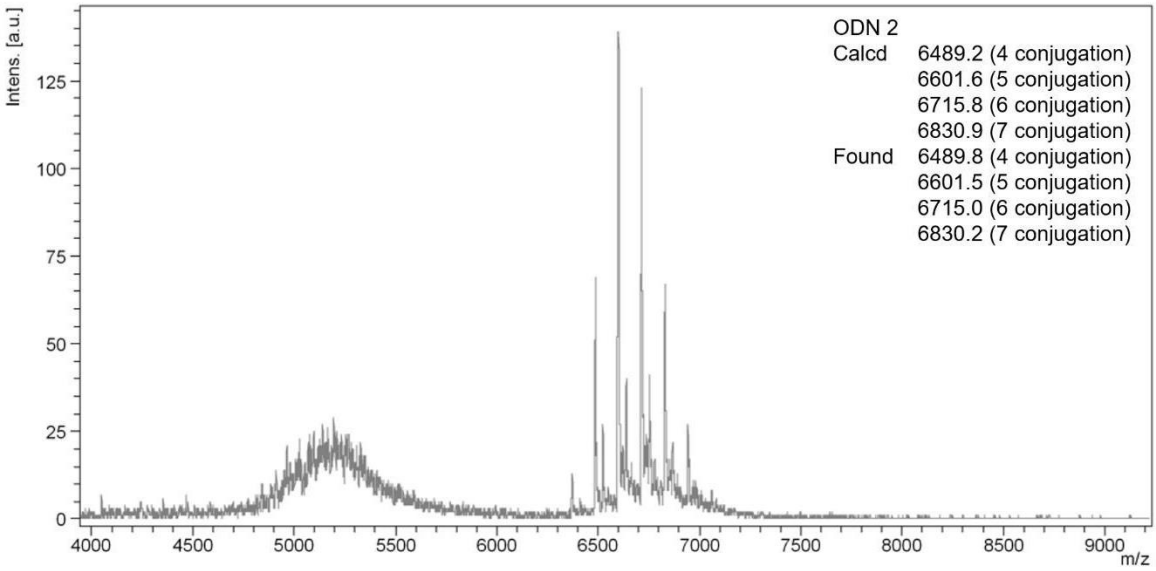

Figure 2-22 MALDI-TOF spectrum of the HPLC peak with R*t* = 16' (see **Figure 2-21**) revealed the 4-7 conjugated pivaloyl oxytrimethyl with poly(dT)sequence (**ODN 2**).

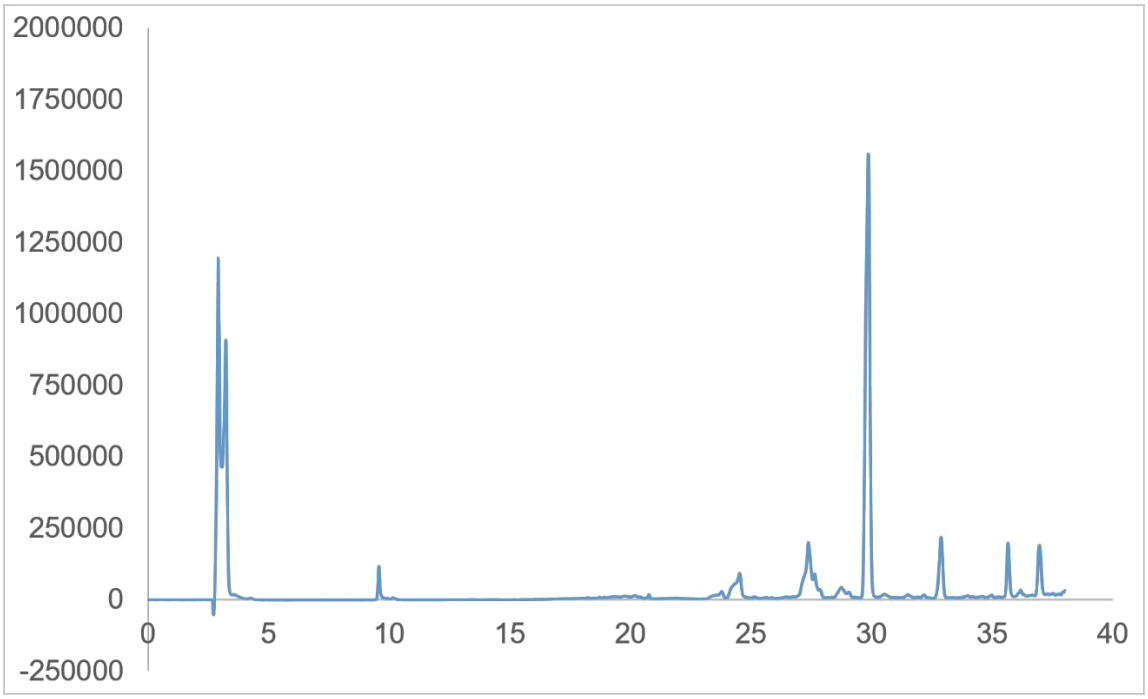

Figure 2-23 HPLC chromatogram of thymine 3-mer conjugation with linolenate (**ODN 3**). Similar chromatogram was obtained when the reaction was performed at 60°C for 6 hours. HPLC condition: 5C18-MS-II column, 4.6 mm I.D. × 250 mm, flow rate: 1 ml/min, gradient: 0 to 45 min 5% to 100% acetonitrile.

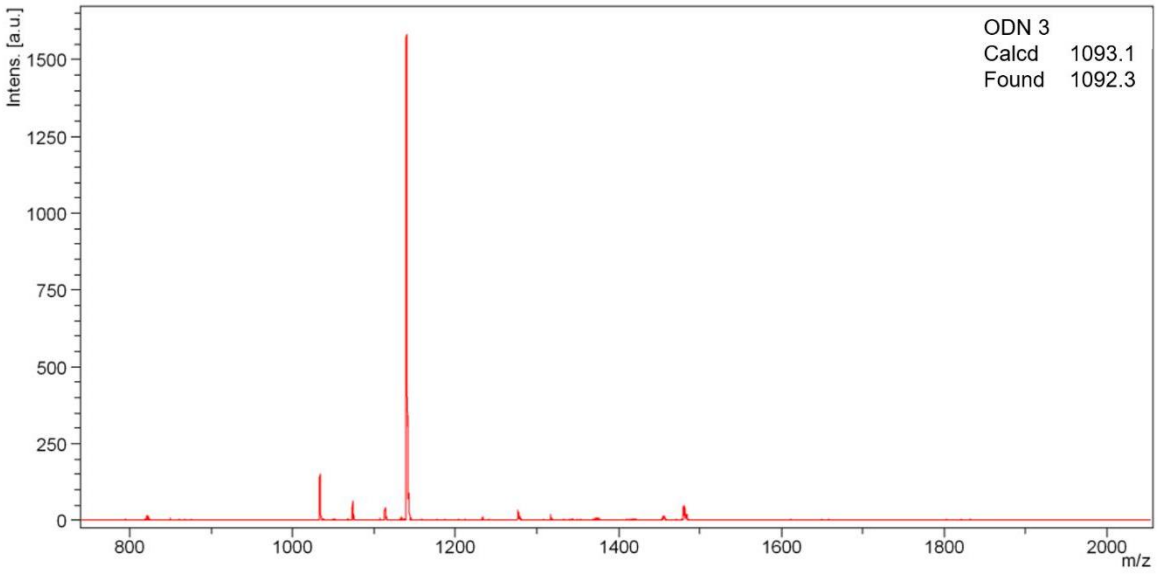

Figure 2-24 MALDI-TOF spectrum of the HPLC peak with R*t* = 27’ (see **Figure 2-23**) revealed the 1 conjugated linolenate with thymine 3-mer (**ODN 3**).

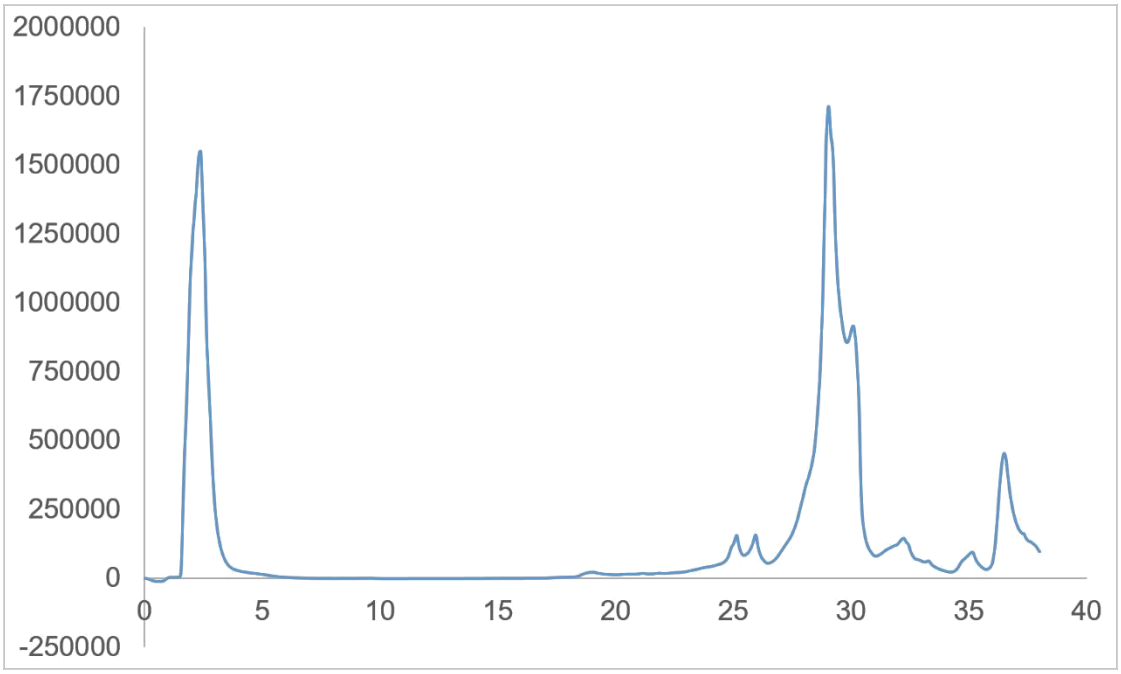

Figure 2-25 HPLC chromatogram of thymine 3-mer conjugation with linoleate (**ODN 4**). Similar chromatogram was obtained when the reaction was performed at 60°C for 6 hours. HPLC condition: 5C18-MS-II column, 4.6 mm I.D. × 250 mm, flow rate: 1 ml/min, gradient: 0 to 45 min 5% to 100% acetonitrile.

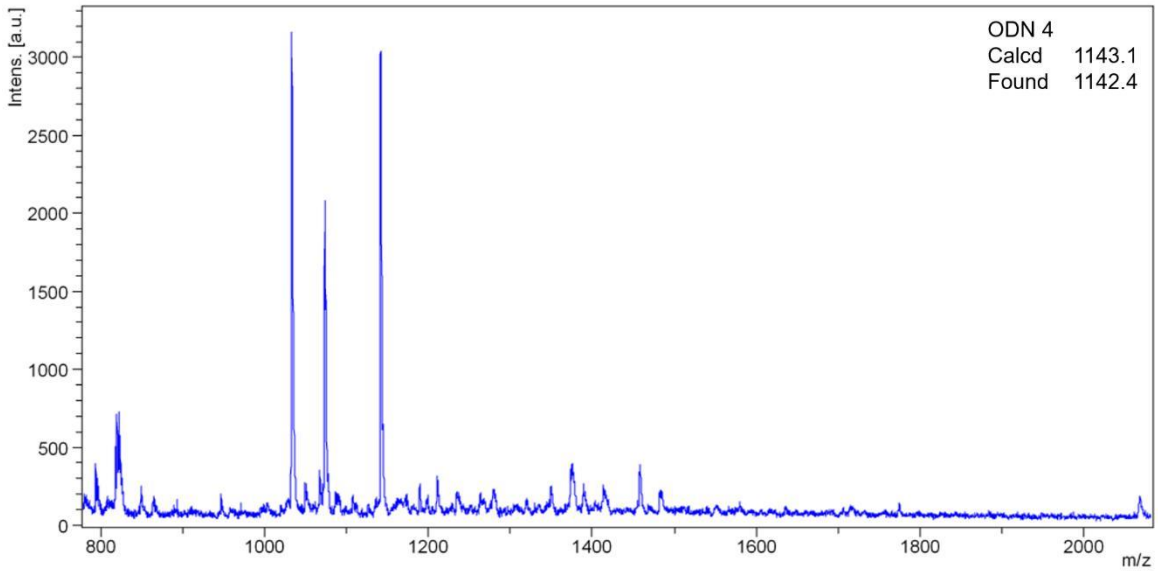

Figure 2-26 MALDI-TOF spectrum of the HPLC peak with R*t* = 27’ (see **Figure 2-25**) revealed the 1 conjugated linoleate with thymine 3-mer (**ODN 4**).

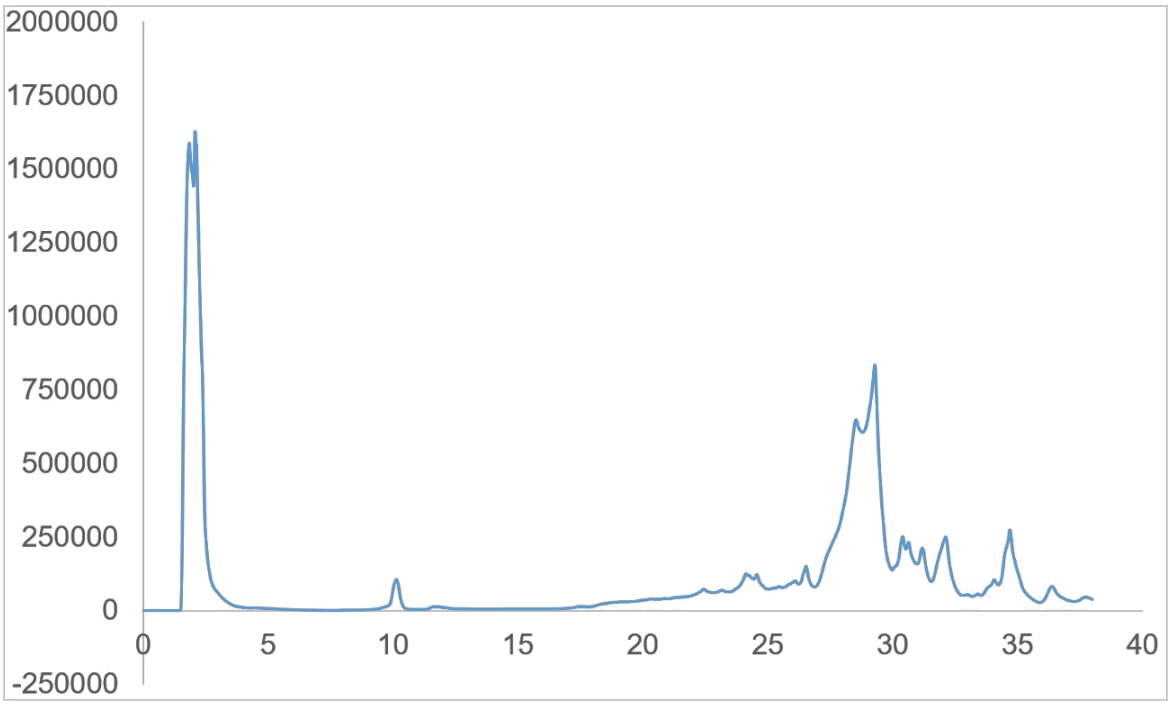

Figure 2-27 HPLC chromatogram of thymine 3-mer conjugation with oleate (**ODN 5**). Similar chromatogram was obtained when the reaction was performed at 60°C for 6 hours. HPLC condition: 5C18-MS-II column, 4.6 mm I.D. × 250 mm, flow rate: 1 ml/min, gradient: 0 to 45 min 5% to 100% acetonitrile.

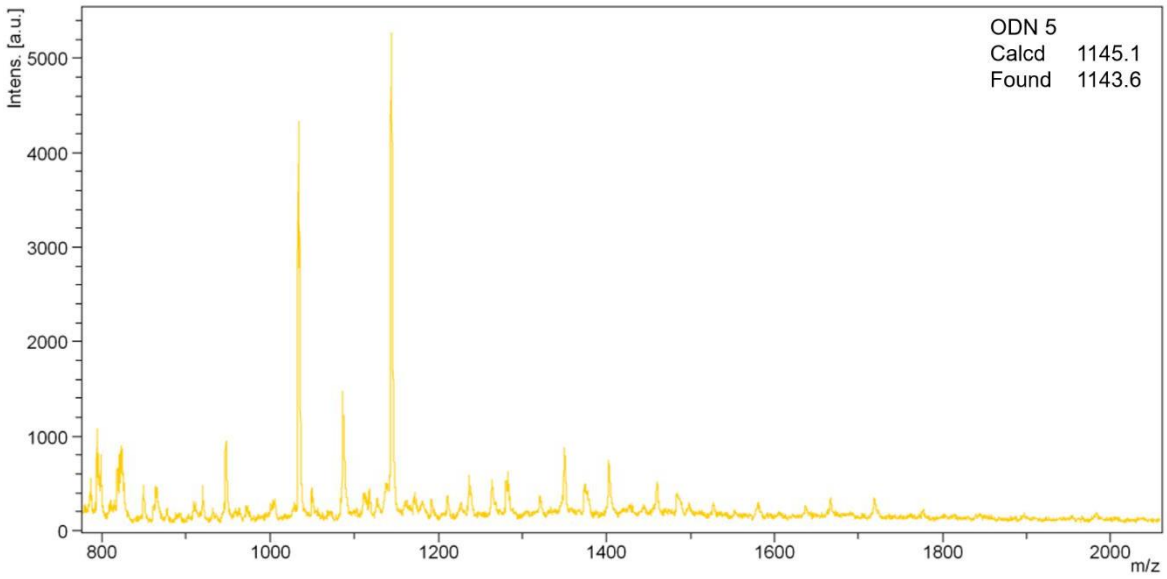

Figure 2-28 MALDI-TOF spectrum of the HPLC peak with R*t* = 30’ (see **Figure 2-27**) revealed the 1 conjugated oleate with thymine 3-mer (**ODN 5**).

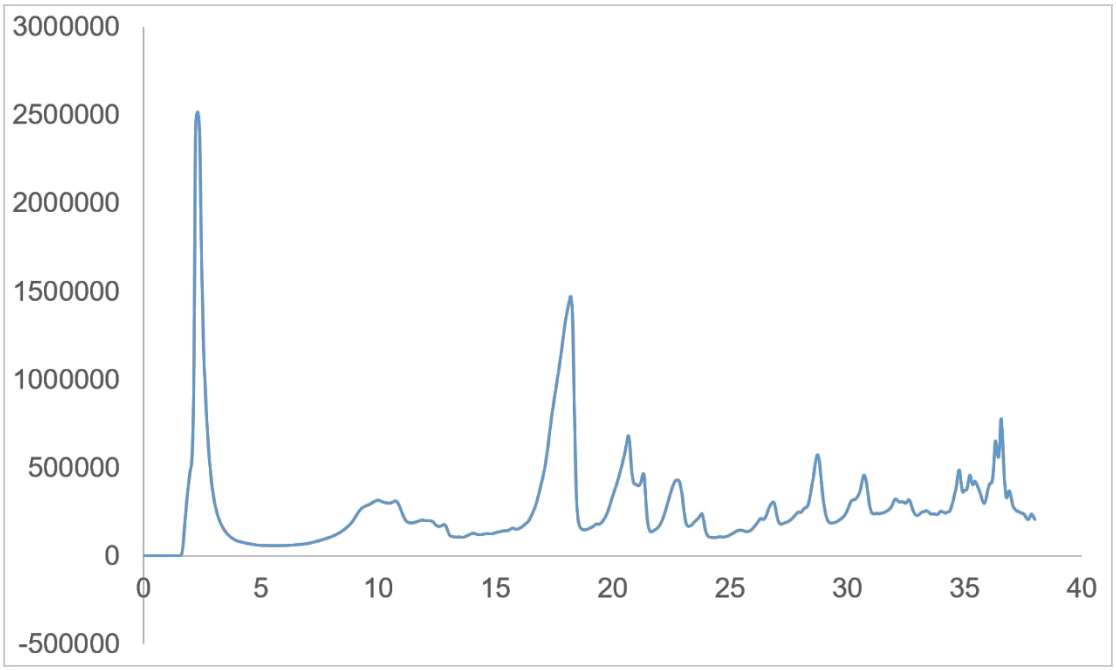

Figure 2-29 HPLC chromatogram of poly(dT)sequence conjugation with linolenate (**ODN 6**). Similar chromatogram was obtained when the reaction was performed at 60°C for 6 hours. HPLC condition: 5C18-MS-II column, 4.6 mm I.D. × 250 mm, flow rate: 1 ml/min, gradient: 0 to 45 min 30% to 100% acetonitrile.

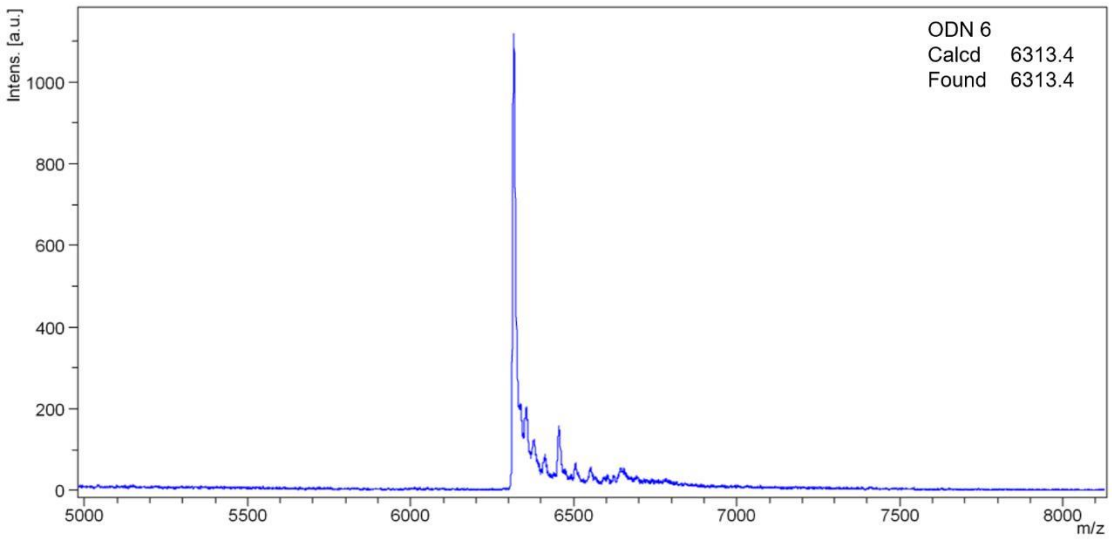

Figure 2-30 MALDI-TOF spectrum of the HPLC peak with R*t* = 10’ (see **Figure 2-29**) revealed the 1 conjugated linolenate with poly(dT)sequence (**ODN 6**).

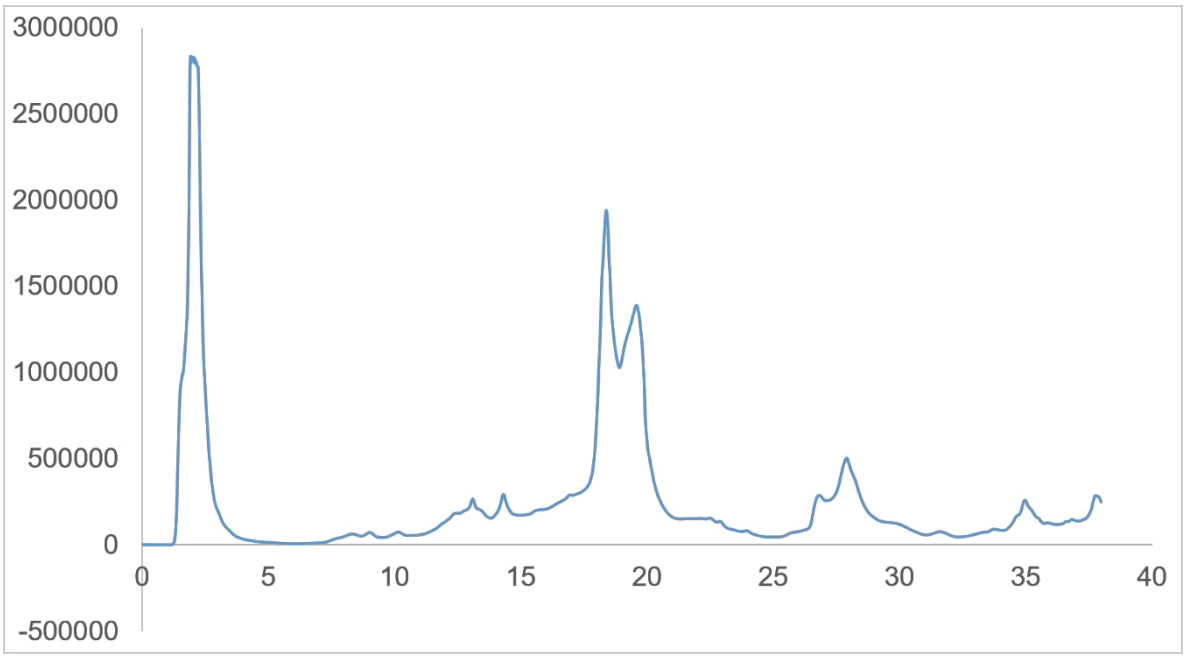

Figure 2-31 HPLC chromatogram of poly(dT)sequence conjugation with linoleate (**ODN 7**). Similar chromatogram was obtained when the reaction was performed at 60°C for 6 hours. HPLC condition: 5C18-MS-II column, 4.6 mm I.D. × 250 mm, flow rate: 1 ml/min, gradient: 0 to 45 min 30% to 100% acetonitrile.

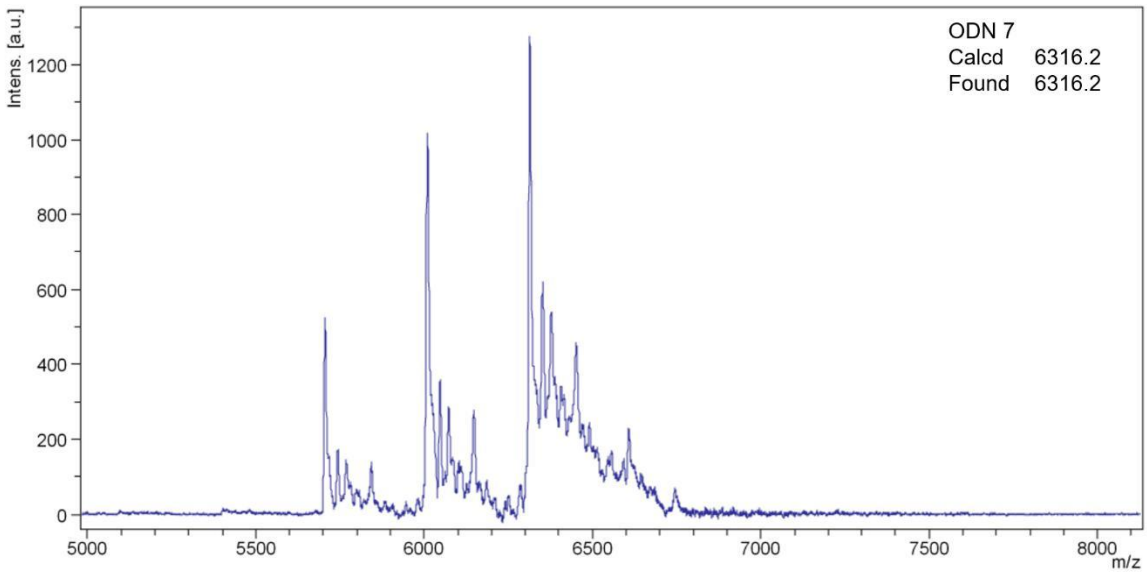

Figure 2-32 MALDI-TOF spectrum of the HPLC peak with R*t* = 13’ (see **Figure 2-31**) revealed the 1 conjugated linoleate with poly(dT)sequence (T20) (**ODN 7**).

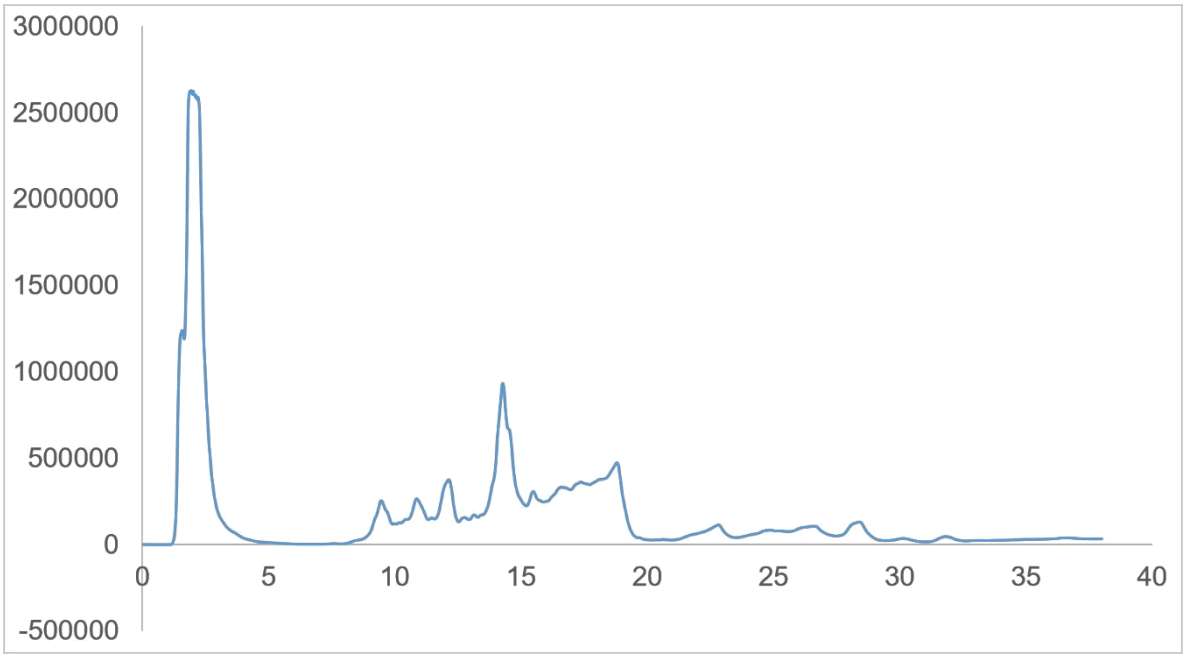

Figure 2-33 HPLC chromatogram of poly(dT)sequence conjugation with oleate (**ODN 8**). Similar chromatogram was obtained when the reaction was performed at 60°C for 6 hours. HPLC condition: 5C18-MS-II column, 4.6 mm I.D. × 250 mm, flow rate: 1 ml/min, gradient: 0 to 45 min 30% to 100% acetonitrile.

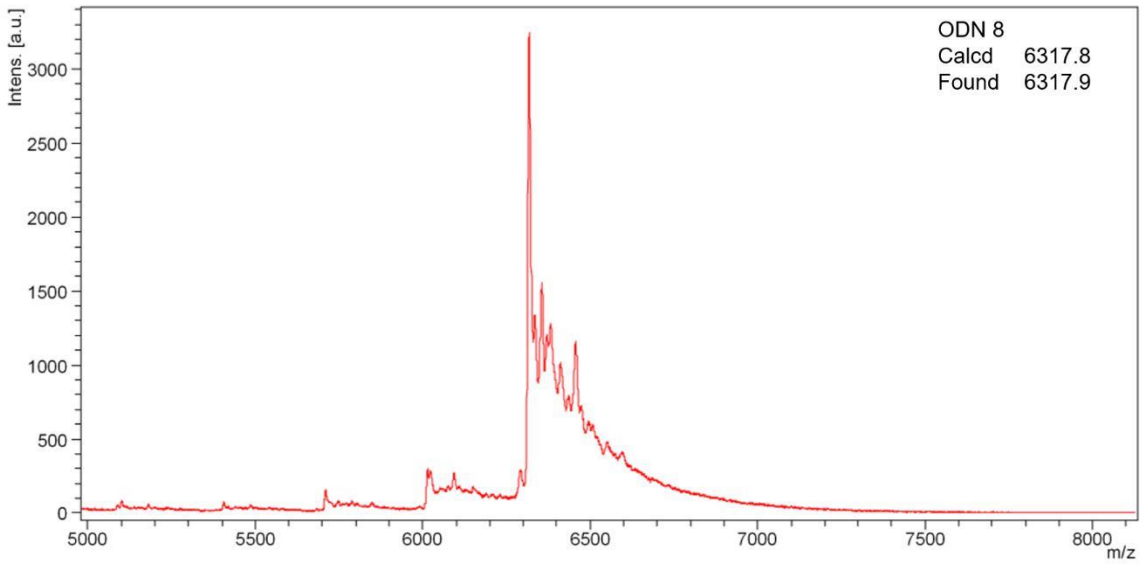

Figure 2-34 MALDI-TOF spectrum of the HPLC peak with R*t* = 11’ (see **Figure 2-33**) revealed the 1 conjugated oleate with poly(dT)sequence (**ODN 8**).

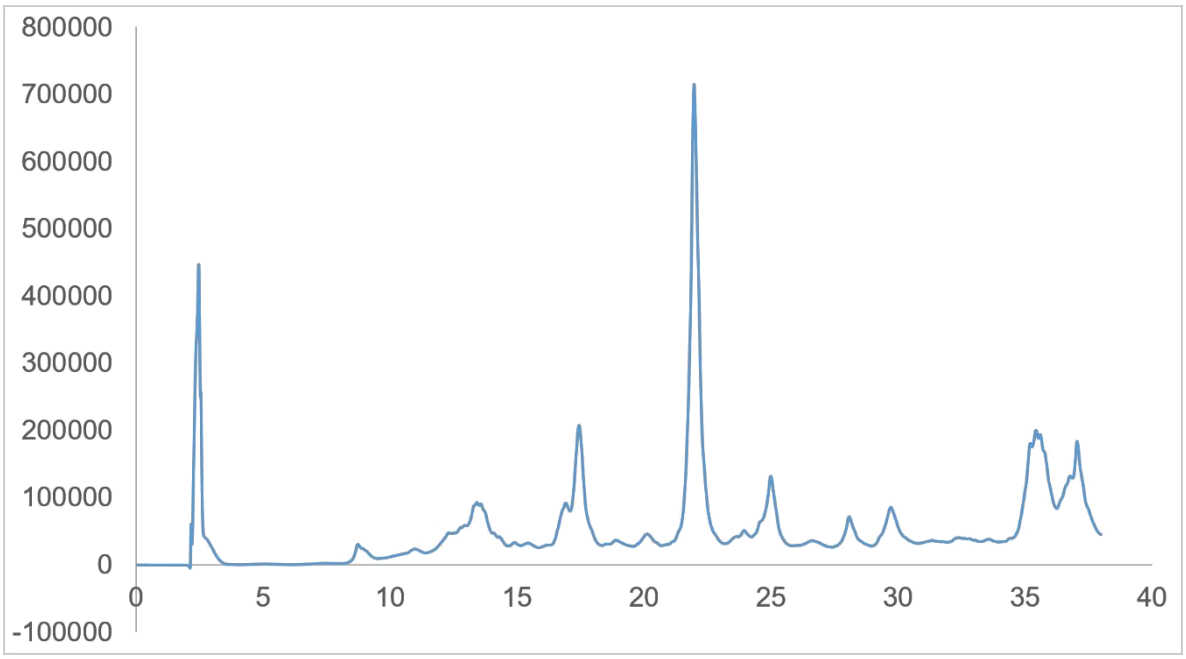

Figure 2-35 HPLC chromatogram of fluorescence poly(dT)sequence conjugation with linolenate (**ODN 9**). Similar chromatogram was obtained when the reaction was performed at 60°C for 6 hours. HPLC condition: 5C18-MS-II column, 4.6 mm I.D. × 250 mm, flow rate: 1 ml/min, gradient: 0 to 45 min 5% to 100% acetonitrile.

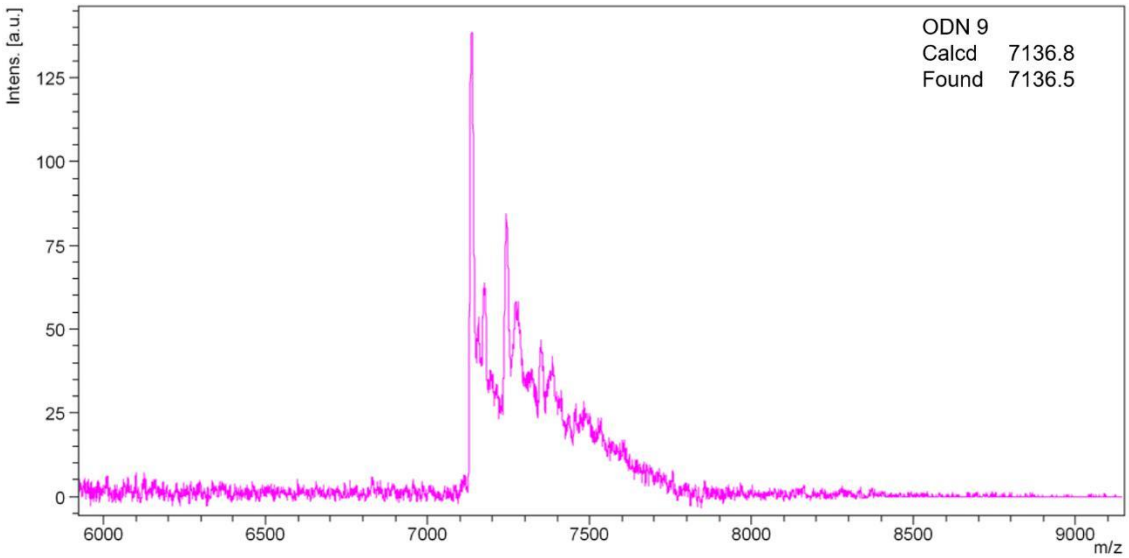

Figure 2-36 MALDI-TOF spectrum of the HPLC peak with R*t* = 17’ (see **Figure 2-35**) revealed the 1 conjugated linolenate with fluorescence poly(dT)sequence (**ODN 9**).

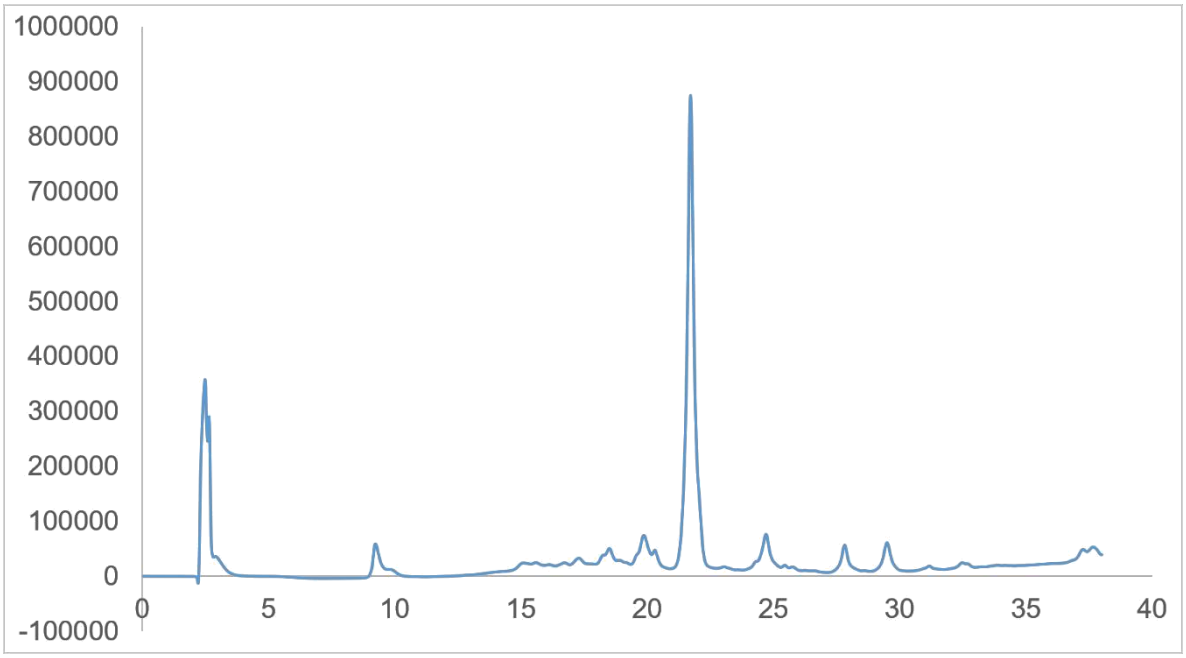

Figure 2-37 HPLC chromatogram of fluorescence poly(dT)sequence conjugation with linoleate (**ODN 10**). Similar chromatogram was obtained when the reaction was performed at 60°C for 6 hours. HPLC condition: 5C18-MS-II column, 4.6 mm I.D. × 250 mm, flow rate: 1 ml/min, gradient: 0 to 45 min 30% to 100% acetonitrile.

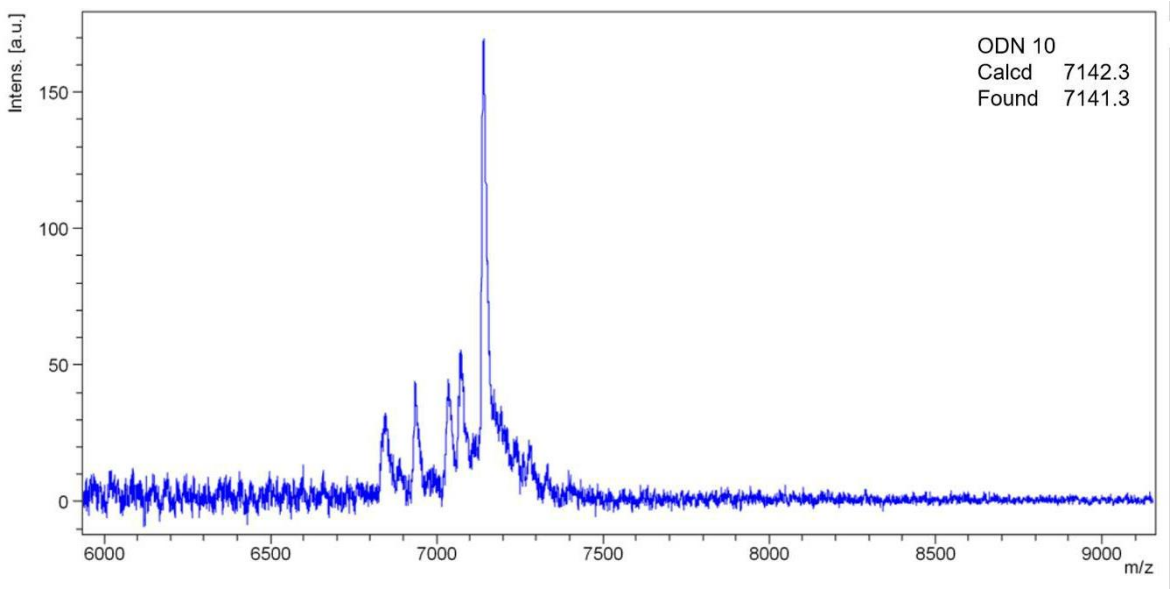

Figure 2-38 MALDI-TOF spectrum of the HPLC peak with R*t* = 17’ (see **Figure 2-37**) revealed the 1 conjugated linoleate with fluorescence poly(dT)sequence (**ODN 10**).

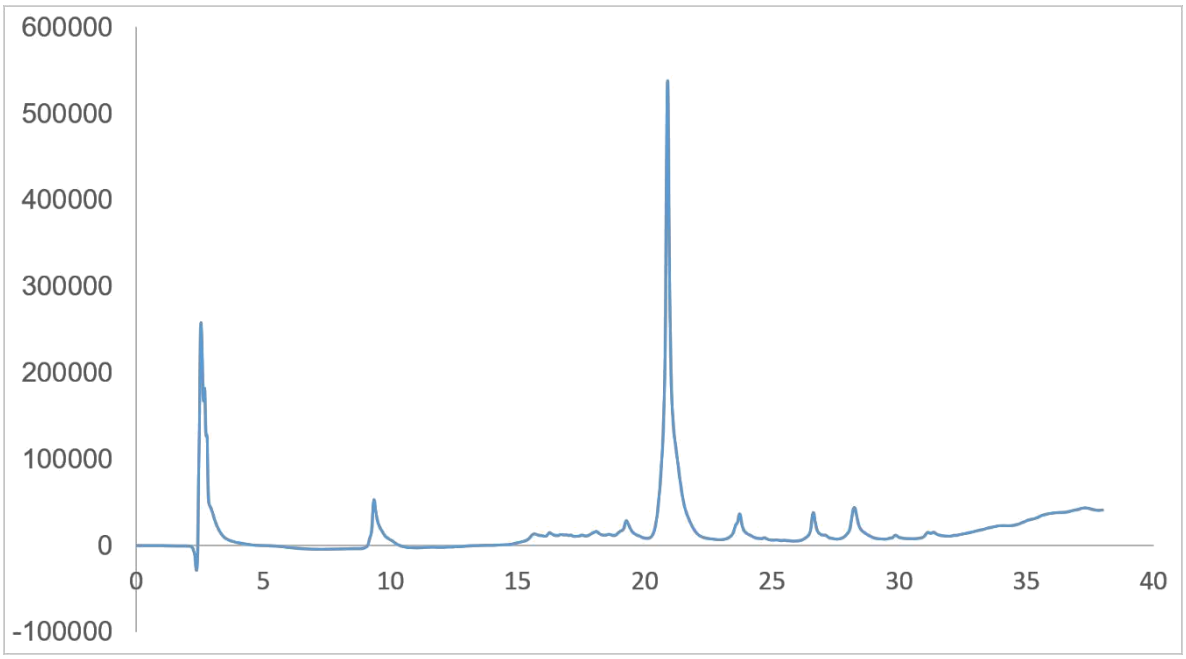

Figure 2-39 HPLC chromatogram of fluorescence poly(dT)sequence conjugation with oleate (**ODN 11**) . Similar chromatogram was obtained when the reaction was performed at 60°C for 6 hours. HPLC condition: 5C18-MS-II column, 4.6 mm I.D. × 250 mm, flow rate: 1 ml/min, gradient: 0 to 45 min 5% to 100% acetonitrile.

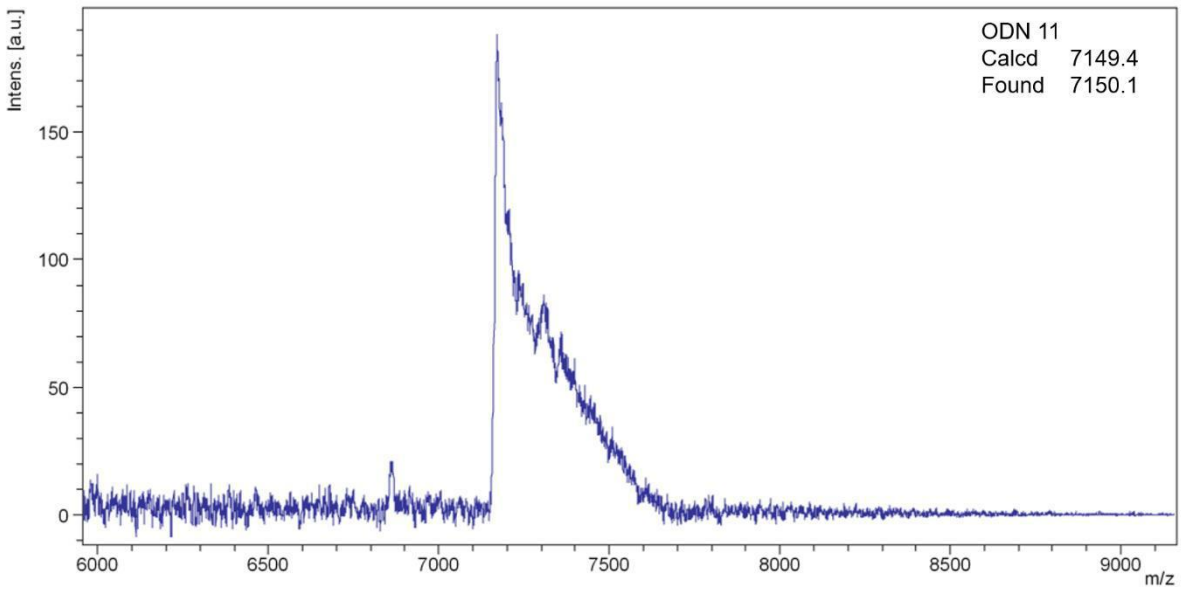

Figure 2-40 MALDI-TOF spectrum of the HPLC peak with R*t* = 17’ (see **Figure 2-39**) revealed the 1 conjugated oleic acid with fluorescence poly(dT)sequence (**ODN 11**).

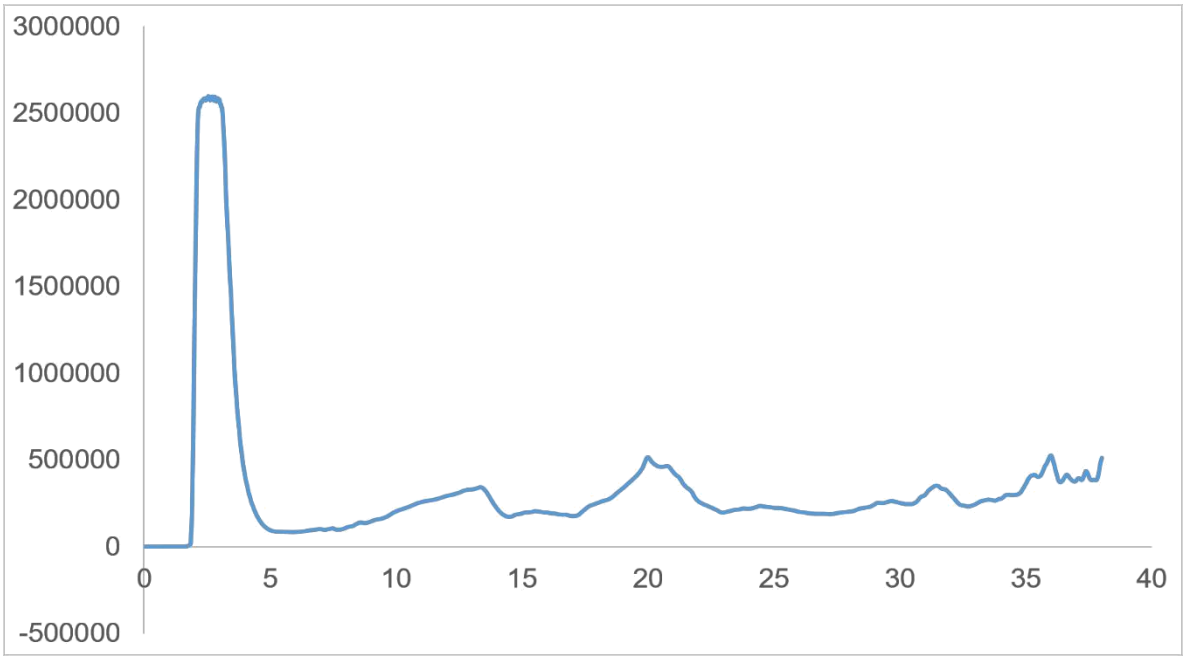

Figure 2-41 HPLC chromatogram of oligonucleotides (**ODN 13**) conjugation with linolenate. Similar chromatogram was obtained when the reaction was performed at 60°C for 6 hours. HPLC condition: 5C18-MS-II column, 4.6 mm I.D. × 250 mm, flow rate: 1 ml/min, gradient: 0 to 45 min 5% to 100% acetonitrile.

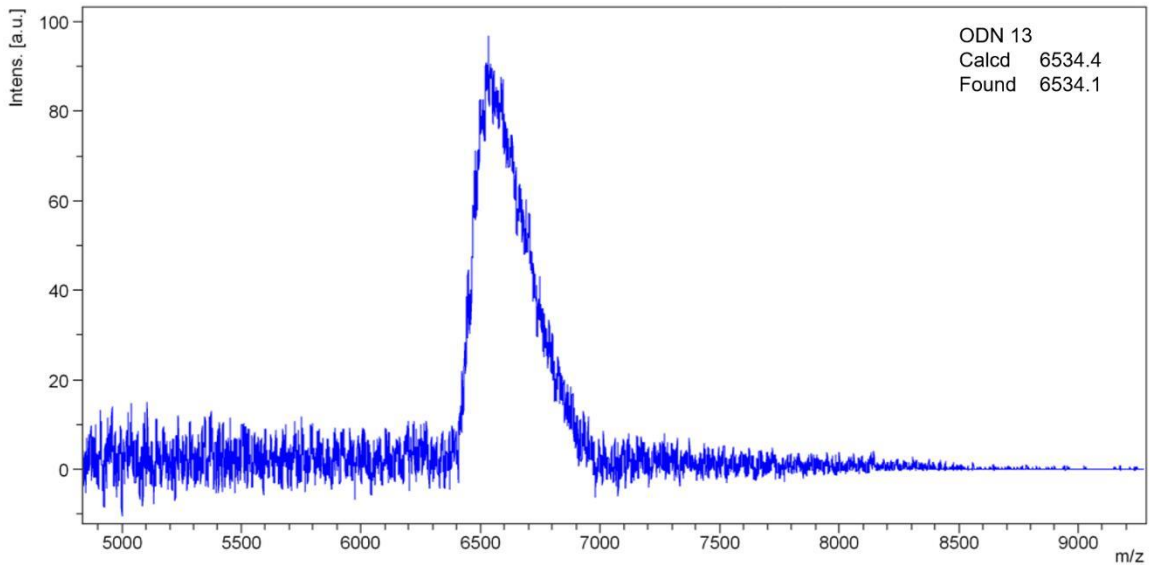

Figure 2-42 MALDI-TOF spectrum of the HPLC peak with R*t* = 9’ (see **Figure 2-41**) revealed the 1 conjugated linolenate with oligonucleotides (**ODN 13**).

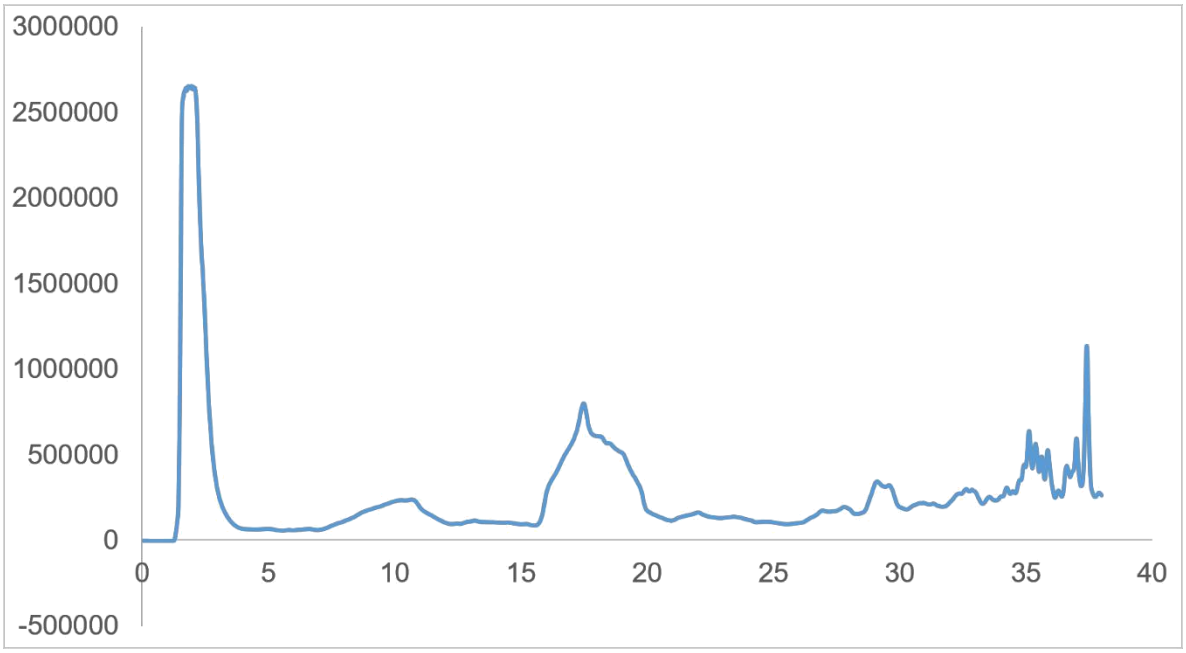

Figure 2-43 HPLC chromatogram of oligonucleotides (**ODN 14**) conjugation with linolenate. Similar chromatogram was obtained when the reaction was performed at 60°C for 6 hours. HPLC condition: 5C18-MS-II column, 4.6 mm I.D. × 250 mm, flow rate: 1 ml/min, gradient: 0 to 45 min 5% to 100% acetonitrile.

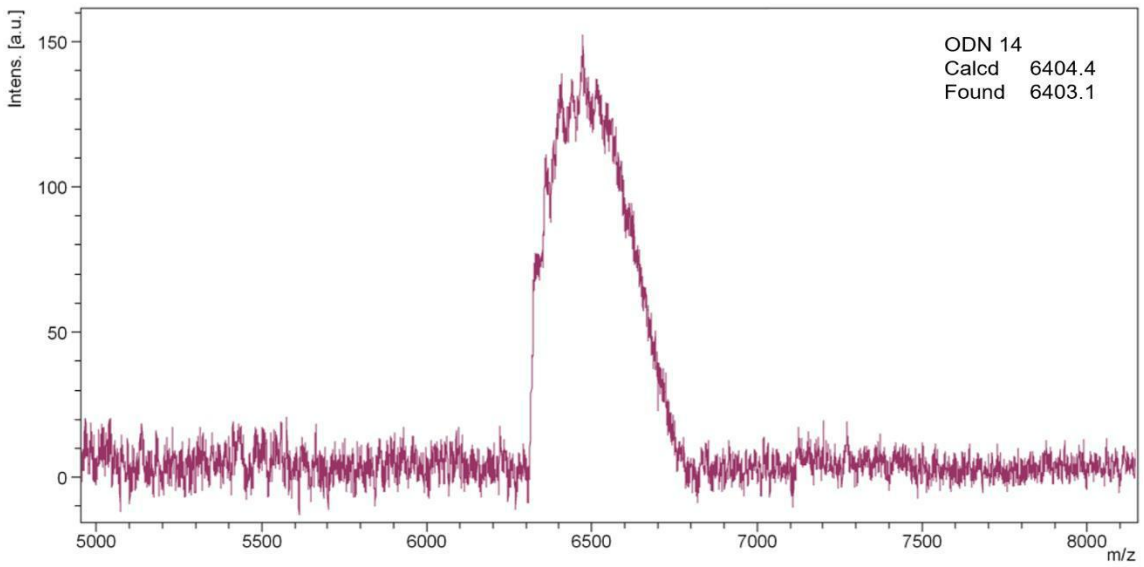

Figure 2-44 MALDI-TOF spectrum of the HPLC peak with R*t* = 9’ (see **Figure 2-44**) revealed the 1 conjugated linolenate with oligonucleotides (**ODN 14**).

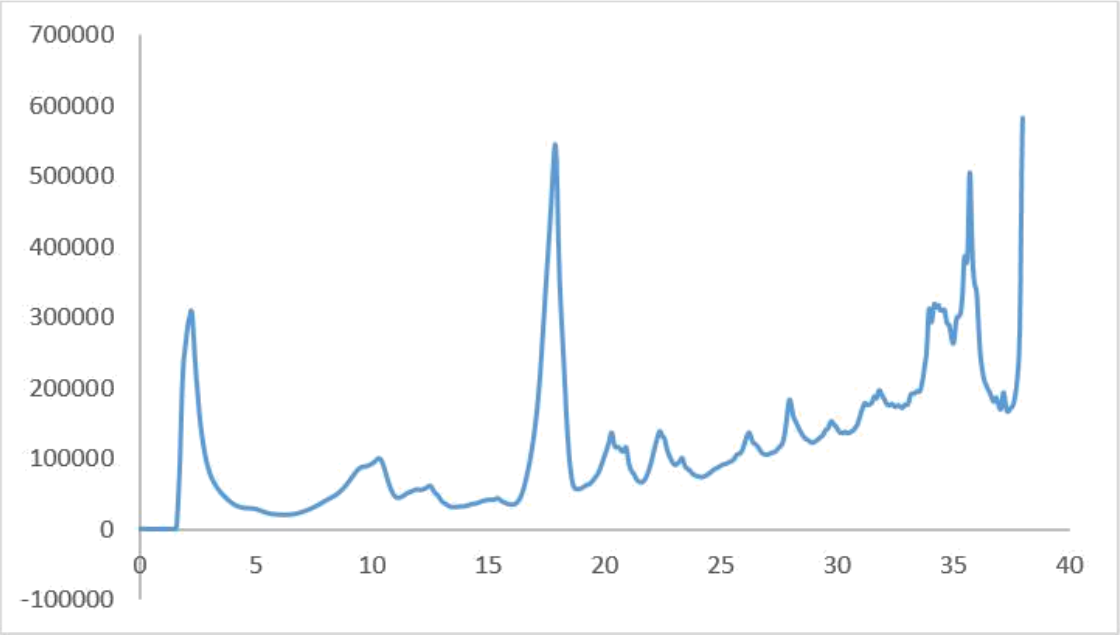

Figure 2-45 HPLC chromatogram of 5'phosphorylation poly(dT) sequence conjugation with linolenic acid. Similar chromatogram was obtained when the reaction was performed at 60°C for 6 hours. HPLC condition: 5C18-MS-II column, 4.6 mm I.D. × 250 mm, flow rate: 1 ml/min, gradient: 0 to 45 min 5% to 100% acetonitrile. No desired products were obtained from HPLC.

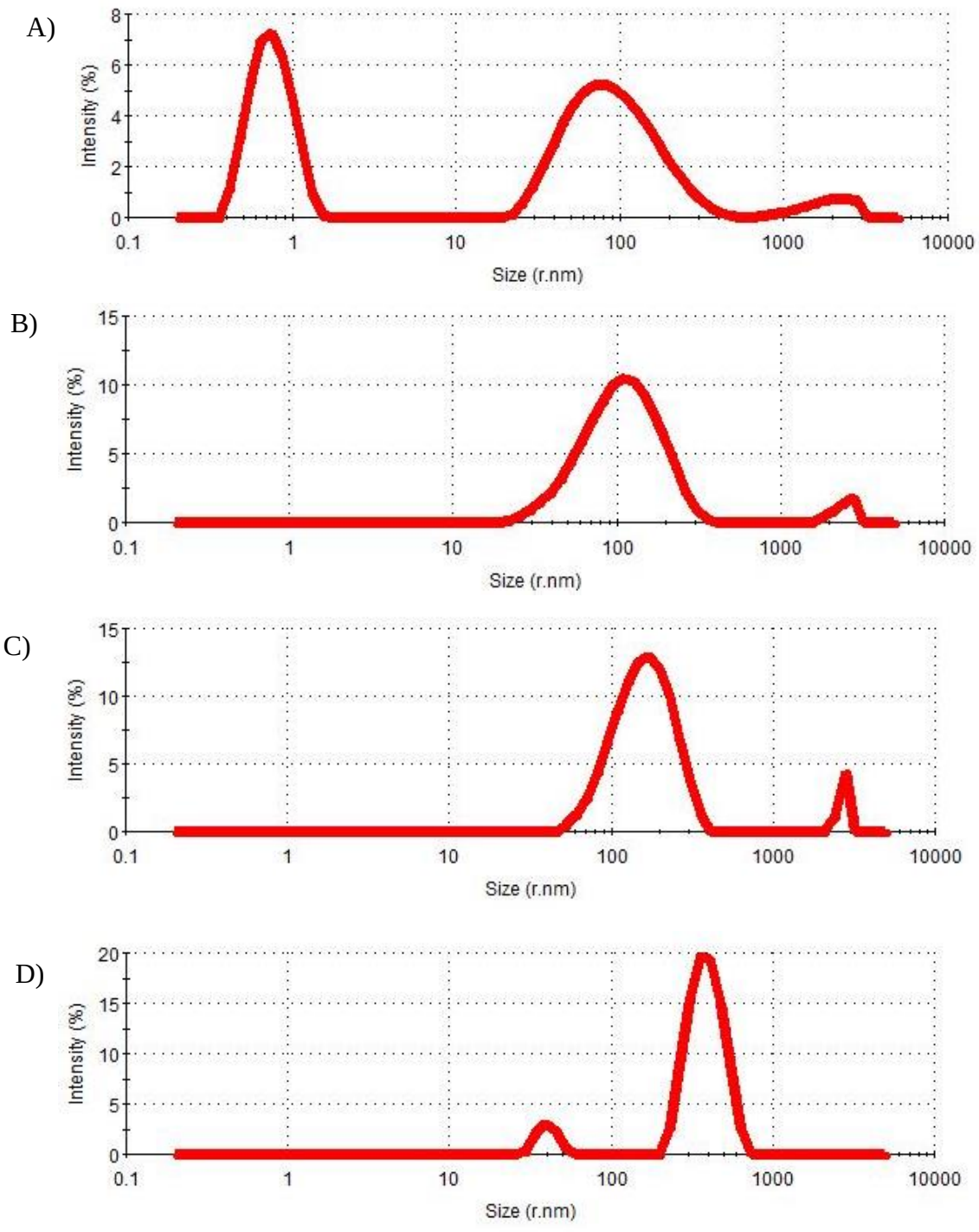

Figure 2-46 Representative size distribution via dynamic light scattering, DLS (A) Poly(dT)sequence (B) Linolenate conjugated poly(dT)sequence (C) Linoleate conjugated poly(dT)sequence (D) Oleate conjugated poly(dT)sequence

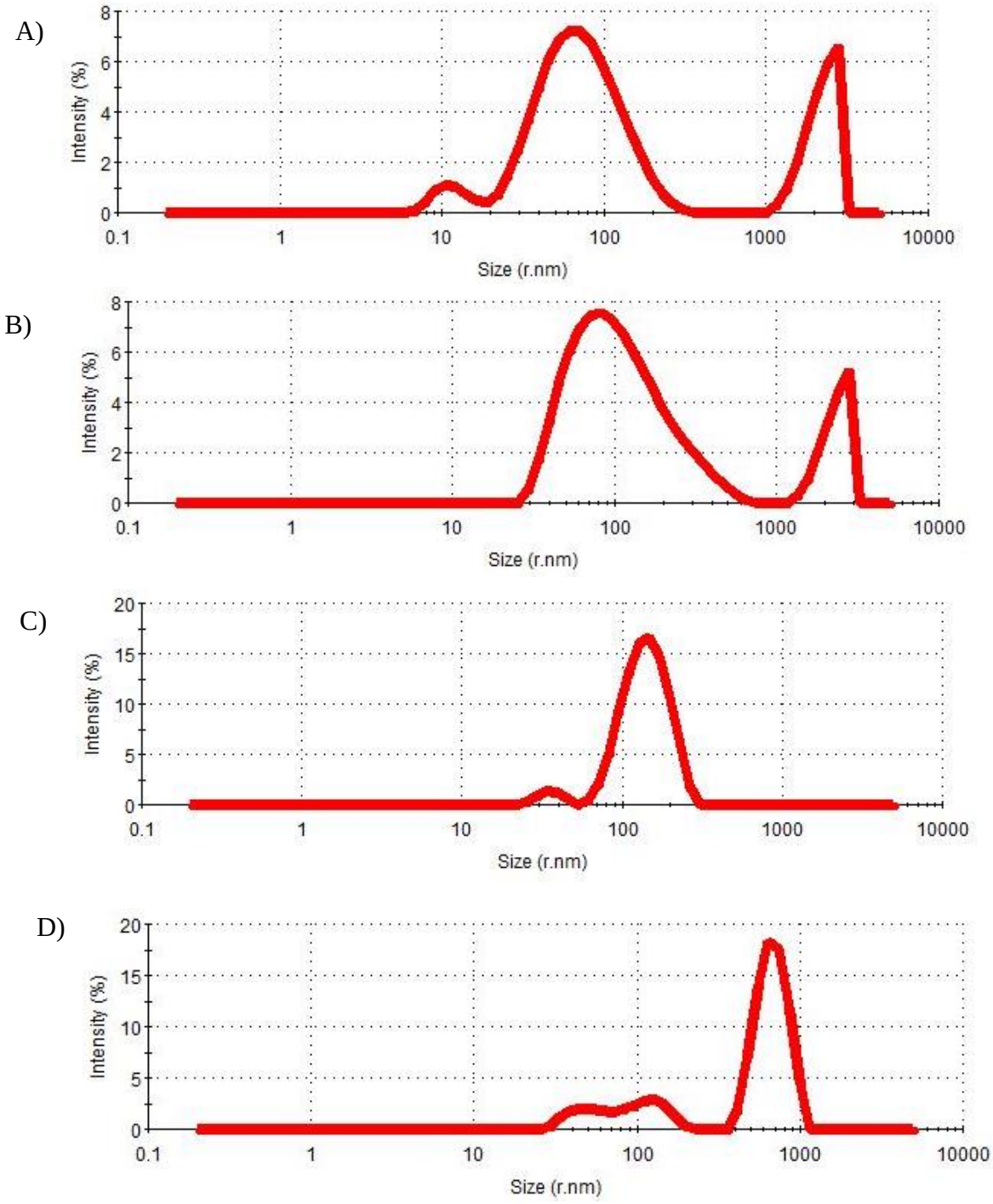

Figure 2-47 Representative size distribution via dynamic light scattering, DLS (A) Fluorescent poly(dT)sequence (B) Linolenate conjugated fluorescent poly(dT)sequence (C) Linoleate conjugated fluorescent poly(dT)sequence (D) Oleate conjugated fluorescent poly(dT)sequence

^{1}H and ^{13}C NMR Charts of Compound **2a**

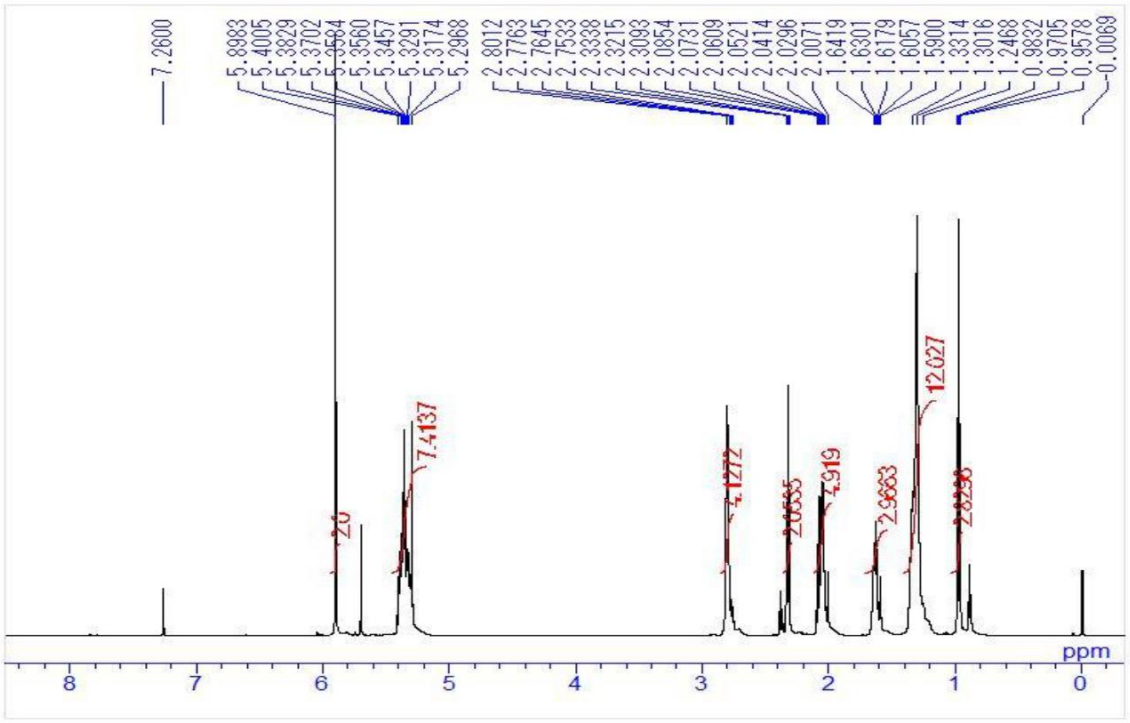

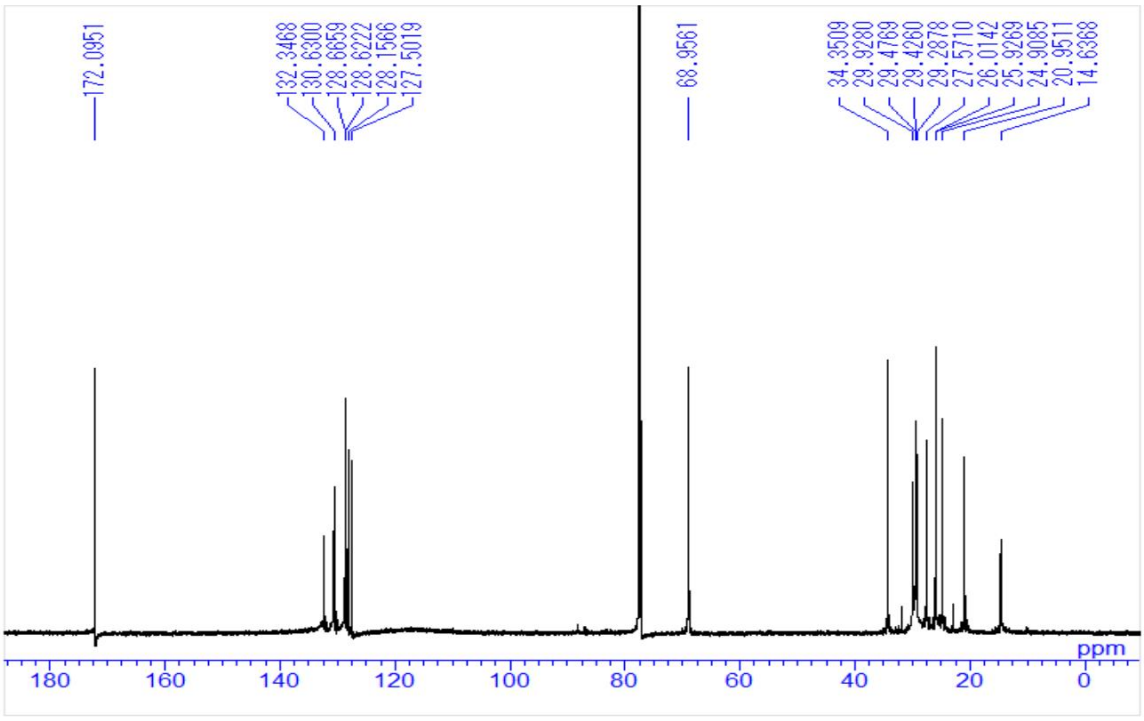

^{1}H and ^{13}C NMR Charts of Compound **2b**

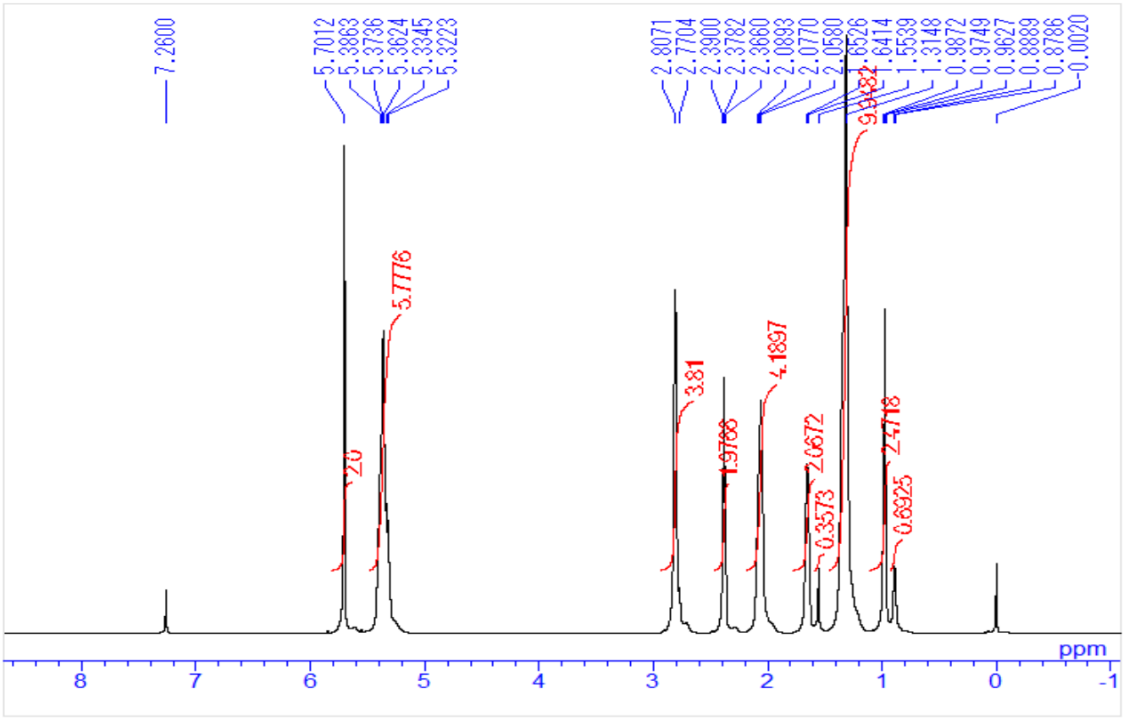

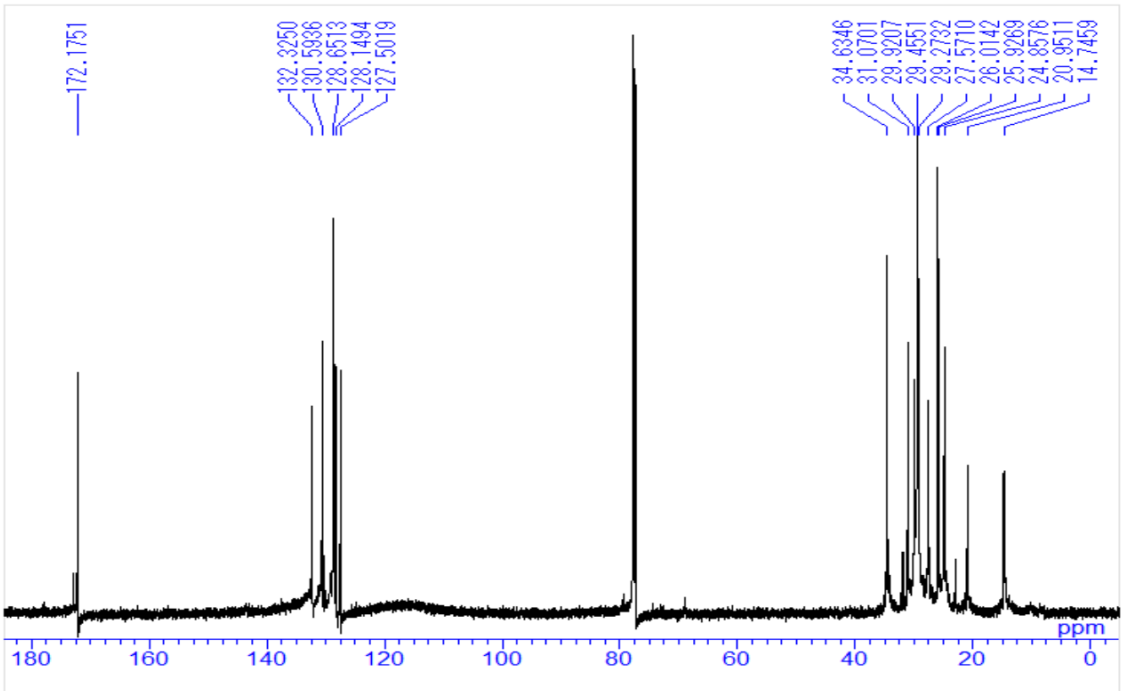

^{1}H and ^{13}C NMR Charts of Compound **2c**

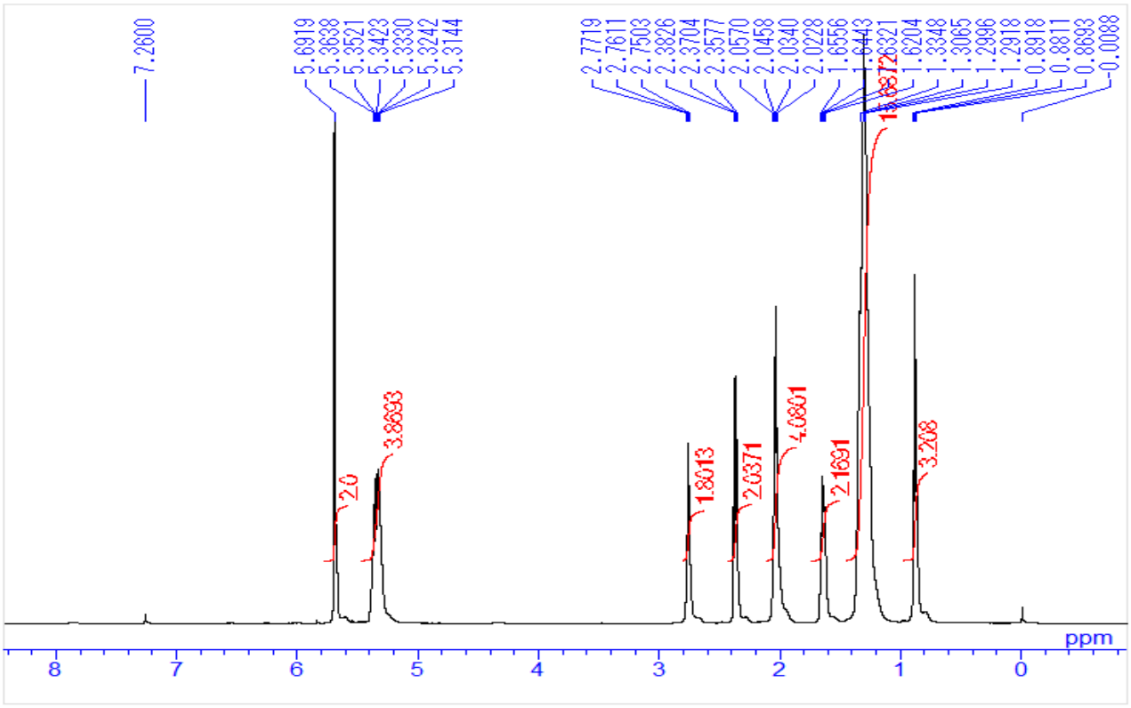

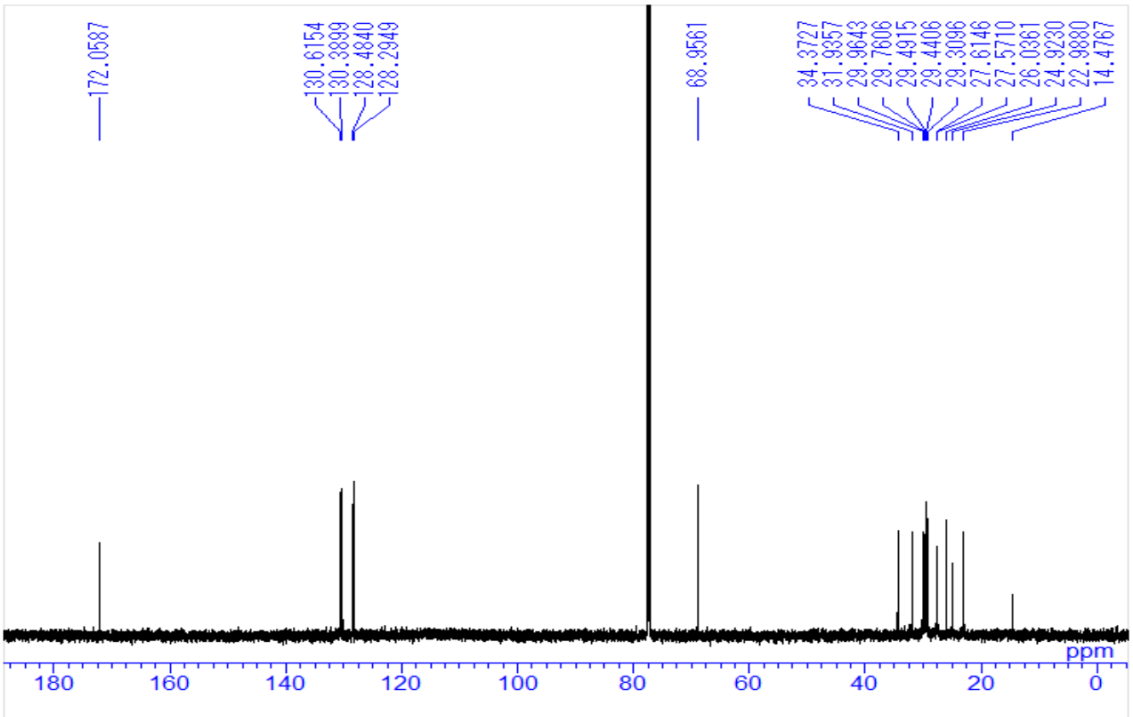

^{1}H and ^{13}C NMR Charts of Compound **3a**

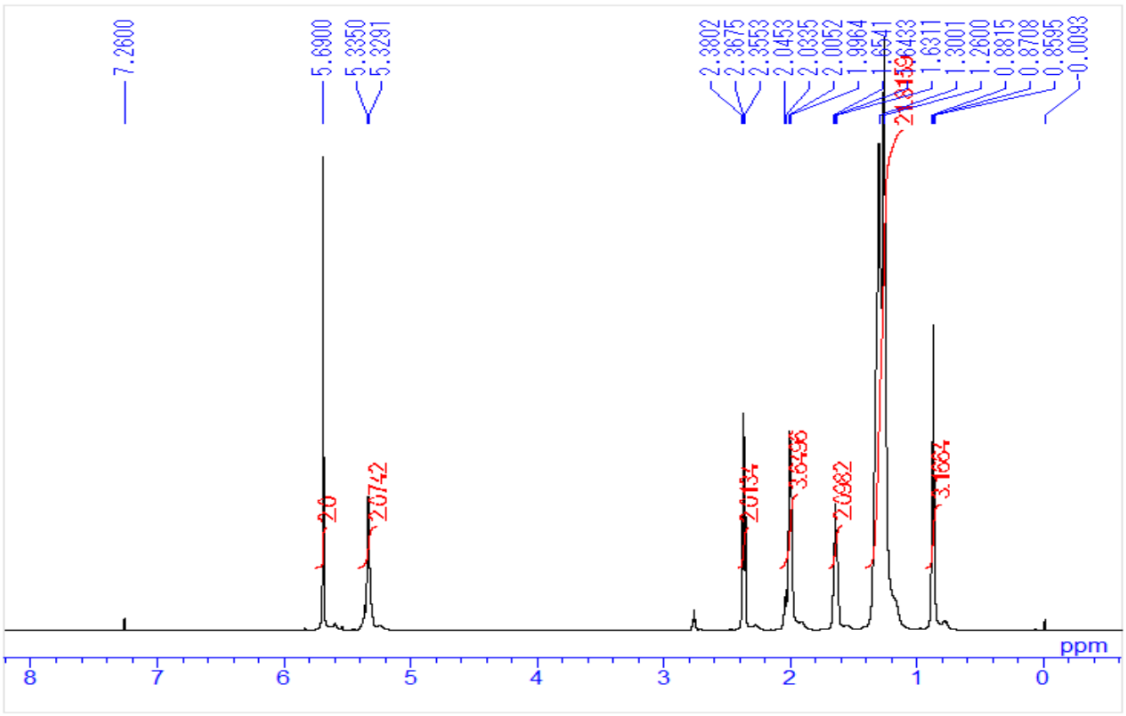

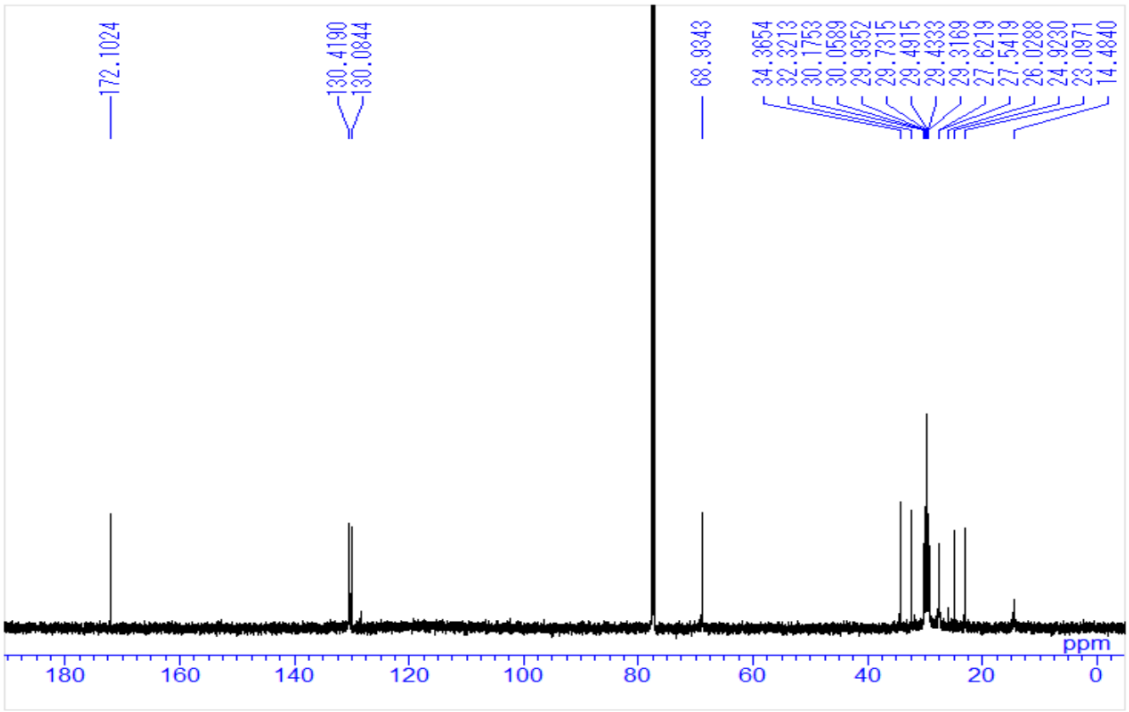

^{1}H and ^{13}C NMR Charts of Compound **3b**

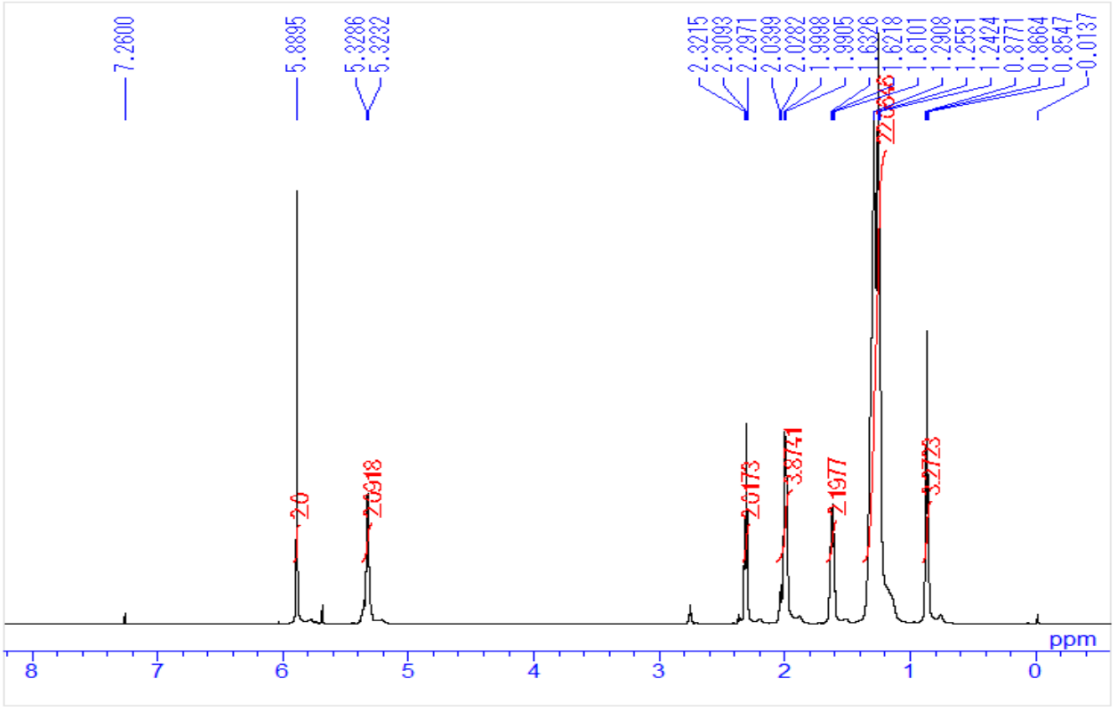

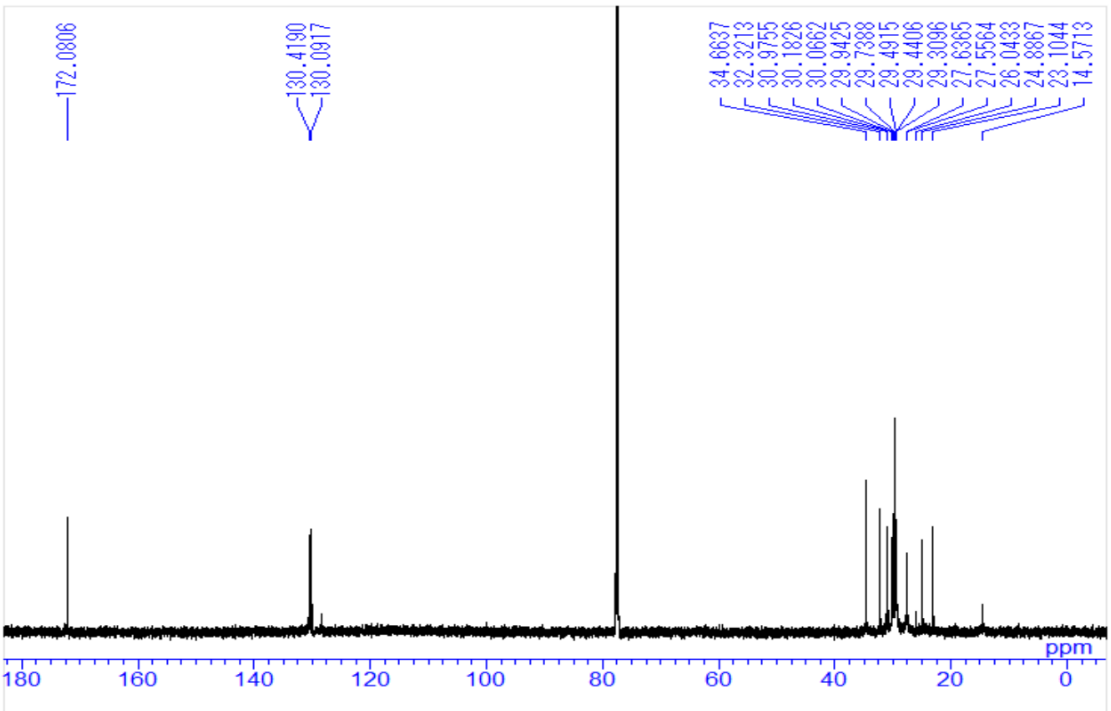

^{1}H and ^{13}C NMR Charts of Compound **3c**

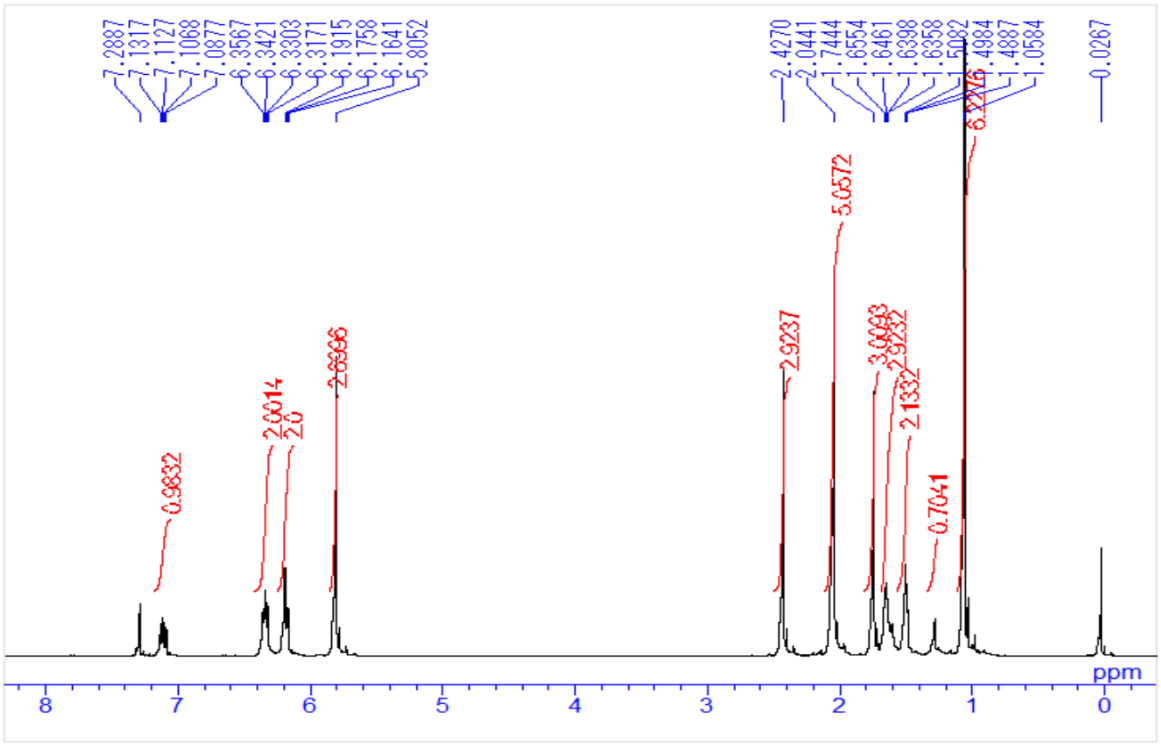

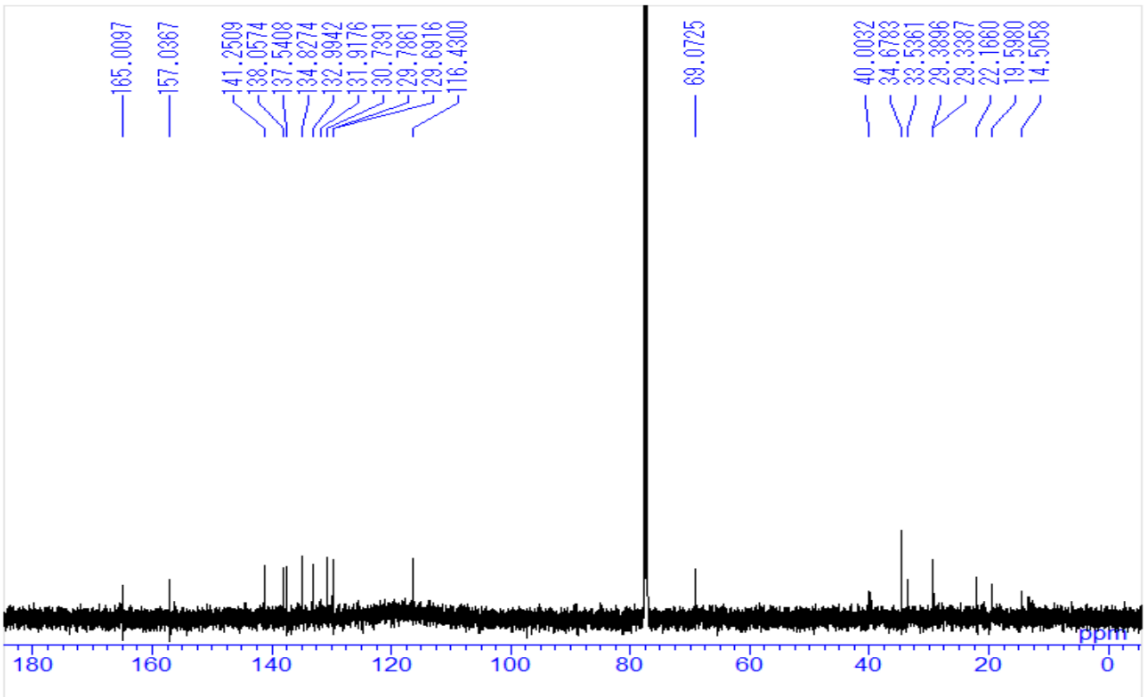

2.6 Reference

1. Opalinska, J.B., and Gewirtz, A.M., Nucleic acid therapeutics: basic principles and recent applications, Nature Reviews of Drug Discovery, 2002, 1: 503-514.

2. Manoharan, M., Oligonucleotide conjugates as potential antisense drugs with improved uptake, biodistribution, targeted delivery, and mechanism of action, Antisense and Nucleic Acid Drug Development, 2002, 12: 103-128.

3. de Fougerolles, A., Vornlocher, H.P., Maragenore, J., and Lieberman, J., Interfering with disease: a progress report on siRNA-based therapeutics. Nature Reviews of Drug Discovery, 2007, 6: 443-453.

4. Lukashev, A., and Zamyatnin, A.A., Viral vectors for gene therapy: current state and clinical perspectives, Biochemistry (Moscow), 2016, 81: 700-708.

5. Kuo, W.T., Huang, H.Y., Huang, Y.Y., Intracellular trafficking, metabolism and toxicity of current gene carriers, Current Drug Metabolism, 2009, 885-894.

6. Raouane, M., Desmaela, D., Urbinati, G., and Massad-Massade, L., Lipid conjugated oligonucleotides: a useful strategy for delivery, Bioconjugate Chemistry, 2012, 23: 1091-1104.

7. Raouane, M., Desmaele, D., Gilbert-Sirieix, M., Gueutin, C., Zouhiri, F., Bourgaux, C., Lepeltier, E., Gref, R., Salah, R.B., Clayman, G., and Massaad-Massade, L., Synthesis, characterization, and *in vivo* delivery of siRNA-squalene nanoparticles targeting fusion oncogene in papillary thyroid carcinoma, Journal of Medicinal Chemistry, 2011, 54: 4067-4076.

8. Sauer, L.A., and Dauchy, R.T., The effect of omega-6 and omega-3 fatty acids on 3H-thymidine incorporation in hepatoma 7288CTC perfused in situ. British Journal of Cancer, 1992, 66: 297-303.

9. Bradley, M.O., Webb, N.L., and Anthony, F.H., Tumor Targeting by Covalent Conjugation of a Natural Fatty Acid to Paclitaxel, Clinical Cancer Research, 2001, 7: 3229-3238.

10. Kuznetsova, L.V., and Chen, J.S., Syntheses and evaluation of novel fatty acid-second-generation taxoid conjugates as promising anticancer agents, Bioorganic Medicinal Chemistry Letter, 2006, 16: 974-977.

11. Wang, Y.L., and Jiang, W., Synthesis and preliminary antitumor activity evaluation of a DHA and doxorubicin conjugate, Bioorganic Medicinal Chemistry Letter, 2006, 16, 2974-2977.

12. Soutschek, J., Akinc, A., Bramlage, B., Charisse, K., Constien, R., Donoghue, M., Elbashir, S., Geick, A., Hadwiger, P., Harborth, J., John, M., Kesavan, V., Lavine, G., Pandey, R. K., Racie, T., Rajeev, K. G., Rohl, I., Toudjarska, I., Wang, G., Wuschko, S., Bumcrot, D., Koteliansky, V., Limmer, S., Manoharan, M., and Vornlocher, H. P., Therapeutic silencing of an endogenous gene by systemic administration of modified siRNAs Nature, 2004, 432, 173– 178.

13. Moschos, S. A., Jones, S. W., Perry, M. M., Williams, A. E., Erjefalt, J. S., Turner, J. J., Barnes, P. J., Sproat, B. S., Gait, M. J., and Lindsay, M. A., Lung delivery studies using siRNA conjugated to TAT(48–60) and penetratin reveal peptide induced reduction in gene expression and induction of innate immunity, Bioconjugate Chemistry, 2007, 18, 1450– 1459.

14. Nishina, K., Unno, T., Uno, Y., Kubodera, T., Kanouchi, T., Mizusawa, H., and Yokota, T., (2008) Efficient in vivo delivery of siRNA to the liver by conjugation of alpha-tocopherol, Molecular Therapy, 2008, 16, 734– 740.

15. Wolfrum, C., Shi, S., Jayaprakash, K.N., Jayaraman, M., Wang, G., Pandey, R.K., Rajeev, K.G., Nakayama, T., Charrise, K., Ndungo, E.M., Zimmermann, T., Koteliansky, V., Manoharan, M., and Stoffel, M., Mechanisms and optimization of in vivo delivery of lipophilic siRNAs, Nature Biotechnology. 2007, 1149-1157.

16. Ueno, Y., Kawada, K., Naito, T., Shibata, A., Yoshikawa, K., Kim, H.S., Wataya, Y., Kitade, Y., Synthesis and silencing properties of siRNAs possessing lipophilic groups at their 3′-termini, Bioorganic Medicinal Chemistry. 2008, 16: 7698-7704.

17. Hecker, S.J., and Erion, M.D., Prodrugs of phosphates and phosphonates, Journal of Medicinal Chemistry. 2008, 51: 2328-2345.

18. Perez, C., Daniel, K.B., and Cohen, S.M., Evaluating prodrug strategies for esterase-triggered release of alcohols, ChemMedChem, 2013, 8, 1662-1667.

19. Burgos-barragen, G., Wit, N., Meiser, J., Dingler, F.A., Pietzke, M., Pontel, L.B., Rosado, I.V., Brewer, T.F., Cordell, R.L., Monks, P.S., Chang, C.J., Vazquez, A., and Petel, K.J., Mammals diverts endogenous genotoxic formaldehyde into one-carbon mechanism, Nature, 2017, 548, 549-612.

20. Irby, D., Du, C., and Li, F., Lipid-drug conjugate for enhancing drug delivery, Molecular Pharmaceutics, 2017, 14, 1325-1338.

21. Schultz, C., Vajanaphanich, M., Harootuniant, A.T., Sammak, P.J., Barrett, K.E., and Tsien, R.Y., Acetoxymethyl esters of phosphates, enhancement of the permeability and potency of cAMP, The Journal of Biological Chemistry, 1993, 268: 6316-6322.

22. Almarrson, O.; Blumberg, L.C.; Remenar, J.F., U.S.Patent, 2010

23. Wang, J., Luo, T., Li, S., and Zhao, J., The powerful application of polyunsaturated fatty acids in improving the therapeutic efficacy, Expert Opinion on Drug Delivery, 2012, 9: 1-7.

24. Kitagawa, M., and Okamoto, A., Rapid nuclear import of short nucleic acids, Bioorganic Medicinal Chemisty Letters, 2016, 26, 4568-4570.

25. Patwa, A., Gissot, A., Bestel, I., and Barthelemy, P., Hybrid lipid oligonucleotide conjugates: synthesis, self-assemblies and biomedical applications, The Royal Society of Chemistry, 2011, 40: 5844-5854.

26. Kwak, M., and Herrmann, A., Nucleic acid amphiphiles: synthesis and self-assembled nanostructures, Chemical Society Reviews, 40: 5745-5755.

27. Gosse, C., Boutorine, A., Aujard, I., Chami, M., Kononov, A., Cogne-Laage, E., Allemand, J.-F., Li, J., and Jullien, L., Micelles of lipid-oligonucleotide conjugates: Implications for membrane anchoring and base paring, Journal of Physical Chemistry, 2004, 108: 6485-6497.

28. Pfeiffer, I, and Hoeoek, F., Bivalent cholesterol-based coupling of oligonucletides to lipid membrane assemblies, Journal of the American Chemical Society, 2004, 126: 10224-10225.

29. Pfeiffer, I, and Hoeoek, F., Quantification of oligonucleotide modifications of small unilamellar lipid vesicles, Analytical Chemistry, 2006, 87: 7493-7498.

30. Bunge, A., Loew, M., Pescador, P., Arbuzova, A., Brodersen, N., Kang, J., Dahne, Lars., Liebscher, Jurgen., Herrmann, Andreas., Stengel, Gudrun., and Huster, Daniel., Lipid membranes carrying lipophilic cholesterol-based oligonucleotides-characterization and application on Layer-by-Layer coated particles, Journal of Physical Chemistry, 2009, 113: 16425-16434.

31. Filippo, G., Banchelli, M., Durand, A., Berti, D., Bronw, T., Caminati, G., and Baglioni, P., Modulation of density and orientation of amphiphilic DNA anchored to phospholipid membrane. I. Supoorted Lipid Bilayers, Journal of Physical Chemistry, 2010, 114: 7338-7347.

32. Rejman, J., Oberle, V., Zuhorn, I.S., and Hoekstra, D., Size-dependent internalization of particles via the pathway of clathrin- and caveolate-mediated endocytosis, Biochemical Journal, 2004, 377: 159-169.

33. Wilner, E.S., Sparks, S.E., Cowburn, D., Girvin, M.E., and Levy, M., Controlling lipid micelle stability using oligonucleotide headgroups, Journal of American Chemical Society, 2015, 137: 2171-2174.

34. Cozzoli, L., Gjonaj, L., Stuart, M., Poolman, B., and Roelfes, G., Responsive DNA G-quadruplex micelles, Chemical Communications, 54: 260-263.

35. Chen, H., Sungwon, K., He, Wei, Wang, H., Low, P.S., Kinam, P., and Ji-xin, C., Fast release of lipophilic agents from circulating PEG-PDLLA micelles revealed by *in vivo* Foerster Resonance Energy Transfer Imaging, Journal of American Chemical Society, 2008, 24: 5213-5217.

36. Abdersona, M., Moshnikovaa, A., Engelmanb, D.M., Reshetyaka, Y.K., and Andreeva, O.A., Prove for the measurement of cell surface pH in vivo and exvivo, PNAS, 2.016, 113: 8177-8181.

*+37. Hayashi, G., Yanase, M., Takeda, K., Sakakibara, D., Sakamoto, R., Wang, D.O., and Okamoto, A., Hybridization-sensitive fluorescent oligonucleotide probe conjugated

with a bulky module for compartment-specific mRNA monitoring in a living cell., Bioconjugate Chemistry, 2015, 26: 412-417.

Chapter 3

4-nitrobenzyl caged oligonucleotides

3.1 Abstract

Intracellular delivery of oligonucleotides is essential for oligonucleotides therapeutics such as antisense oligonucleotides, miRNAs and siRNAs. The methodologies involving the molecular modification of oligonucleotides with synthetic moieties have emerged as promising strategy for the effective delivery of oligonucleotides. In this report, we synthesized oligonucleotide pro-drugs bearing 4-nitrobenzyl reduction-activated protecting groups. 4-nitrobenzyl caged oligonucleotides were amenable to post DNA modification and purification. Moreover, alkyne-linked 4-nitrobenzyl caged oligonucleotides was synthesized and incorporated into oligonucleotides. Subsequently, these oligonucleotides were conjugated to linolenate molecules using a copper-catalyzed alkyne-azide cycloaddition.

3.2 Introduction

Oligonucleotides-based therapeutics such as antisense oligonucleotides, miRNAs and siRNAs have been developed to treat various human disorders including to increase the understanding of pharmacological processes in human body [1-3]. However, the application of oligonucleotides-based therapeutics has been limited due to poor bioavailability and cellular penetration. The physicochemical properties of cell membranes are the barriers of the oligonucleotides delivery into the cells. In addition, the polyanionic and hydrophilic properties of oligonucleotides are the major factors that prevent the passive diffusion to the cells. The development of the efficient delivery of oligonucleotides-based therapeutics to the target cell is highly desired for the therapeutic purpose[4-5]. To date, various delivery systems of oligonucleotide delivery including viral and nonviral vector oligonucleotides delivery has been developed[6]. In addition, the pro-oligonucleotides method was developed in the -1990s[7-10]. This method is depended on the biodegradable functional group for the protection of phosphate group on the internucleotide linkages of oligonucleotides. After transferring pro-oligonucleotides into the cell, the endogenous enzyme such as esterase in the cells will be cleaved pro-oligonucleotides to release the active oligonucleotides without any transfection reagent. The advantages of this methods are typically resistant to nucleases, no need any transfection reagents and the amenable to protect phosphate group with several functional group[5].

The development of hypoxia-activated prodrugs are preferably attracted for the therapeutic entity under hypoxic conditions[11 -12]. Hypoxia is the conditions of advanced solid tumors, which produce insufficient of oxygen and has poorly developed vasculature. Hypoxia can induce the resistant of chemotherapy and radiation therapy[13]. There are several reports about the hypoxic tumors treatment by using pro-drug under this conditions[14]. The prodrugs are normally protected with hypoxia-labile protecting groups. Prodrugs are can be removed into the active forms under hypoxic conditions.

There are several reports mentioned about the synthesis of pro-oligonucleotide containing 4-nitrobenzyl group that is applied for hypoxic conditions[15-19]. The 4-nitrobenzyl groups are cleaved by the nitro group reduction to the hydroxyamino group following by a 1,6- elimination process to release the active oligonucleotides (**Figure 3-1**). Therefore, the hypoxic tumor can converted pro-oligonucleotides to active oligonucleotides that hybridizes to the target RNA sequences in the target cells.

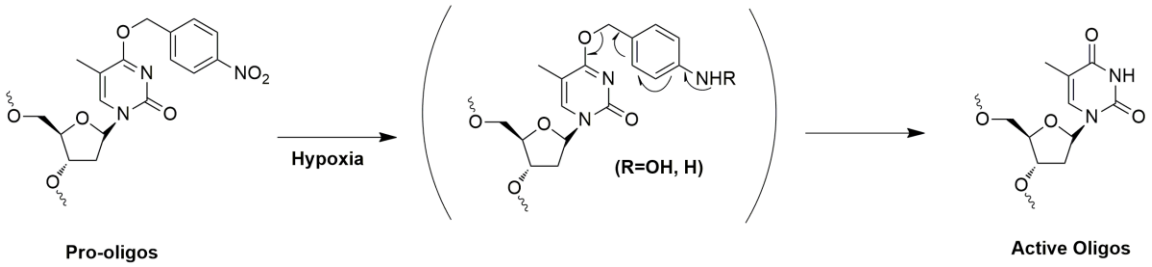

Figure 3-1 Proposed reaction process for the deprotection of 4-nitrobenzyl groups under hypoxic conditions

In this study, we design and synthesize oligonucleotides containing 4-nitrobenzyl groups on phosphate internucleotide linkages via post-modification of DNA strands for the application in a large oligonucleotides. As a model experiment in hypoxic cells, oligonucleotides containing 4-nitrobenzyl group were treated with nitro-reductase in the presence of NADPH for the conversion into free oligonucleotides. Moreover, according to my previous studies of polyunsaturated fatty acids conjugated oligonucleotides, linolenic acid conjugated fluorescence poly(dT)sequence showed the outstanding cellular uptake in HeLa cells. I tried to link linolenic acid to 4-nitrobenzyl group to improve the cellular uptake.

3.3 Results and Discussion

Rationale

Light-activated RNA Interference (LARI) is an effective way to control gene expression with light. This, in turn, allows for the spacing, timing and degree of gene expression to be controlled by the spacing, timing and amount of light irradiation. The key meidiators of this process are siRNA or dsRNA that have been modified with four photocleavable groups of dimethoxy nitro phenyl ethyl (DMNPE), located on the four terminal phosphate groups of the duplex RNA. The modification is performed by using a of dimethoxy nitro phenyl ethyl (DMNPE) group by the oxidation of a hydrazone precursor into the diazo form, which then efficiently reacts with the four terminal phosphate groups of RNA duplex[20] (**Figure 3-2**).

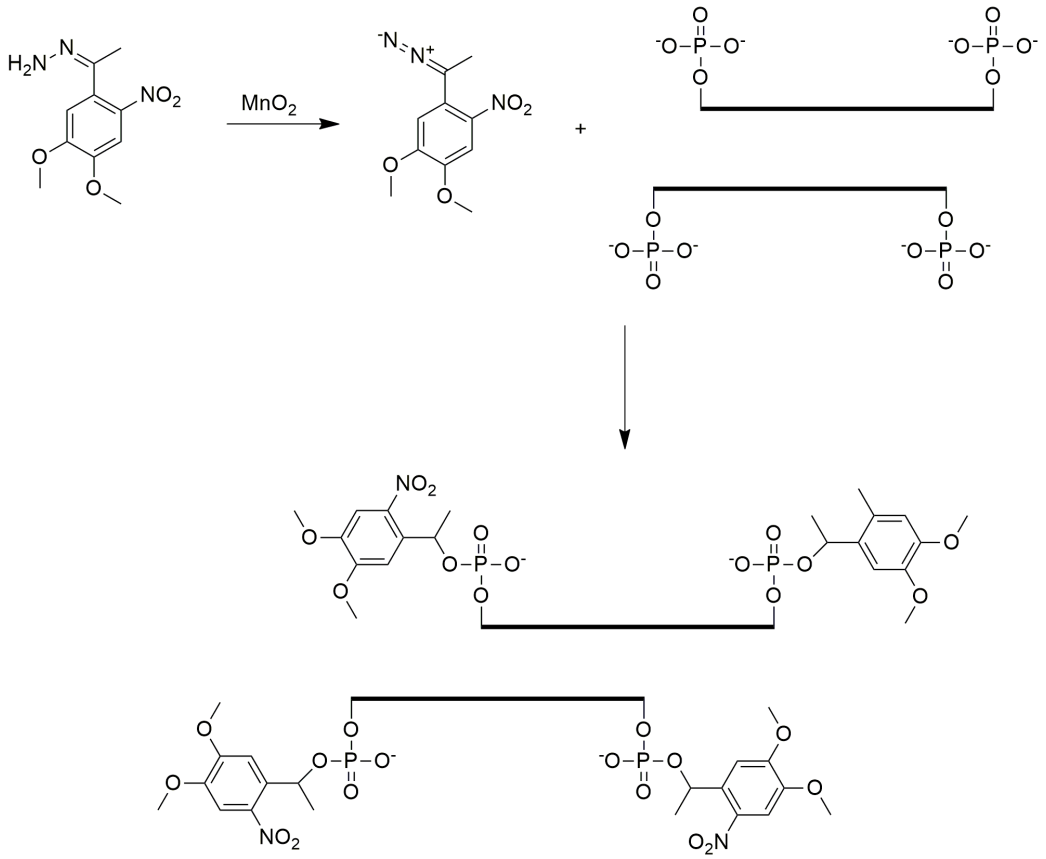

Figure 3-2 Introduction of four photocleavable DMNPE groups into siRNA/dsRNA. Four phosphate groups are introduced synthetically into the four termini of the RNA duplex. DMNPE hydrazone is converted into diazo-DMNPE, which then regiospecifically reacts with the four terminal phosphates to make the final tetra-modified species

The caging reaction via the oxidation of a hydazone precursor is also used with the compound 6-bromo-4-diazomethyl-7-hydroxycoumarin (Bhc-diazo), which forms phosphate moiety of the sugar-phosphate of RNA[21] (**Figure 3-3**). The 6-bromo-7-hydroxycoumarin-4-ylmethyl (Bhc) group binds to approximately 30 sites on the phosphate moieties per 1 kb of RNA sequence.

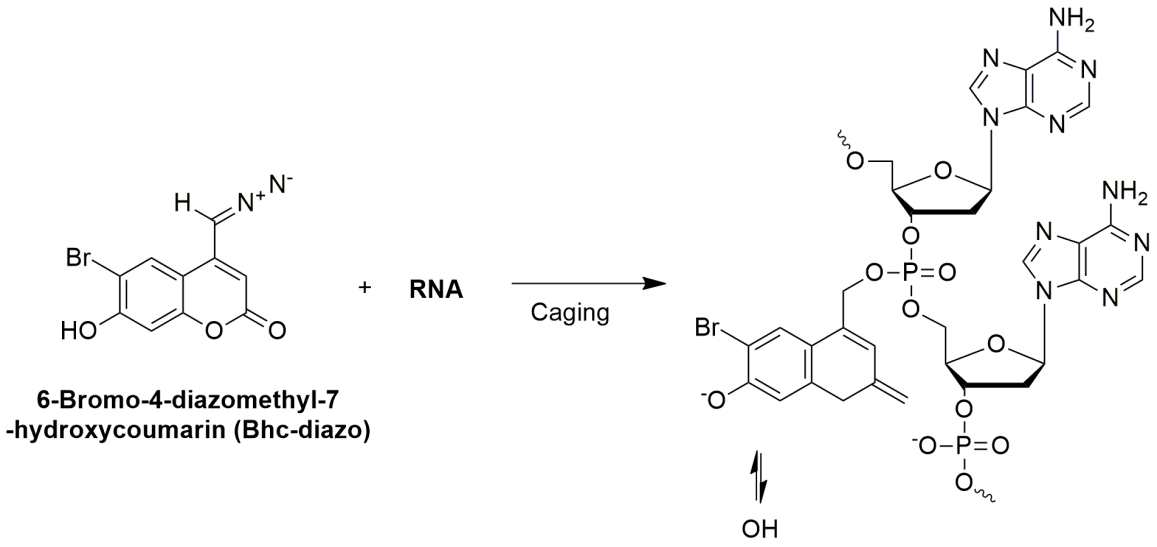

Figure 3 -3 Caging reaction of 6-bromo-4-diazomethyl-7-hydroxycoumarin to the phosphate group of RNA.

Research Strategy

In my research, hydrazone precursor conjugation method was applied to react at the phosphate groups on the internucleotides linkages. Protecting phosphate groups on the internucleotides linkages will remove the anionic properties of oligonucleotides that is one of the barrier of oligonucleotides delivery.

The caging reaction of 4-nitrobenzyl group started from the transformation of 4-nitrobenzyldehyde to 4-nitrophenylhydrazone by substitution reaction using anhydrous hydrazine. Hydrazone group of 4-nitrophenylhydrazone was oxidized into diazo form, followed by the reaction of diazo form at the phosphate groups on the inter nucleotides linkages.

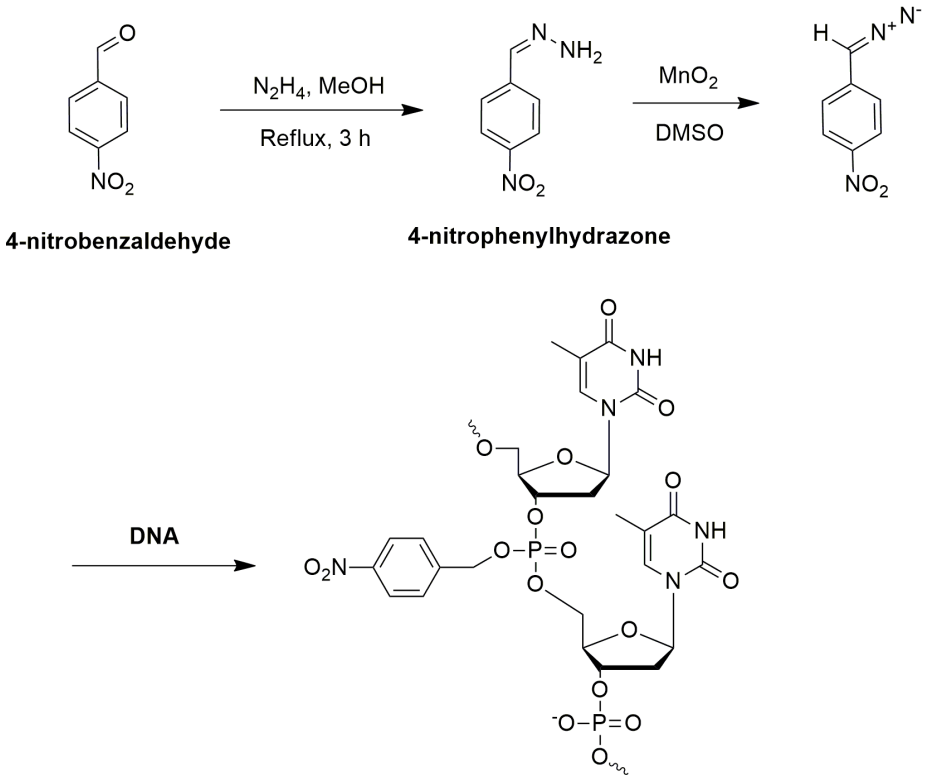

Figure 3-4 Conjugation of 4-nitrobenzyl group to phosphate group of oligonucleotides

Preparation of 4-nitrophenylhydrazone

4-nitrophenylhydrazone was prepared according to the previous reports[22]. Anhydrous hydrazine was added to the solution of 4-nitrobenzaldehyde in methanol, then reflux the reaction for 3 hours. The keto group of 4-nitrobenzaldehyde was substituted by amine group resulting 4-nitrophenylhydrazone (**Figure 3-5**).

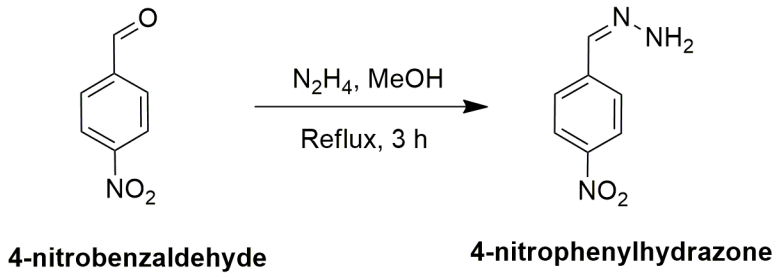

Figure 3-5 Preparation of 4-nitrophenylhydrazone

Caging reaction of 4-nitrophenylhydrazone to the phosphate group of oligonucleotides

4-nitrophenylhydrazone-diazo form was freshly prepared before caging reaction. MnO_2 was added to 4-nitrophenylhydrazone in dehydrated DMSO. After agitation at room temperature for 45 min, the reaction solution turned from yellow to yellow-brown, indicating the formation of diazo group. The caging reactions of oligonucleotides with 4-nitrophenylhydrazone (diazo form) were carried out in dehydrated DMSO solutions in dark place. After ethanol precipitation, the reaction mixture was subjected to MALDI-TOF-MS measurements, which was expected to determine the caging number. 12, 6, and 2 of 4-nitrobenzyl caged oligonucleotides were identified with **ODN 1**, **ODN 2** and **ODN 3** respectively (**Table 3-1**).

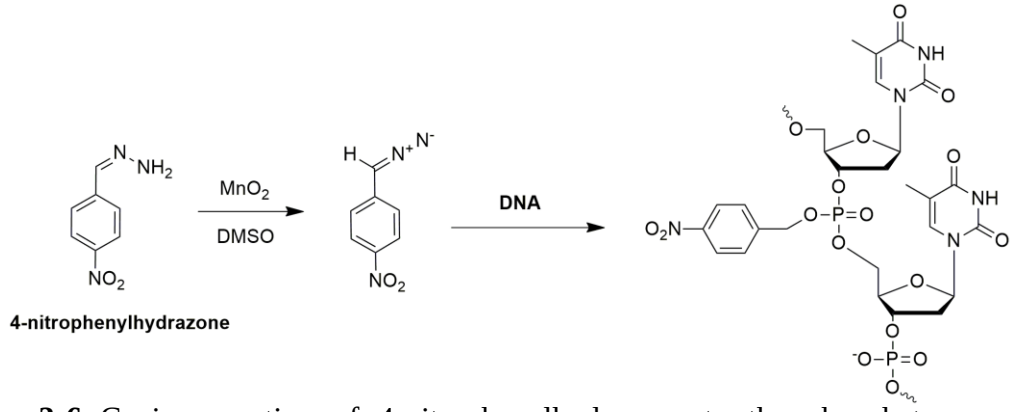

Figure 3-6 Caging reaction of 4-nitrophenylhydrazone to the phosphate group of oligonucleotides

Table 3-1 The caging number of 4-nitrobenzyl group on oligonucleotides

	Sequence[a]	**Maximum Caging Number**
ODN 1	5'-TTT TTT TTT TTT TTT TTT TT-3'	12
ODN 2	5'-CTC TAG CGT CTT AAA GCC GA-3'	6
ODN 3	5'-F-TTT TTT TTT TTT TTT TTT TT-3'	2

[a]F: fluorescein-labeled dT (**Figure 3-7**).

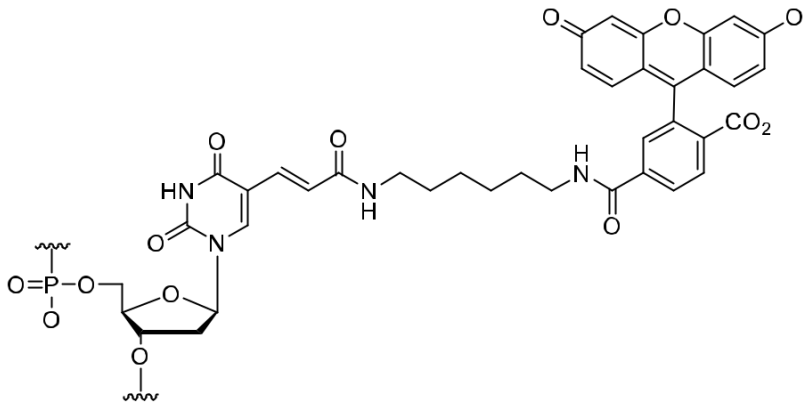

Figure 3-7 Structure of Fluorescein-labeled dT (F in **Table 3-1**).

Caging reaction of linolenate-linked 4-nitrobenzyl group with oligonucleotides

The synthesis started from 3-hydroxy -4-nitrobenzaldehyde (**1**) was selectively alkylated with propargyl bromide in the presence of K_2CO_3 to give compound (**2**), which was converted to compound (**3**) under the solution of methanol of compound in anhydrous, then reflux the reaction for 3 hours. The diazo form of compound (**3**) was freshly prepared before caging reaction by adding MnO_2 in dehydrated DMSO. After agitation at room temperature for 45 min, the reaction solution turned from yellow to yellow-brown, indicating the formation of diazo group. The caging reactions of oligonucleotides with compound (**4**) (diazo form) were carried out in dehydrated DMSO solutions in dark place. After ethanol precipitation, the reaction mixture was subjected to MALDI-TOF-MS measurements, which was expected to determine the caging number. 7 and 1 of alkyne-linked 4-nitrobenzyl caged oligonucleotides were identified with ODN 4 and ODN 5 respectively (**Table 3-1**). Purification of the alkyne-linked 4-nitrobenzyl caged oligonucleotides are required before the next step.

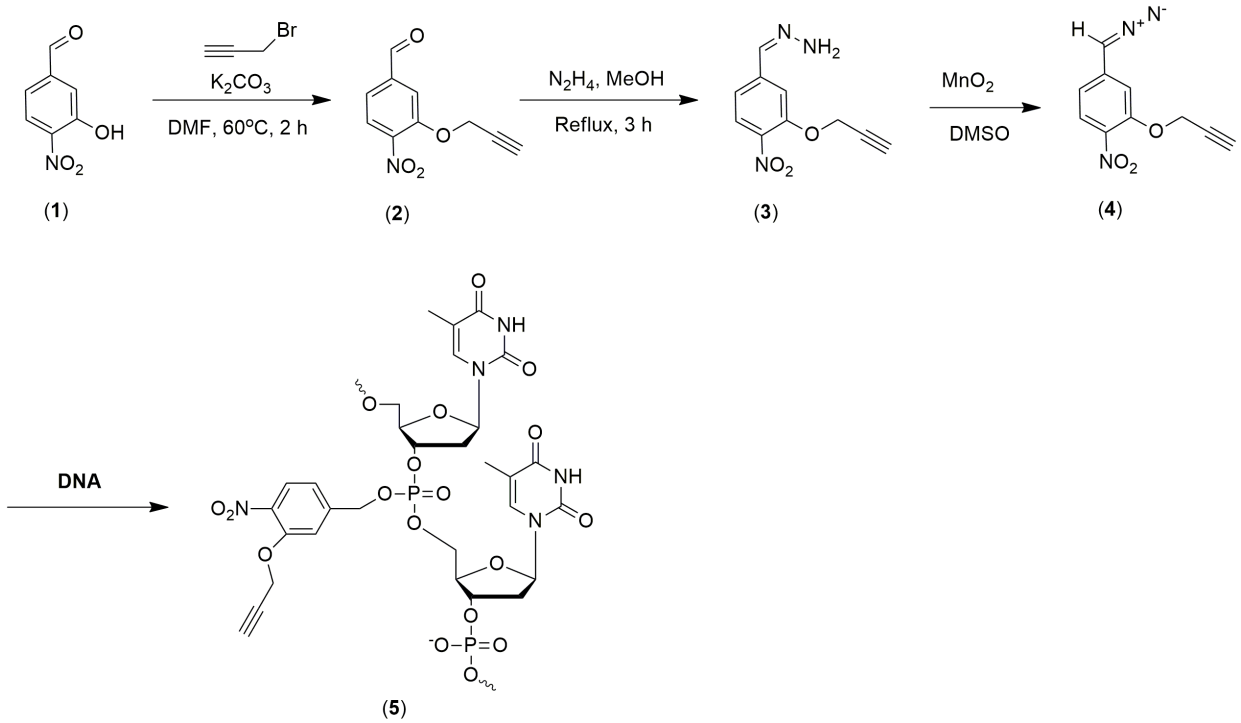

Figure 3-8 Caging reaction of 3-hydroxyalkyne-4-nitrophenylhydrazone to the phosphate group of oligonucleotides

Table 3-2 The caging number of alkyne-linked 4-nitrobenzyl group on oligonucleotides

	Sequence[a]	**Maximum Caging Number**
ODN 4	5'-TTT TTT TTT TTT TTT TTT TT-3'	7
ODN 5	5'-F-TTT TTT TTT TTT TTT TTT TT-3'	1

[a]F: fluorescein-labeled dT (**Figure 3-7**).

Linolenic acid were modified to linolenate azide derivatives through the attachment of amino-PEG3-azide in anhydrous CH_2Cl_2 (**Figure 3-9**). The alkyne-linked 4-nitrobenzyl caged oligonucleotides were coupled with linolenate azide derivatives to generate the triazoled-linked oligonucleotides (**Figure 3-10**). The reaction mixtures were subjected to HPLC purification and confirmed by MALDI-TOF-MS. The summary of linolenate-linked 4-nitrobenzyl caged oligonucleotides, which were coupled with 2 alkyne-linked 4-nitrobenzyl caged oligonucleotides and linolenate azide derivatives were summarize in **Table 3-3**. Nevertheless, **ODN 6-8** were mixed in the same fractions.

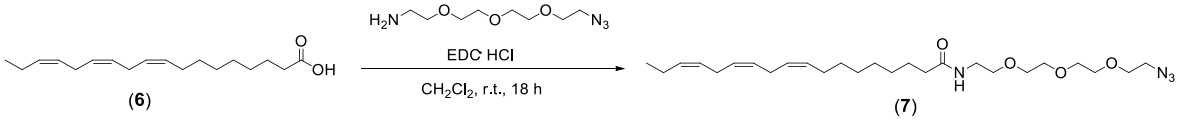

Figure 3-9 Synthesis of linolenic acid azide derivatives (**7**)

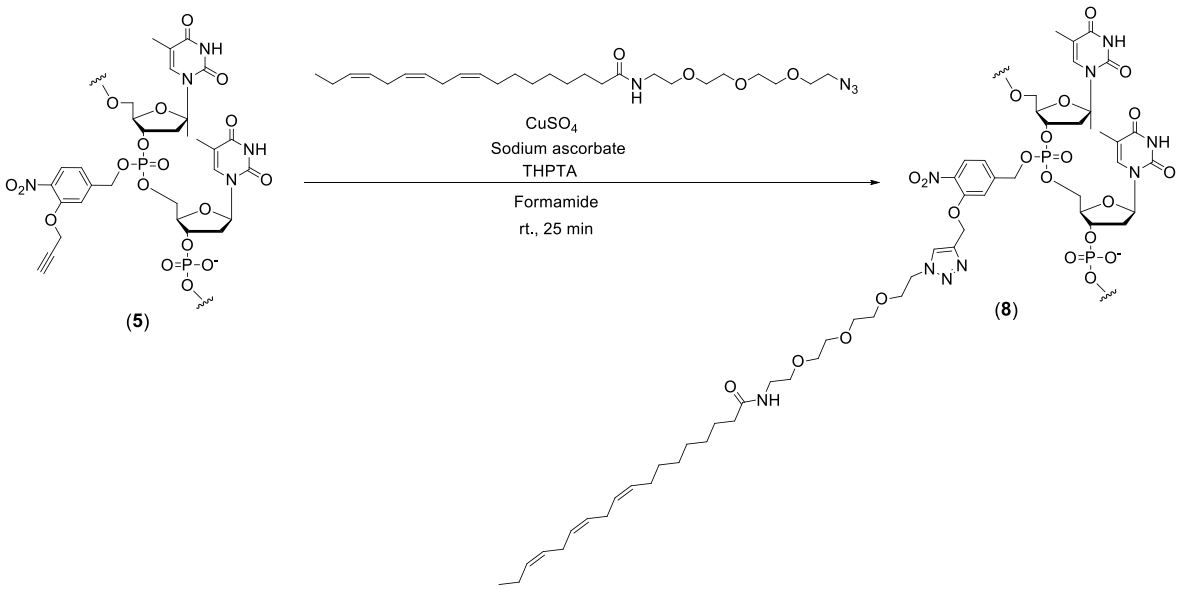

Figure 3-10 Conjugation of linolenic acid-linked 4-nitrobenzyl group with oligonucleotides

Table 3-3 The caging number of linolenate-linked and alkyne-linked 4-nitrobenzyl group on oligonucleotides (The starting material are 2 alkyne-linked 4-nitrobenzyl caged oligonucleotides)

	Sequence	**Caging Number**	
		Alkyne	Linolenate
ODN 6	5'-TTT TTT TTT TTT TTT TTT TT-3'	1	1
ODN 7	5'-TTT TTT TTT TTT TTT TTT TT-3'	0	1
ODN 8	5'-TTT TTT TTT TTT TTT TTT TT-3'	0	2

[a]F: fluorescein-labeled dT (**Figure 3-7**)

Cell culture, Oligonucleotides treatment, and Imaging Analysis

Investigation the cellular uptake properties of the polyunsaturated fatty acids conjugated oligonucleotides (**ODN 3, 5**). **ODN 3** and **ODN 5** were individually incubated with HeLa cells without any transfecting reagent at 37ºC for 2 h. The sample solutions containing 4 μM probes were incubated for 2 h with cultured HeLa cells and fluorescence positive cells were then detected for the non-modified probe and **ODN 3, 5** under a confocal microscope. The results suggest that **ODN 5** exhibited the slightly of the cellular uptake intensity through 1 conjugation of alkyne-linked 4-nitrobenzyl was attached to fluorescence poly(dT)sequence.

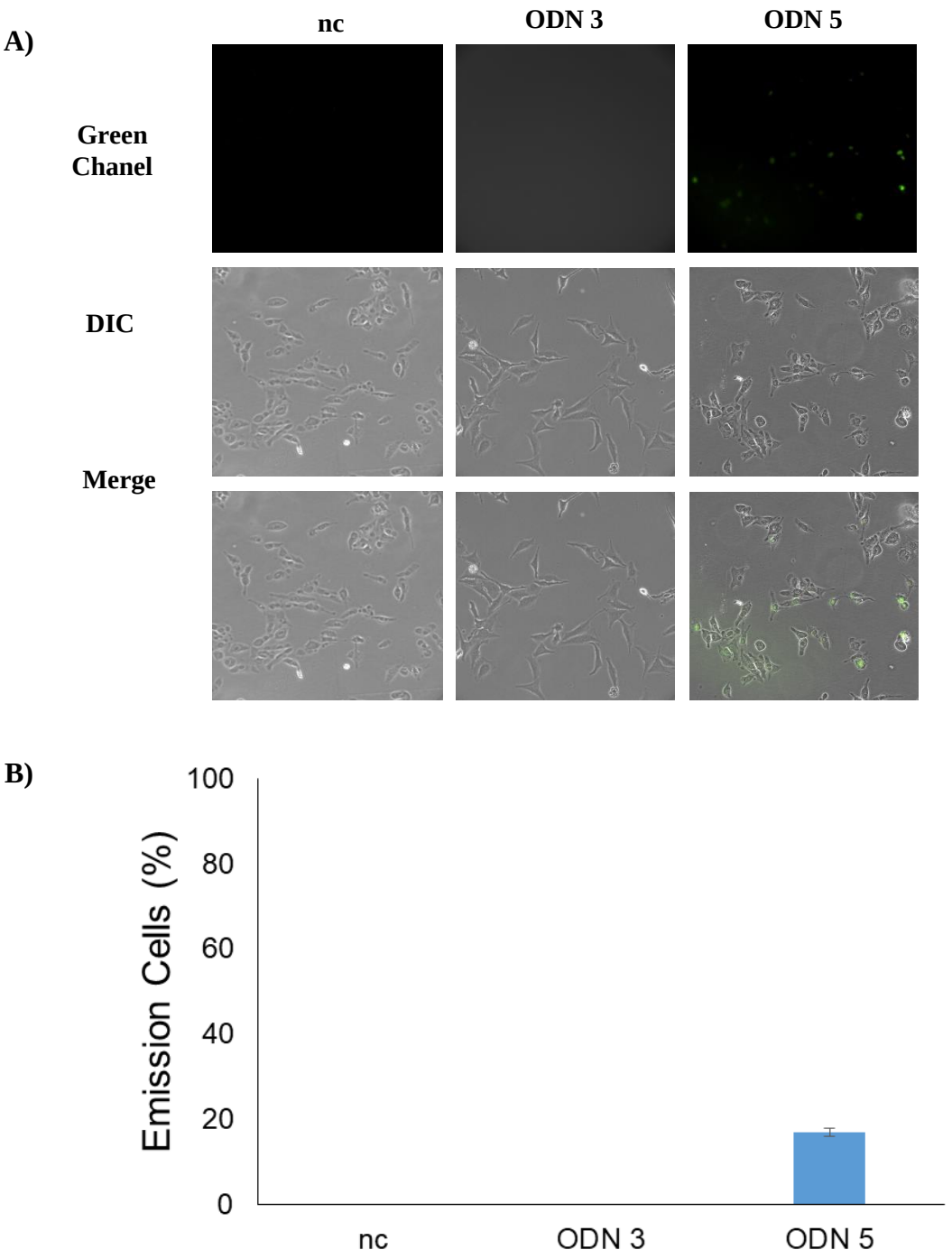

Figure 3-11 Cellular uptake experiments of 4-nitrobezyl and alkyne-linked 4-nitrobenzyl caged fluorescent poly(dT)sequence. (A) Fluoresecence imaging of living HeLa cells treated with 4-nitrobezyl and alkyne-linked 4-nitrobenzyl caged fluorescent poly(dT) sequences, **ODN 3** and **ODN 5**. Negative control (nc): unconjugated fluorescent poly(dT)sequences. Bar: 50 μm. (B) Statistic analysis of cellular uptake efficiency by counting fluorescent cells (200 cells each) from imaging data. The values indicate mean percent of each sample, with error bars showing standard errors (*n* = 257 for **ODN 5**)

3.4 Summary

We have synthesized pro-oligonucleotides, which bearing 4-nitrobenzyl reduction activated groups via post-synthesis DNA modification. Furthermore, alkyne-linked 4-nitrobenzyl caged oligonucleotides were synthesized and incorporated with modified linolenate azide derivatives by a subsequent CuAAC reaction. We can observed some linolenate-linked 4-nitrobenzyl caged oligonucleotides. Our methods could be useful for the development of oligonucleotides prodrugs by conjugation various functional molecules to discover the best functional group for oligonucleotides delivery.

3.5 Experimental procedures

General. All chemicals were purchased from Sigma-Aldrich, Wako Chemicals, and Tokyo Chemical Industry. 1H and 13C NMR spectra were measured with a Bruker Avance 600 (600 MHz). Electrospray ionization mass spectra (ESI-MS) were recorded by a Bruker microTOF II-NAC. MALDI-TOF mass spectra were recorded by a Bruker microflex - NAC. DNA was synthesized on a NTS H-8 DNA/RNA synthesizer (Nihon Techno Service). DNA oligonucleotides were purified by HPLC system composed by GILSON Inc. and JASCO Inc. modules. Absorption were recorded on Shimadzu UV-2550 spectrophotometer and RF-5300PC spectrofluorophotometer.

Preparation of 4-nitrophenylhydrazone 4-nitrobenzaldehyde (3.00 mmol) in 100 ml methanol was added dropwise to rapidly stirring anhydrous hydrazine (18 mmol, 575.34 mg). After stirring, the mixture was refluxed for 3 hours. After cooling, the acquired product was recrystallized by ethanol providing 4-nitrophenylhydrazone as yellow precipitate at a yield of 80.3%, 438.7 mg. ^{1}H-NMR ($CDCl_3$, 600 MHz) δ 8.20 (s, 2-H), 7.73 (s, 1-H), 7.67 (s, 1-H), 5.88 (s, 1-H), 1.58 (s, 2-H).

Preparation 4-nitrophenylhydrazone (diazo form) in diazo solution 3-hydroxy-4-nitrophenylhydrazone (20 µmol, 1 eq) was dissolved in dehydrated DMSO (600 µl), MnO_2 (200 µmol, 10 eq) was added and the reaction mixture was agitated at room temperature for 45 minutes. The color of the solution changes from yellow to yellow-brown, which is an indicator of diazo formation. The mixture was centrifuged at 2,000 g for 1 minute at room temperature and the supernatant was collected. After filtration, the diazo solution was freshly used for caging reactions.

Caging reaction of 4-nitrobenzyl group with oligonucleotides To a solution of oligonucleotides (10 nmol) in dehydrated DMSO 35 µl, the 4-nitrophenylhydrazon (diazo form) in diazo solution 90 µl was added. After shaking at room temperature for 24 hours in dark place, 12 M ammonium acetate 25 µl aqueous solution was added and the mixture was shaked for 15 min at room temperature upon which ethanol precipitation.

Preparation of 4-nitro-3-(prop -2-yn-1-yloxy)benzaldehyde (2) 3-hydroxyl-4-nitrobenzaldehyde (**1**) (500 mg, 1 eq) and K_2CO_3(1.24 g, 3 eq) were dissolved in DMF (10 mL), and a solution was stirred at 60°Cfor 1 h. To the solution was added propargyl bromide (272.78µL, 1.2 eq), and the solution was stirred at 60°C for 1 h. The solution wasdiluted with EtOAc and washed with H_2O. The organic solution was dried ($MgSO_4$), filtered, and evaporated in vacuo. The residue was purified by column chromatography on a silica gel eluted with hexane:EtOAc (7:3) to give 4-nitro-3-(prop-2-yn-1-yloxy)benzaldehyde (**2**) (630.8 mg, 100%). ^{1}H-NMR ($CDCl_3$, 600 MHz) δ 10.06 (s, 1-H), 7.95 (s, 1-H), 7.75 (s, 1-H), 7.61 (s, 1-H), 7.59 (s, 1-H), 4.92 (s, 2-H), 4.12 (s, 1-H).

Preparation of 4-nitro-3-(prop-2-yn-1-yloxy)benzylidene hydrazine (3) 4-nitro-3-(prop-2-yn-1-yloxy)benzaldehyde (300 mg, 1 eq) in 60 ml methanol was added dropwise to rapidly stirring anhydrous hydrazine (280µL, 6 eq). After stirring, the mixture was refluxed for 3 hours. After cooling, the acquired product was recrystallized by ethanol providing 4-nitrophenylhydrazone as yellow precipitate at a yield of 37.79%, 241.7 mg. ^{1}H-NMR ($CDCl_3$, 600 MHz) δ 7.87 (s, 1-H), 7.68 (s, 1-H), 7.48 (s, 1-H), 5.86 (s, 2-H), 4.88 (s, 1-H).

Preparation of 4-nitro-3-(prop-2-yn-1-yloxy)benzylidene hydrazone (4) in diazo solution Compound (**4**) was prepared by following the preparation 4-nitrophenylhydrazone (diazo form) in diazo solution. 4-nitro-3-(prop-2-yn-1-yloxy)benzylidene hydrazine (**3**) was employed as the starting material.

Preparation of linolenate azide derivatives (**7**) Linolenic acid (100 mg, 1 eq) and 1-amino-11-azido-3, 6, 9-trioxaundecane (108 µl, 1.5 eq) were dissolved in CH_2Cl_2 (2 mL). To the solution was added EDC·HCl (82.81 mg, 1.2 eq). The resulted mixture was stirred at room temperature for 18 h. The mixture was evaporated in vacuo. The residue was purified by column chromatography on a silica gel elutedwith CH_2Cl_2/MeOH (50:1) to give linolenic acid azide derivatives (**7**) (172.2 mg, 99.17%) as a yellow oil. ^{1}H-NMR ($CDCl_3$, 600 MHz) δ 5.35-5.24 (m, 6-H), 3.68-3.32 (m, 14-H), 2.77 (s, 3-H), 2.16-2.05 (m, 7-H), 1.58 (s, 2-H), 1.27-1.23 (m, 11-H), 0.97 (s, 3-H).

Conjugation of linolenate-linked 4-nitrobenzyl group with oligonucleotides Alkyned-linked 4-nitrobenzyl caged oligonucleotides (0.86 nmol, 1 eq)was dissolved in water 50 µl and formamide 50 µl. Copper sulfate (II) (2.15 µg, 100 eq), Tris(3-hydroxypropyltriazolymethyl)amine (THPTA) (7.47 µg, 200 eq), linolenate azide derivatives (0.5 µl, 100 eq) were added to the solution. Sodium ascorbate (1.36 µg, 80 eq) was added to start the reaction. The reaction mixture was vigorously stirred by vortex for 5 min, then put on MicroMixer E-36 (TAITEC) for 25 min. The product was purified by HPLC, lyophilized and identified by MALDI-TOF mass spectrometry.

Cellular Uptake of Conjugated Alkyne-linked and 4-nitrobezyl Fluorescein Labeled Pro-oligonucleotides Conjugated alkyne-linked and 4-nitrobezyl fluorescein labeled pro-oligonucleotides (4 µM, 1.0 µL) was mixed with OPTI-MEM (9.0 µL). Each cultured cells in 3.5 cm glass bottom dish containingg 1×10^5cells were washed with 1 mL of 1 × PBS (-) once and the sample solution was added to the center of glass base. These dishes were incubated at 37^{o}C for 2 hours. Subsequently, the sample solution was discarded and each dish was washed with 1 × PBS (-) and OPTI-MEM. The fluorescence images were recorded under confocal laser scanning microscope (Ex: 488 nm, wavelength longer than 505 nm was detected).

^{1}H NMR Charts of 4-nitrophenylhydrazone

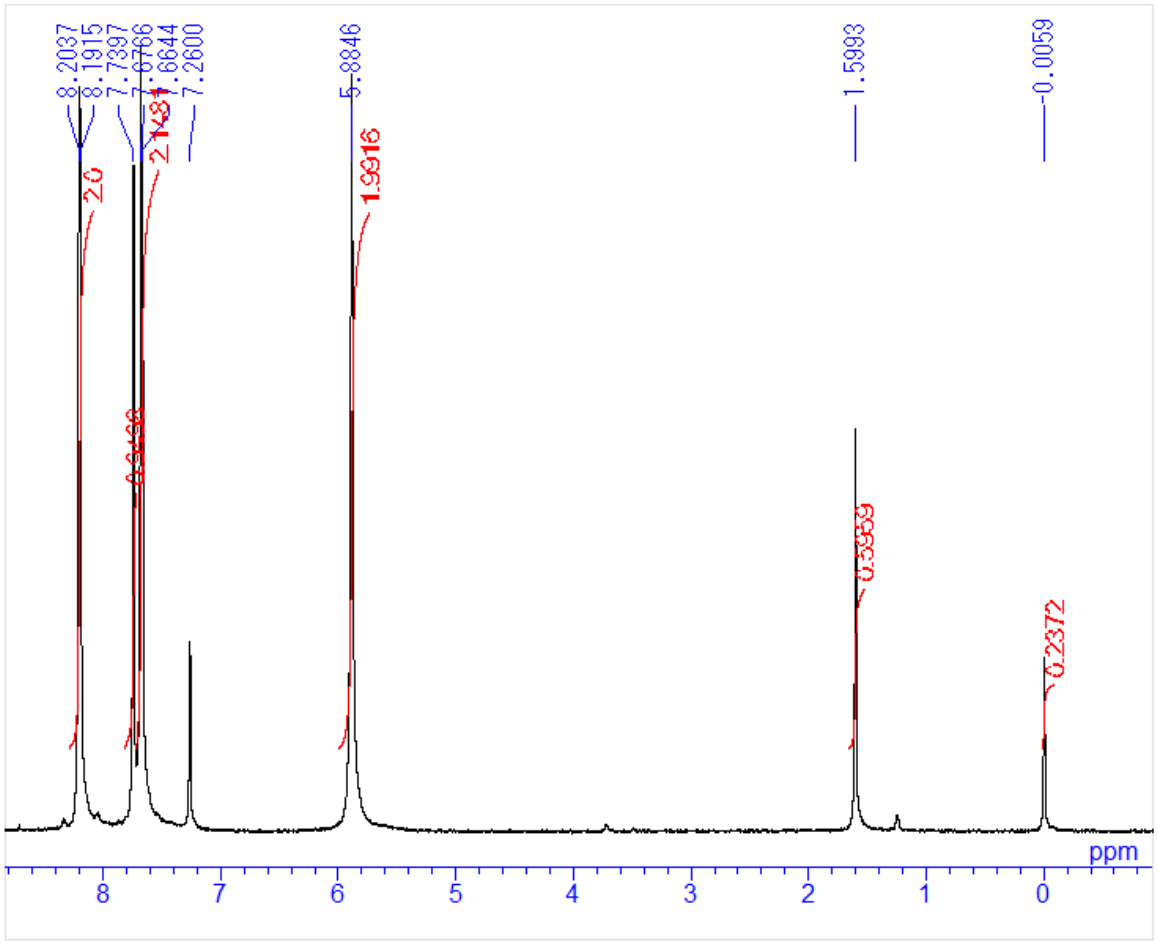

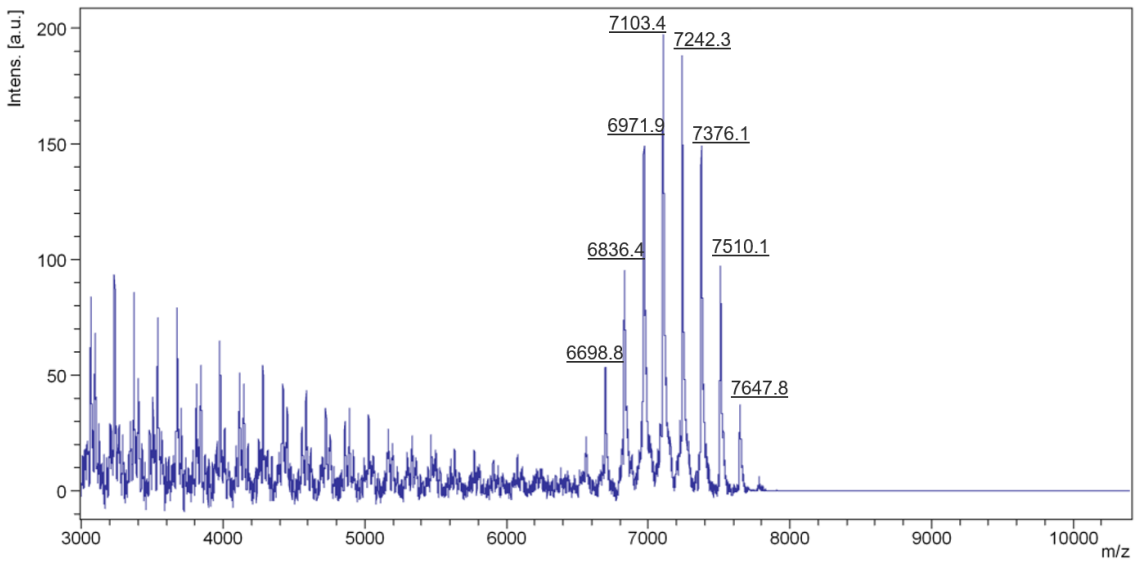

Figure 3-12 MALDI-TOF spectrum revealed the 5-12 conjugated 4-nitrophenylhydrazone with poly(dT)sequence (**ODN 1**).

Table 3-4 Caging number of 4-nitrophenylhydrazone with poly(dT)sequence (**ODN 1**)

Caging number	Cal.	Found.
5	6697.5	6698.8
6	6836.6	6836.4
7	6970.4	6971.9
8	7102.8	7103.4
9	7242.9	7242.3
10	7375.1	7376.1
11	7508.2	7510.1
12	7643.3	7648.8

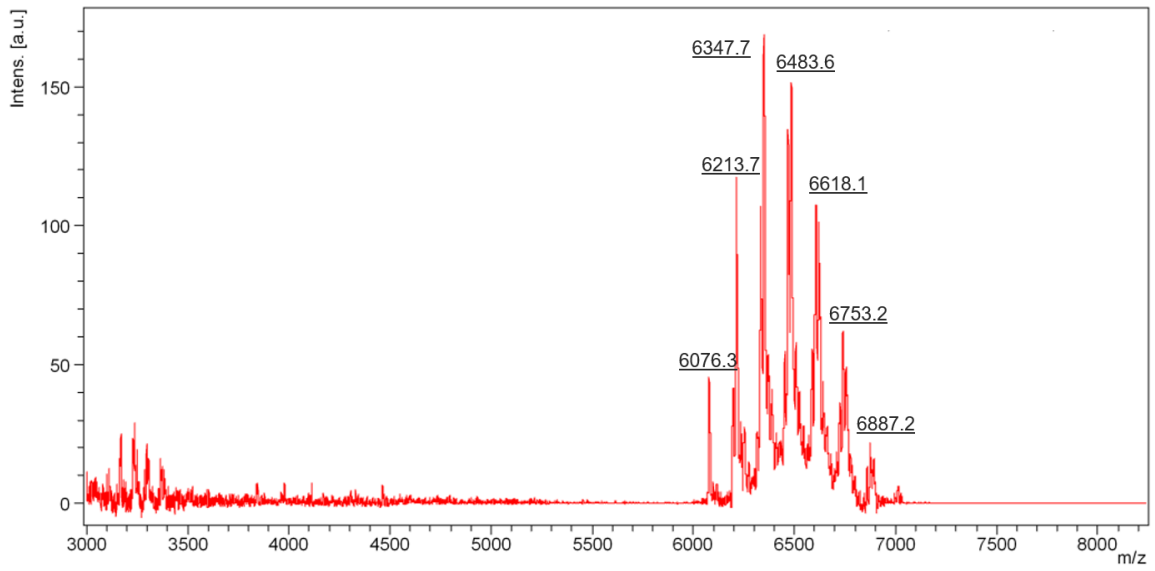

Figure 3-13 MALDI-TOF spectrum revealed the 1-6 conjugated 4-nitrophenylhydrazone with **ODN 2**.

Table 3-5 Caging number of 4-nitrophenylhydrazone with poly(dT)sequence (**ODN 2**)

Caging number	Cal.	Found.
0	6076.9	6076.3
1	6212.1	6213.7
2	6347.2	6347.7
3	6482.3	6483.7
4	6617.4	6618.1
5	6752.5	6753.2
6	6887.7	6887.3

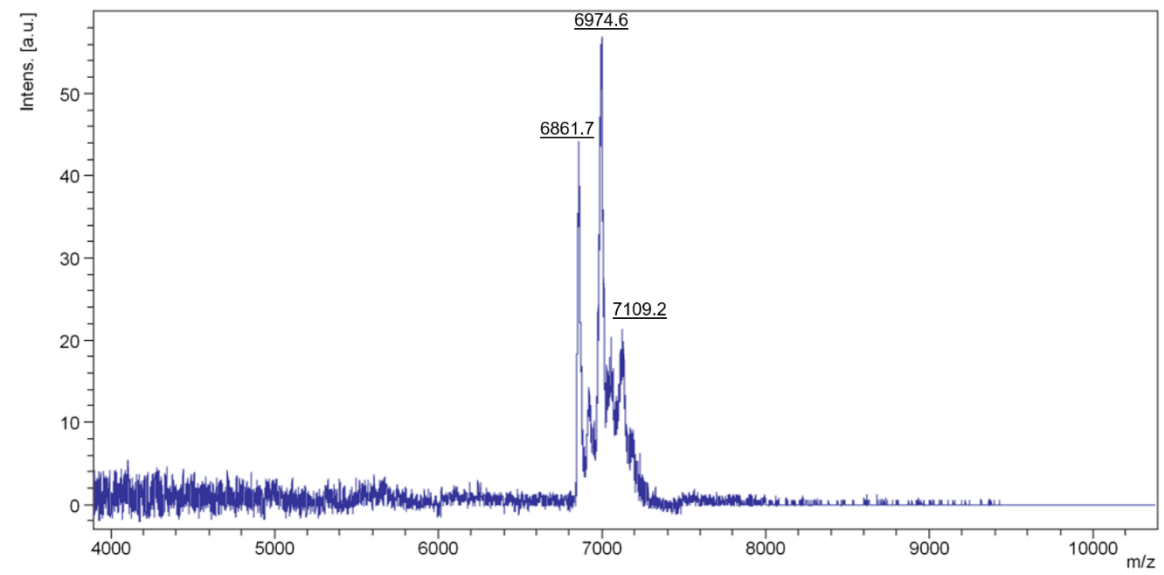

Figure 3-14 MALDI-TOF spectrum revealed the 2 conjugated 4-nitrophenylhydrazone with fluorescein poly(dT)sequence (**ODN 3**).

Table 3-6 Caging number of 4-nitrophenylhydrazone with fluorescein poly(dT)sequence (**ODN 3**)

Caging number	Cal.	Found.
0	6838.6	6861.7
1	6973.7	6974.6
2	7108.8	7109.2

^{1}H NMR Charts of 4-nitro-3-(prop-2-yn-1-yloxy)benzaldehyde (**2**)

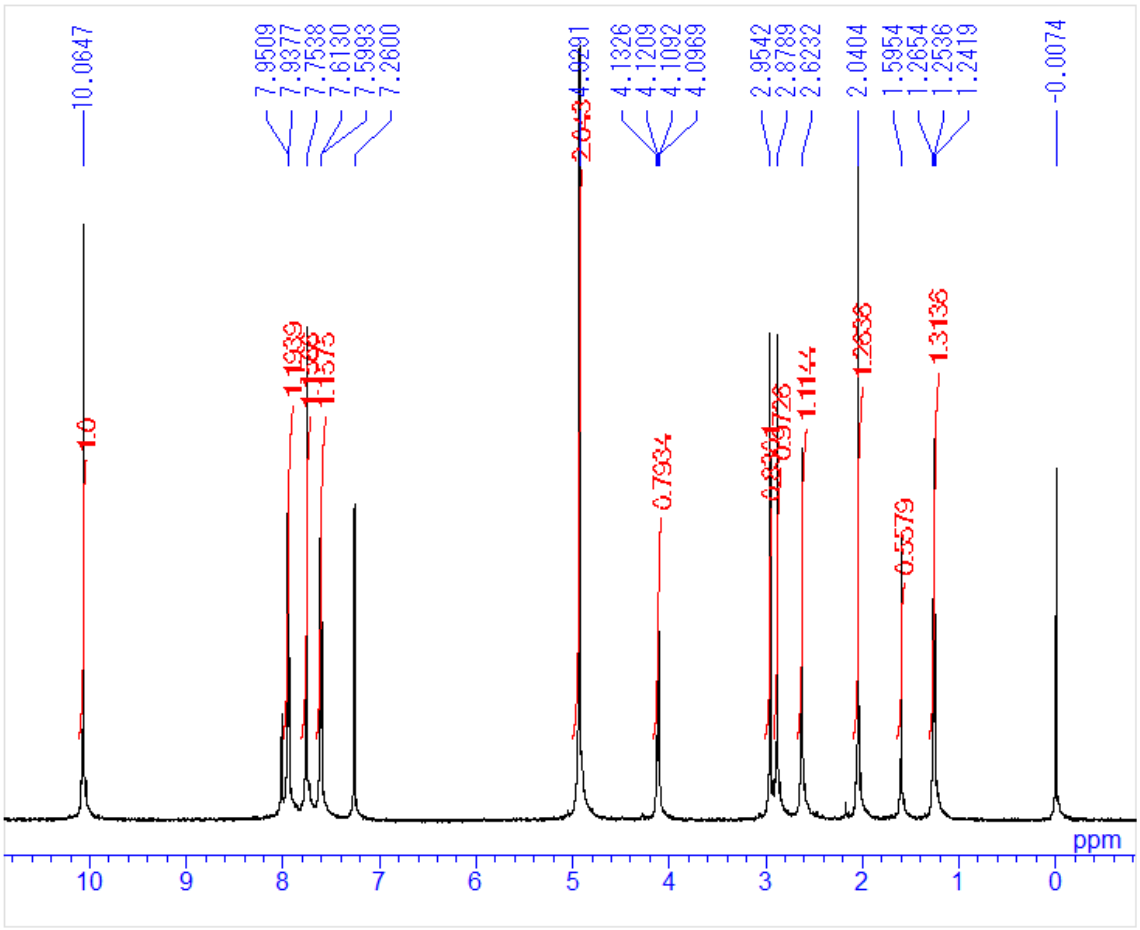

^{1}H NMR Charts of 4-nitro-3-(prop-2-yn-1-yloxy)benzylidene hydrazine (**3**)

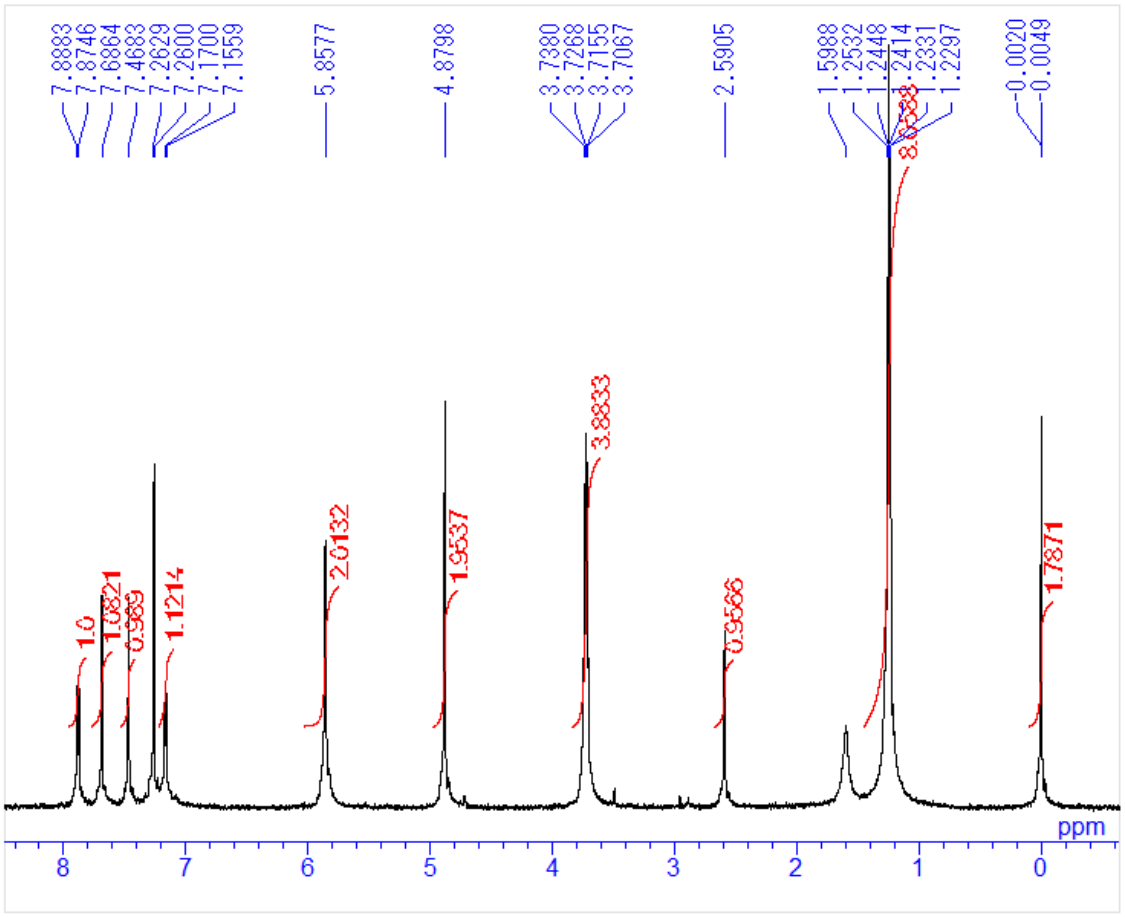

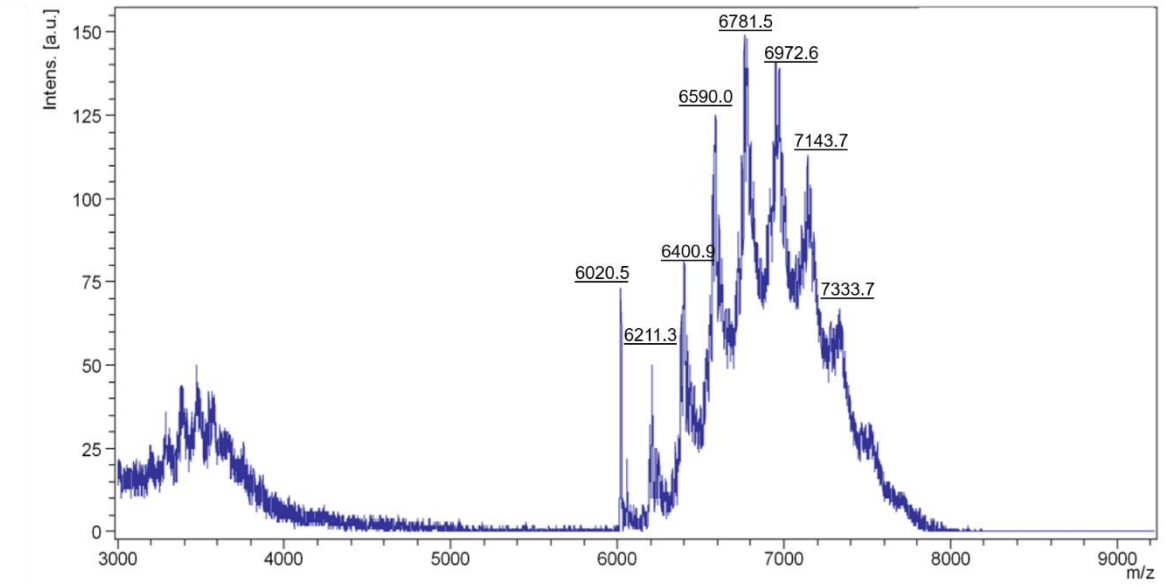

Figure 3-15 MALDI-TOF spectrum revealed the 1-7 conjugated 3-hydroxyalkyne-4-nitrophenylhydrazone with poly(dT)sequence (**ODN 4**)

Table 3-7 Caging number of 3-hydroxyalkyne-4-nitrophenylhydrazone with poly(dT)sequence (**ODN 4**)

Caging number	Cal.	Found.
0	6021.8	6020.5
1	6211.1	6211.3
2	6400.2	6400.9
3	6589.4	6590.0
4	6778.6	6781.5
5	6967.7	6972.6
6	7158.5	7143.7
7	7346.1	7333.7

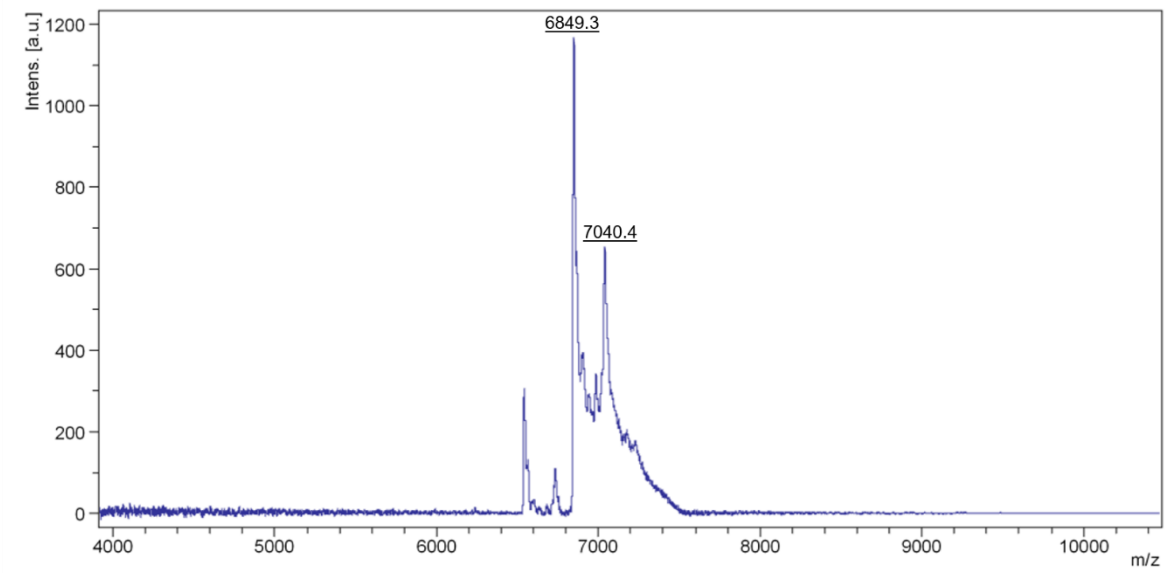

Figure 3-16 MALDI-TOF spectrum revealed the 1 conjugated 3-hydroxyalkyne-4-nitrophenylhydrazone with fluorescein poly(dT)sequence (**ODN 5**)

Table 3-8 Caging number of 3-hydroxyalkyne-4-nitrophenylhydrazone with fluorescein poly(dT)sequence (**ODN 5**)

Caging number	Cal.	Found.
0	6838.6	6849.3
1	7027.8	7040.4

^{1}H NMR Charts of linolenate azide derivatives (**7**)

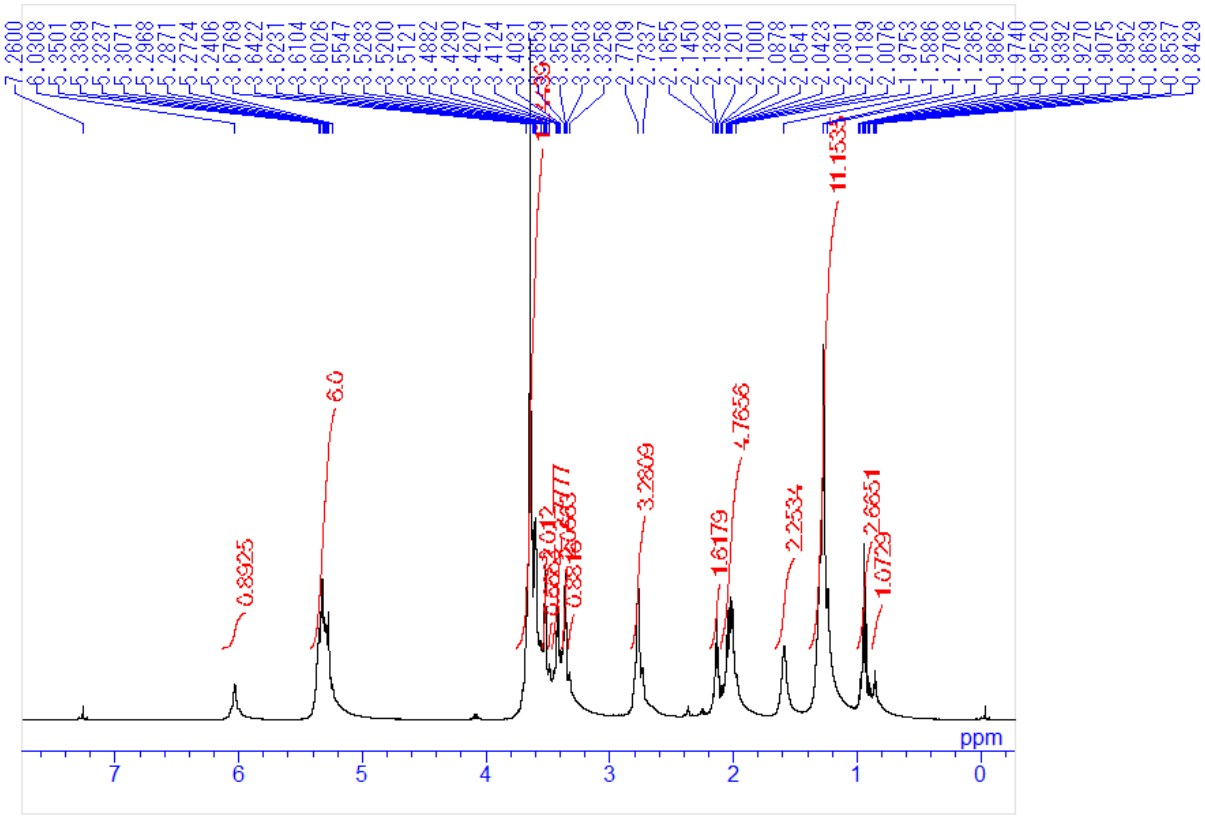

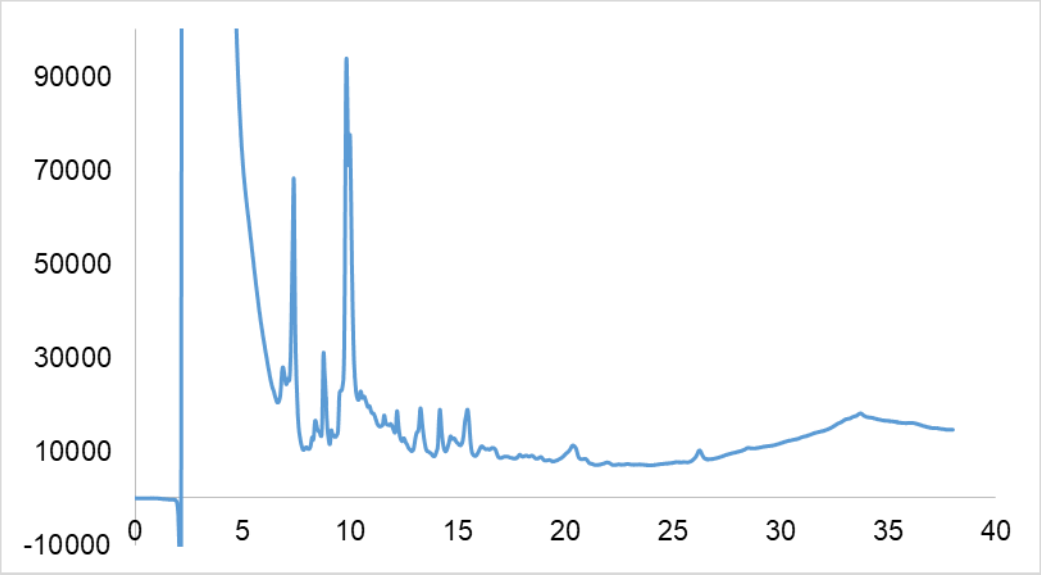

Figure 3-17 HPLC chromatogram of linolenate-linked and alkyne-linked 4-nitrobenzyl group on poly(dT)sequence (**ODN 6-8**). HPLC condition: 5C18-MS-II column, 4.6 mm I.D. × 250 mm, flow rate: ml/min, gradient: 0 to 45 min 30% to 100% acetronitrile.

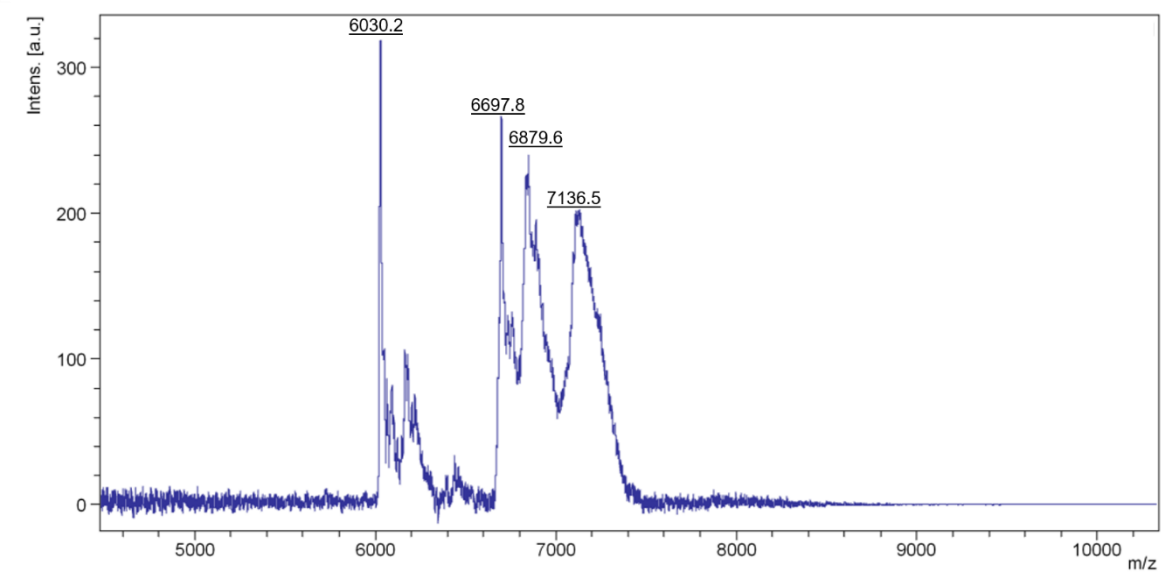

Figure 3-18 MALDI-TOF spectrum of the HPLC peak with R*t* = 15’ (see Figure) revealed the linolenate-linked and alkyne-linked 4-nitrobenzyl group on poly(dT)sequence (**ODN 6-8**)

Table 3-9 The caging number of linolenate-linked and alkyne-linked 4-nitrobenzyl group on poly(dT)sequence (**ODN 6-8**)

Caging Number		Calcd.	Found
Alkyne	Linolenate		
1	1	6878.9	6879.6
0	1	6689.7	6697.8
0	2	7357.6	7136.5

3.6 Reference

1. Takeshita, F., and Ochiya, T., Therapeutic potential of RNA interference against cancer, Cancer Science, 2006, 97, 689– 696

2. Devi, G.R., siRNA-based approaches in cancer therapy, Cancer Gene Therapy, 2006, 13, 819– 829

3. Mescalchin, A., and Restle, T., Oligomeric Nucleic Acids as Antivirals Molecules, 2011, 16, 1271– 1296

4. Debart, F., Abes, S., Deglane, G., Moulton, H.M., Clair, P., Gait, M.J., and Vasseur, J., Chemical modifications to improve the cellular uptake of oligonucleotides, Current Topics in Medicinal Chemistry, 2007, 7, 727-737.

5. Saneyoshi, H., Iketani, K., Kondo, K., Saneyoshi, T., Okamoto, I., and Ono, A., Synthesis and characterization of cell-permeable oligonucleotides bearing reduction-activated protecting groups on the internucleotide linkages, Bioconjugate Chemistry, 2016, 27, 2149-2156.

6. Mintzer, M.A., and Simanek, E., E., Nonviral vectors for gene delivery, Chemical Reviews, 2009, 109, 259– 302.

7. Barber, I., Rayner, B., and Imbach, J.-L., The prooligonucleotide approach. I: esterase-mediated reversibility of dithymidine S-alkyl-phosphorothiolates to dithymidine phosphorothioates, Bioorganic Medicinal Chemistry Letters, 1995, 5, 563– 568.

8. Mignet, N., Morvan, F., Rayner, B., and Imbach, J.-L., The pro -oligonucleotide approach. V: Influence of the phosphorus atom environment on the hydrolysis of enzymolabile dinucleoside phosphotriesters, Bioorganic Medicinal Chemistry Letters, 1997, 7, 851– 854.

9. Tosquellas, G., Alvarez, K., Dell'Aquila, C., Morvan, F., Vasseur, J.-J., Imbach, J.-L., and Rayner, B., The pro-oligonucleotide approach: Solid phase synthesis and preliminary evaluation of model pro-dedecanthymidylates, Nucleic Acid Research, 1998, 26, 2069-2074.

10. Bologna, J.C., Morvan, F., and Imbach, J.L., The pro-oligonucleotide approach: Synthesis of mixed phosphodiester and SATE phosphotriester pro-oligonucleotides using H-phosphonate and phosphoramidite chemistries, European Journal of Organic Chemistry, 1999, 2353-2358.

11. Cowen, R.L., Williams, K.J., Chinje, E.C., Jaffar, M., Sheppard, F., Telfer, B.A., Wind, N.S., and Stratford, I.J., Hypoxia targeted gene therapy to increase the efficacy of tirapazamine as an adjuvant to radiotherapy, Cancer Research, 2004, 64, 1396-1402.

12. Failes, T.W., and Hambley, T.W., Models of hypoxia activated prodrugs: Co(III) complexes of hydroxamic acids, Dalton Transactions, 2006, 15, 1895-1901.

13. Hockel, M., and Vaupel, P., Tumor hypoxia: definitions and current clinical, biologic, and molecular aspects, Journal of the National Cancer Institute, 2001, 93, 266-276.

14. Wilson, W.R., and Hay, M.P., Targeting hypoxia in cancer therapy, Nature Reviews Cancer, 2011, 11, 393-410.

15. Saneyoshi, H., Hiyoshi, Y., Iketani, K., Kondo, K., and Ono, A., Bioreductive deprotection of 4-nitrobenzyl group on thymine base in oligonucleotides for the activation of duplex, Bioorganic and Medicianl Chemistry Letter, 2015, 25, 5632-5635.

16. Ikeda, M., Kamimura, M., Hayakawa, Y., Shibata, A., and Kitade, Y., Reduction-responsive guanine incorporated into G-quadruplex-forming DNA, Chembiochem Communcations, 2016, 17, 1304-1307.

17. Khalaj, A., Abdi, K., Ostad, S.N., Khoshayand, M.R., Lamei, N., and Nedaie, H.A., Synthesis, In Vitro cytotoxicity and radiosensitizing activity of novel 3-[(2,4-dinitrophenylamino)alkyl]derivatives of 5-fluorouracil, Chemical Biology and Drug Design, 2013, 83, 183-190.

18. Yamazoe, S., McQuade, L.E., and Chen, J.K., Nitroreductase-activated morpholino oligonucleotides for In Vivo gene silencing, Chemical Biology, 2014, 9, 1985-1990.

19. Guo, T., Cui, L., Shen, J., Zhu, W., Xu, Y., and Qian, X., A highly sensitive long-wavelength fluorescence probe for nitroreductase and hypoxia: selective detection and quantification, Chemical Communications, 2013, 92, 10820-10822.

20. Kala, A., Jain, P.K., Karunakaran, D., Shah, S., and Friedman, S.H., The synthesis of tetra-modified RNA for the multidimensional control of gene expression via light-activated RNA interference, Nature Protocols, 2014, 9, 11-20.

21. Ando, H., Furuta, T., Tsien, R.Y., and Okamoto, Y., Photo-mediated gene activation using caged RNA/DNA in zebrafish embryos, Nature Genetics, 2001, 28, 317-325.

22. Huang, W., Yu, X., Lin, H., and Lin, H., A colorimetric sensor for the recognition of biologically important anions, Journal of Inclusion Phenomena and Macrocyclic Chemistry, 2011, 69, 69-73

Chapter 4

Conclusion and Future Perspective

Conclusion

This doctoral dissertation describes the development of the pro-oligonucleotides using caging reaction for oligonucleotides strands to attain the efficient delivery of oligonucleotides to a specific target site. In this study, we developed new method for the conjugation of the functional groups to the oligonucleotides via post-synthesis DNA modification.

In chapter 2, several esters of polyunsaturated fatty acids, which are able to attach to oligonucleotides were synthesized. The conjugation of oligonucleotides with polyunsaturated fatty acids was proceeded through postsynthetic modification of oligonucleotides by using the activated esters of polyunsaturated fatty acids such as poly(dT)sequence, which is complementary to the poly(A)tails of mRNA was modified. The reaction mixture was incubated 60^{o}C for 6 h, and attachment of a polyunsaturated fatty acid to DNA strands was confirmed by MALDI-TOF mass spectroscopy. In investigation of the cellular uptake properties without any transfecting reagent, the polyunsaturated fatty acids conjugated fluorescent oligonucleotides were used. The fluorescent poly(dT) DNA modified with a polyunsaturated fatty acid showed the outstanding cellular uptake into HeLa cells. In addition, the polyunsaturated fatty acid attached to DNA was removed by esterases to give the unmodified original DNA.

In chapter 3, the synthetic compound 4-nitrophenylhydrazone (diazo form) construct covalent bonds with the phosphate moiety of the sugar-phosphate backbone of oligonucleotides such as poly(dT)sequence. Moreover, an alkyne-linked protecting group as a conjugatable protecting group was designed and incorporated into oligonucleotides. A subsequent CuAAC reaction with linolenate azide derivatives was carried out to obtain linolenate-linked 4-nitrobenzyl oligonucleotides. Despite, fluorescent poly(dT)sequence DNA modified with linolenate-linked 4-nitrobenzyl oligonucleotides was not observed. In examination of cellular uptake properties, 4-nitrobenzyl and alkyne-linked 4-nitrobenzyl caged fluorescent oligonucleotides were used. Surprisingly, alkyne-linked 4-nitrobenzyl caged oligonucleotides showed slightly cellular uptake into HeLa cells.

Our DNA modified with a polyunsaturated fatty acid gave us the simple methods for DNA functionalization, cellular uptake, and defunctionalization. Moreover, our DNA modified with alkyne-linked protecting group as a conjugatable protecting group could be useful for the development of oligonucleotide prodrugs.

Future Perspective

Oligonucleotides delivery is the transferring therapeutics oligonucleotides into the target cell. These oligonucleotides are nucleic acid-based molecules (DNA, RNA) that are easily degraded when administered into the body. There are several issues to be addressed for oligonucleotides delivery. According to data obtained from the previous research[1], a total of 1387 patent applications are about gene transfer system and 639 of these are directly disease related. The distribution ratio of these applications is viral vector, 63%; non-viral vectors, 35% and hybrid vectors, 2%.

As seen below, **viral vectors** are still the most preferred methods for oligonucleotides delivery because of their **effective** transduction. It is clearly that researchers are focused on the development of viral vectors with minimal cytotoxic, tumorogenic, and immunogenic effects. **Safety** is the key points to discover the oligonucleotides delivery system.

Recently, chemists have developed stimuli-responsive **caged oligonucleotides**[2] both external stimuli (such as light, magnetic field, and temperature) as well as internal stimuli (such as biomarkers, enzymes and pH) to release the oligonucleotides from the cage. Especially, internal stimuli like enzymes have been traditionally and actively examined to install stimuli-responsive properties into smaller molecules in order to develop prodrugs. However, the functional diversity and bioapplication of the chemically caged oligonucleotides reported is still limited. Moreover, most of the bond-cleaving reactions built into the molecular designs are irreversible and thereby their stimuli-responsive functions will work only once in their lifetimes.

According to our research, linolenate conjugated oligonucleotides have been achieved the bond-cleaving reactions with the esterase. Besides, linolenate conjugated oligonucleotides can effective assist delivering oligonucleotides into the cells. Although, our post-synthesis caged DNA modification strategy can obtain the low yield of linolenate conjugated oligonucleotides. Additionally, the iodomethyl alkyl group might react with guanine base causing oligonucleotides breakage.

4-nitrobenzyl caged oligonucleotides have been demonstrated the bond-cleaving reactions with the nitroreductase in previous report. The caging reaction of 4-nitrophenylhydrazone via oxidation can form 4-nitrobenzyl moiety on the sugar-phosphate of oligonucleotides without any side reactions. Despite, 4-nitrobenzyl group was failed to assist oligonucleotides entry into the cells. Alkyne-linked 4-nitrobenzyl group was designed as a conjugatable functional group to help oligonucleotides delivery.

To apply the chemically caged oligonucleotides to assist oligonucleotides delivery, **specificity and sensitivity** of chemical reaction are the most important factors to be considered and improved. Likewise, chemistry based on **bio-orthogonal reactions** will play a crucial role in this research area and should be expanded. To apply **antidote**[3] for error- correcting mechanisms may be needed for medicinal applications. The lifetimes of the oligonucleotides released from the chemical cages under physiological conditions would not be long. Antidote control is the safest way to regulate drug activity, because the drug activity is independent of underlying patient physiology and co-morbidities. Overall, we thus believe that the target-directed construction of chemically caged oligonucleotides, which have several responsive units can modulate their function autonomously in response to their surrounding environments. Chemically caged oligonucleotides presents and excitement of research and will lead to a wide range of future bioapplications.

Reference

1. Kuscu, L., and Sezer, A.D., Future prospects for gene delivery systems, Expert Opinion on Drug Delivery, 2017, 14, 1205-1215.

2. Ikeda, M., and Kabumoto, M., Chemically caged nucleic acids, Chemistry Letters, 2017, 46, 634-640.

3. Rusconi, C.P., Roberts, J.D., Pitoc, G.A., Nimjee, S.M., White, R.R., Quick, G., Scardino, E., Fay, W.P., and Sullenger, B.A., Antidote-mediated control of an anticoagulant aptamer *in vivo*, Nature Biotechnology, 2004, 22, 1423-1428.

List of Achievements

Research Papers:

Karnsomwan, W., and Okamoto, A., Drastic improvement of cell uptake efficiency of nucleic acids by direct modification with linolenate. (in preparation now)

Proceedings:

Karnsomwan, W., and Okamoto, A., Cellular uptake properties of the polyunsaturated fatty acids conjugated oligonucleotides. The 99th Annual Meeting 2019 of CSJ. Kobe, Japan. 16-19 March 2019.

Acknowledgements

Firstly, I would like to express my sincere gratitude to my supervisor Professor Akimitsu Okamoto for the continuous support of my PhD study and related research, for his patience, motivation and immense knowledge. His guidance helped me in all the time of research and writing of this thesis.

I would like to thank my thesis committee: Associate Professor Dr. Kanjiro Miyata, Associate Professor Dr. Sadao Ota, Associate Professor Dr. Tsuyoshi Osawa and Dr. Satoshi Yamaguchi for their critical remarks on their insightful comments and also for the hard question which incented me to widen my research from various perspectives.

I am greatly thankful to the Mitsui sumitomo bank international cooperation foundation scholarship for providing the scholarship to do my PhD work in Japan.

I would like to acknowledge all members of Okamoto lab, especially, Assistant Professor Dr. Kunihiko Morihiro, Dr. Zhu Hao, Mei Takenaka, Kenta Kohyama, Kaho Usami, Tsuyoshi Hosogane, Yuya Moriyama, Fumika Takeuchi, Miho Kisaka, Wakako Dewa, Xiao Keijing for their various help regarding the laboratory instruments and fruitful discussions. I would also thank to our lab secretary Ms. Chie Shishido and Ms. Kanae Yamanaka (RCAST office) for helping me to complete various official works and protocol.

I would like to thank my family in Thailand: my father Suchin Karnsomwan, my mother Chutima Karnsomwan, my brother Nattakit Karnsomwan and my sister Sujaree Karnsomwan for supporting me during my PhD study and my life in general.

Finally, my sincere thanks to my husband Yuta Hayashi for supporting my life in Japan, the encouragement and spiritually throughout my PhD study.